Efficient methods for recycling cathodes of spent lithium-ion batteries

by

Nianji Zhang

A thesis submitted in partial fulfillment of the requirements for the degree of

Master of Science

in

Materials Engineering

Department of Chemical and Materials Engineering

University of Alberta

Abstract

The ever-growing market share of electrical transportation and energy storage stations has led to a demand surge for lithium-ion batteries (LIBs). Despite their popularity in global energy storage market, an efficient, sustainable and green method that can recycle spent LIBs is also in active exploration. Currently, recycling methods that destructively extract valuables from spent cells, pyro- and hydro-metallurgy, have demonstrated their feasibility at industrial scale, yet both approaches are criticized of generation of undesired environmental concerns. Both metallurgical methods aimed at extracting valuable metals only, however, suffer from the market trend shifting towards cobalt-poor and even cobalt-free chemistry. Recently guided by circular and green economy, alternative innovative strategies are emerging in order to achieve an "closed-loop" recycling of spent LIBs. What is interesting in these strategies is a complete recovery of the pristine structure and functionality of cathode materials in non-destructive methods. Despite the great promise and advantages of the direct recovery method in terms of simplicity, low energy consumption and low stress on the environment, it is still inadequate and ineffective to process obsolete cathodes, such as $LiCoO_2$ and NCM111, to meet the current market. In view of this, another nondestructive method, upcycling, is developed, which aims at either recycling spent cathodes with increased functionality for new applications, or regenerating cathodes with increased performance. This thesis includes fundamental development of cathode recycling strategies, and focuses on developing efficient and effective upcycling method.

This thesis starts with a literature review (Chapter 1) on necessary pretreatment process and recent advances in current four recycling methods, where their ascendancy, challenges, and perspectives are also discussed. Then, the focus of this thesis is extended to a research attempt on testing the feasibility of upcycling methods (Chapter 2). In this research, a 5% $LiMn_{0.75}Ni_{0.25}O_2$

coating is manufactured on spent $LiCoO_2$ cathode material through a modified hydrothermal treatment coupled with a short annealing. With this coating, the upcycled cathode shows a capacity of 160.23 mAh/g with a capacity retention of 91.2% after 100 cycles which are much improved comparing with pristine $LiCoO_2$.

Preface

The work included in the Chapter 1 has been written as a manuscript submitted under peer review. I finished the original draft, Mr. Zhixiao Xu (PhD candidate) and Ms. Wenjing Deng (PhD candidate) helped to review and polish it. Dr. Xiaolei Wang contributed in conceptualization, supervision, and review and editing of the manuscript.

The work in Chapter 2 has been written in a manuscript. I proposed the idea, performed the experiments, analyzed the data, and wrote the manuscript.

Acknowledgements

At the end of my M.Sc. program, I would like to thank everyone who helped me during my studies. I would like to express my greatest gratitude, first and foremost, to my supervisor, Dr. Xiaolei Wang, for offering me such opportunity to work in this project, and the support, guidance, and encouragement throughout the program. I also would like to thank my colleagues in NanoFACE group for their assistance, and inspiration. My thanks especially go to Mr. Zhixiao Xu and Ms. Wengjing Deng for their help in precursor preparation, essay polishing for the literature review, and characterizations of the experimental project. I also want to thank Ms. Xiaolan Gao for providing me spent alkaline batteries in another project. Ms. Zhiping Deng, and Ms. Rujiao Ma are acknowledged for valuable discussions.

Financial support from the Natural Sciences and Engineering Research Council of Canada (NSERC), the Discovery Grant Program and the Discovery Accelerator Supplement Grant program, New Frontiers in Research Fund-Exploration program, and the department of Chemical and Materials Engineering is gratefully acknowledged.

Thanks to all stuff in the Chemical and Materials Engineering department, including our respected professors, and helpful administrative staff.

At last, many thanks to my family members for their love and support in my life. It is impossible for me to even start the journey without them.

Table of Contents

Abstract……ii

Preface……iv

Acknowledgements……v

Table of Contents……vi

List of Tables……viii

List of Figures……ix

Chapter 1. Literature review……1

1.1. Introduction……1

1.2. Significance for recycling spent LIBs……3

1.3. Pretreatment……6

1.4. Pyrometallurgy……8

1.4.1. Conventional pyrometallurgy……8

1.4.2. Fine pyrometallurgy……10

1.5. Hydrometallurgy……12

1.5.1. Leaching……13

1.5.2. Separation……18

1.6. Direct recycling……26

1.6.1. Degradation mechanism in $LiMO_2$ cathodes……26

1.6.2. Direct recycling methods……32

1.7. Upcycling……38

1.7.1. Upcycling towards greater performance……39

1.7.2. Upcycling towards new applications……43

1.8. Conclusions and perspectives……...46

Chapter 2. Surface coating enabled upcycling of spent lithium-cobalt oxide cathodes……...49

2.1. Introduction……..…….49

2.2. Experimental……...……..51

2.3. Results and Discussion…….…….53

2.4. Conclusions……..….58

2.5. Supplementary Information…….….59

Chapter 3. Conclusions and future work……..……..62

References……..63

List of Tables

Table 1 $I_{(003)}/I_{(104)}$ ratios of spent cathode materials and treated cathode materials. ……54

Table S1 Potential change of redox peaks in CV curves of coated, and pristine LCO samples. .60

Table S2 Potential of main peaks, and their voltage differences at 4th, and 100th cycle in dQ/dV plots. ……..61

Table S3 Resistance values of various samples obtained after fitting Nyquist plots. ……..61

List of Figures

Figure 1 (a) Intercalation mechanism of conventional graphite/$LiCoO_2$ LIBs. (b) Structure of a cylindrical cell. ……3

Figure 2 (a) Historical worldwide sales of plug-in hybrid EV (PHEV) and battery EV (BEV) from 2010 to 2020, and projections at 2025 and 2030. Based on data from IEA (2021) [3], all rights reserved; (b) Historical price for the three critical elements for LIBs: cobalt, nickel, and lithium. Based on data from ref. 4, in which the annual average price of Co and Ni from London Metal Exchange (LME), cash, is selected here. (c) The contribution of every component to the whole cost of LIBs. Based on data from ref. 7. (d) The four strategies dealing with spent LIB cathodes: the destructive pyro- and hydrometallurgical, and non-destructive direct recycling and upcycling methods. ……..……5

Figure 3 Workflow diagram of (a) Umicore process and (b) Accurec process. ……....8

Figure 4 pH number of various metals start and end precipitation as hydroxides. Inset: The K_{sp} values [108, 112] of various metal hydroxides, and pH values when the precipitation starts and ends calculated from the definition of K_{sp} ($K_{sp} = [M][OH]_n$ for $M(OH)_n$). Note: the concentration range of metal ions is set between 10^{-5} - 5.0 M. ……20

Figure 5 (a) Degradation mechanism of LIBs as shown in the discharging curve (left) and two main factors(right). Reprinted from ref. 127, copyright 2015 Elsevier. (b) The variations in *c*, and *a* lattice parameters, and corresponding phase transitions during Li^+ deintercalation. Adapted from ref. 148, copyright 2018 Royal Society of Chemistry. Inset: comparison between energy diagrams of $Li_{0.5}CoO_2$ and $Li_{0.5}NiO_2$. Reprinted from ref. 143 with permission, copyright 2001 Elsevier. (c) Time-resolved (TR) XRD patterns (middle) and trace oxygen gas release results (right) from simultaneously measured mass spectroscopy (MS) from the overcharged $Li_{0.33}Ni_{0.8}Co_{0.15}Al_{0.05}O_2$ during heating up to 500 °C. Reprinted from ref. 149, copyright 2013 Wiley. (d) The degraded structure of NCM523 cycled under different voltage windows. Reprinted with permission from ref. 147, copyright 2014 Wiley. (e) The effect of Ni content on the temperature inducing irreversible phase transformations. (f) Schematic illustration of one transition metal migration route inducing irreversible phase transformations. e-f: reprinted from ref. 129 with permission, copyright 2014 American Chemical Society. ..……30

Figure 6 (a) Schematic illustration of hydrothermal relithiation method, where Fe^{3+} cations disordered in Li sites are reduced by with presence of citric acid in LiOH solution. (b) The evolution of LFP composition during relithiation at different temperatures. a-b: reprinted with permission from ref. 169, copyright 2020 Elsevier. (c) Illustration for recovering Li composition of degraded cathodes by eutectic molten salts relithiation approach. (d) Phase diagram of $LiNO_3$:LiOH system. c-d: reprinted with permission from ref. 26, copyright 2019 Wiley. (e)

Reaction scheme for relithiation of the EOL cathode materials via redox mediation: Li-deficient transition-metal oxide ($Li_{1-x}MO_2$) is relithiated via shuttling of quinone molecules, the redox mediator (RM). Left: relithiation process; Middle: whole process; Left: regeneration of LiRM from the reaction of 3,5-di-tert-butyl-o-benzoquinone (DTBQ), the RM, with metallic Li. Reprinted with permission from ref. 159, copyright 2021 American Chemical Society. …….35

Figure 7 Upcycling strategies for spent cathodes, achieving different applications or with improved performance. Upper left: reprinted from ref. 184 with permission. Copyright 2019 American Chemical Society. …….42

Figure 8 (a) Illustration on the application of spent LCO as lubricate additive. Reprinted from ref. 184 with permission. Copyright 2019 American Chemical Society. (b) Catalysis mechanism of toluene oxidation over upcycled MnO_x. Adapted with permission from ref. 188. Copyright 2019 Elsevier. (c) Schematic illustration of the mechanochemical process of spent NCM523 with Na2S·9H2O. Reprinted with permission from ref. 187, copyright 2019 Elsevier. (d) Schematic diagram of upcycling process transforming spent NCM523 into OER catalysts with Li salts extracted electrochemically. (e) The polarization curves (top left), and Tafel slopes (top right) at 20 mA/cm^2 of the delithiated $Li_{1-\delta}Ni_{0.5}Co_{0.2}Mn_{0.3}O_2$ (δ = 0.9, 0.6, 0.4, 0) samples, and the long-term chrono-potentiometric stability (bottom) of $Li_{0.4}Ni_{0.5}Co_{0.2}Mn_{0.3}O_2$ and $LiNi_{0.5}Co_{0.2}Mn_{0.3}O_2$ at 20 mA/cm^2. d-e: reprinted/adapted with permission from ref. 186. Copyright 2019 Elsevier. (f) Polarization curves of $M(OH)_2$ (M: $Ni_{0.5}Co_{0.2}Mn_{0.3}$), $LiNi_{0.5}Co_{0.2}Mn_{0.3}O_2$, and IrO_2. Reprinted with permission from ref. 187, copyright 2019 Elsevier. ……..45

Figure 9 Process workflows for pyrometallurgical, hydrometallurgical, direct recycling, and upcycling processes. ……..46

Figure 10 (a) XRD patterns of DLCO, LCO-pri, and NM-DLCO-5%, and the (b) enlarged view.

……53

Figure 11 SEM images and corresponding EDX mapping images of DLCO (a-d), and NM-DLCO-5% (e-h). ……55

Figure 12 Cycling performance of degraded, pristine, and regenerated cathode materials. (Initial three cycles: 0.4 C (1 C = 140 mAh/g) from 3.0 to 4.2 V; the following cycles: 1 C from 3.0 to 4.35 V). (b) Rate capability of the regenerated and pristine cathode materials with a cut-off voltage of 4.35 V. ……..56

Figure 13 Voltage profiles of the regenerated (a) and pristine (c) cathode materials at the initial three cycles at 0.4 C in the volatage range of 3.0 – 4.20 V. The differential specific capacity vs. voltage (dQ/dV) curves for the regenerated (b) and pristine (d) cathode materials. ……57

Figure 14 (a) Nyquist plots of regenerated, pristine, and degraded LCO samples after 100 cycles, equivalent circuit (inset), and (b) enlarged view. …….58

Figure S1 Cycling performance of the LCO commercial cylindrical cell which was cycled in a voltage range of 3.0 - 4.2 V at 825 mA (total capacity: 1650 mAh). ……59

Figure S2 XRD patterns of all LCO samples. ……..59

Figure S3 Cycling performance of upcycled cathode materials with different coating contents. (Initial three cycles: 0.4 C (1 C = 140 mAh/g) from 3.0 to 4.2 V; the following cycles: 1 C from 3.0 to 4.35 V). ……....60

Figure S4 CV curves of NM-DLCO-5%, and LCO-pri samples in a scan rate of 0.1 mV/s from 3.0 V to 4.5 V. ……60

Figure S5 EDX-ray spectrometry analysis, and content of various elements. …….61

Chapter 1. Literature review

1.1 Introduction

Due to high capacity, high energy density, admirable lifespan, and low carbon footprints, LIBs are regarded by many governments to be the next-generation power source for electric vehicles (EVs), replacing fossil fuel-based automobiles. Simultaneously, the market of portable electronics also produced numerous spent LIBs annually. However, with tons of LIBs disposed each year, the regeneration and recycling of LIBs became more and more urgent considering the huge market share of LIBs in energy storage field and their growing popularity. As organic solvent containing fluoride was vastly used as electrolytes for LIBs and safety hazards coupled with short circuit, recycling of spent LIBs is imperative. In addition to the environmental and safety concerns, recycling of spent LIBs could also be profitable, able to alleviate the stress on supply chain due to the uneven distribution of critical elements and environmental-benign as many valuable elements (Co, Ni, Cu, Li, etc.) are used and accumulated in spent LIBs, from which makes it easier and greener to collect than from crust of the earth.

The success of lithium for energy storage started from the early 1970s with the primary lithium-ion battery. A very famous example is the lithium thionyl chloride battery, which is a primary battery developed by Adam Heller and is still being utilized in pace makers due to its ultra-long lifetime. In the same period, a reversible process in which lithium can be intercalated into layered transition metal dichalcogenides (sulfides and selenides) was found by Whittingham et al. [1]. The reversible intercalation process made a rechargeable high-energy storage system possible. As a layered transition metal disulfide, TiS_2 attracted a lot of interest as it offers low molecular weight, admirable electronic conductivity and low cost. As a positive electrode material, it showed an average specific capacity of 240 mAh/g with an intercalation voltage of 2.0 V versus Li/Li^+. However, TiS_2 can react with water and decompose into titanium oxide and hydrogen sulfide, meaning the synthesis of TiS_2 must be performed under an inert atmosphere. As TiS_2 was excluded from candidate materials due to its safety issues and elaborate synthesis, the need to find workable high-energy cathode material drove more attention to other transition metal chemicals. Goodenough et al. reported lithium intercalation process in Li_xCoO_2 ($0<x\leq1$), a layered cobalt oxide compound, which was later developed into “rocking chair” rechargeable lithium-ion battery with carbonaceous material as the anode, as shown in Figure 1a. In 1991, Sony Corporation

commercialized rechargeable LIBs using $LiCoO_2$ as cathode and carbon as anode. Such battery was led by Yoshio Nishi, who won the Nobel Prize in Chemistry with Goodenough and Whittingham for their efforts in the development of lithium-ion battery.

Basically, a LIB is made of a cathode, an anode, and a polymer separator, which all are soaked in organic electrolyte, as shown in Fig.1a. The mechanism of battery depends on a redox reaction, where the reduction and oxidation reaction are separated with each other, and potential difference between two electrodes drives electrons to move and perform work to external circuit. While discharging, a reduction reaction happens on the positive electrode (cathode) which is connected with a negative electrode (anode) by the external circuit and the electrolyte, the former one is a pathway for election motion while the latter is a pathway for ion transfer, offering the cathode both Li^+ ions and electrons. The charging process happens reversely, with electrons move through the external circuit from the positive electrode to the negative electrode where happens an electron-consuming reduction reaction while Li^+ ions move in the same direction with electrons but through electrolyte. The electrolyte is made of a mixture of organic solvents, typically contain ethylene carbonate (EC), dimethyl carbonate (DMC) and etc., with a Li-salt (e.g., $LiPF_6$) dissolved. The separator is an electrochemically insulating membrane, usually made of polymer, separating anode and cathode from short-circuit but is porous, allowing Li^+ ion diffusion. Generally, in LIB fabrication industry, the active materials on the electrode need to be mixed with conductive agents like carbon black while both are binding with each other and to metal foil (Al and Cu) through a polymer binder, commonly polyvinylidene fluoride (PVDF), to form a slurry latter coated on Al or Cu current collector.

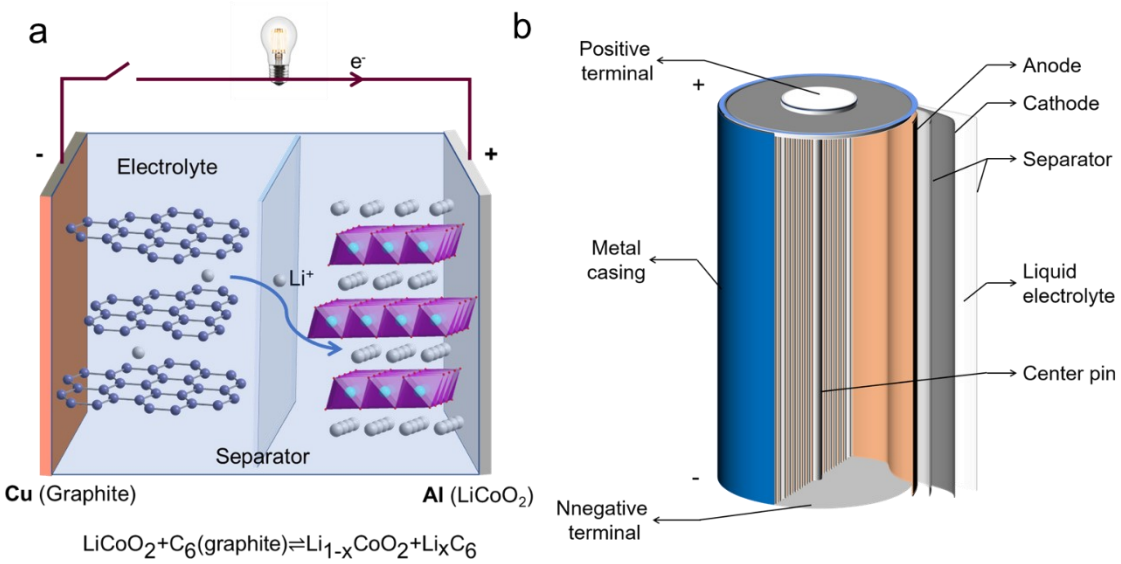

Figure 1 (a) Intercalation mechanism of conventional graphite/$LiCoO_2$ LIBs. (b) Structure of a cylindrical cell.

The market of LIBs started growing since 1991 when Sony Inc. developed the first commercial LIB using graphite anodes and $LiCoO_2$ cathodes, following the Li^+-ion intercalation and deintercalation mechanism (Fig. 1a). After 30 years, the market is shifting from $LiCoO_2$ (LCO) to Co-poor cathodes such as $LiNi_{1/3}Mn_{1/3}Co_{1/3}O_2$ (NCM111), and $LiNi_{0.8}Co_{0.15}Al_{0.05}O_2$ (NCA) or even Co-free cathodes like $LiFePO_4$ (LFP) and $LiMn_2O_4$. Reports pointed the average price for LIBs pack has reached 137 $/kWh in 2020, 89% decreased than that one decade ago, partly owing to the increasing popularity of Co-less chemistry [2]. However, LCO still dominate the market for consumer electronics industry due to its high energy density, while NMC is expected to grow in the highest rate for automotive application, in which the cylindrical structured cell (as shown in Figure 1b) dominates. Commonly, graphite is utilized as anodes for LIBs while SiO_x is now also introduced as an additive to improve the performance.

1.2. Significance for recycling spent LIBs

The success of LIBs in consumer electronics market has driven more and more application for EVs in the past decade. In such case, the market is expected to keep expanding (Figure 2a), to reach ~11 million EV-sales at 2025 and ~20 million at 2030 according to a projection from International Energy Agency (IEA) [3]. Meanwhile, the increasing demand for LIBs, in which the

cathode materials account for 30% material cost of the whole battery, not only drives the popularity of Co-deficient cathodes but also exacerbates the stress on the supply chain, also stating the significance of recycling spent LIBs on the other hand. For instance, the vast majority of cobalt resources are in sediment-hosted stratiform copper deposits in Congo (Kinshasa) and Zambia, from where at least 60% of Cobalt is produced [4]. Recycling the critical elements from spent LIBs at least brings three benefits: (1) a combined treatment on spent LIBs can benefit from scale effect, and safety and environmental hazards dealing with degraded LIBs can be controlled; (2) recycling critical metals from spent LIBs secures the supply chain that is circular in nature, and alleviates materials scarcity and enhances environmental sustainability; (3) using recycled materials through a direct recycling method has potential to decrease costs by 44%, energy consumption by 83%, water use by 79%, and SO_x emission by 99%, comparing producing 1 kg NCM111 from mineral ores [5]. 5-15 tons of spent LIBs can be used to manufacture 1 ton of battery-grade cobalt, equivalent to about 300 tons of mineral ores [5-6].

Recycling of spent LIBs mainly focuses on valuable metals, which are mainly concentrated in cathodes. In general, pre-treatment like disassembly, crushing, and separation, is necessary to recycle more efficiently and remove toxic electrolytes. Since charged batteries are located at a thermodynamically active state, great danger is associated with recycling, requiring a qualified waste management system.

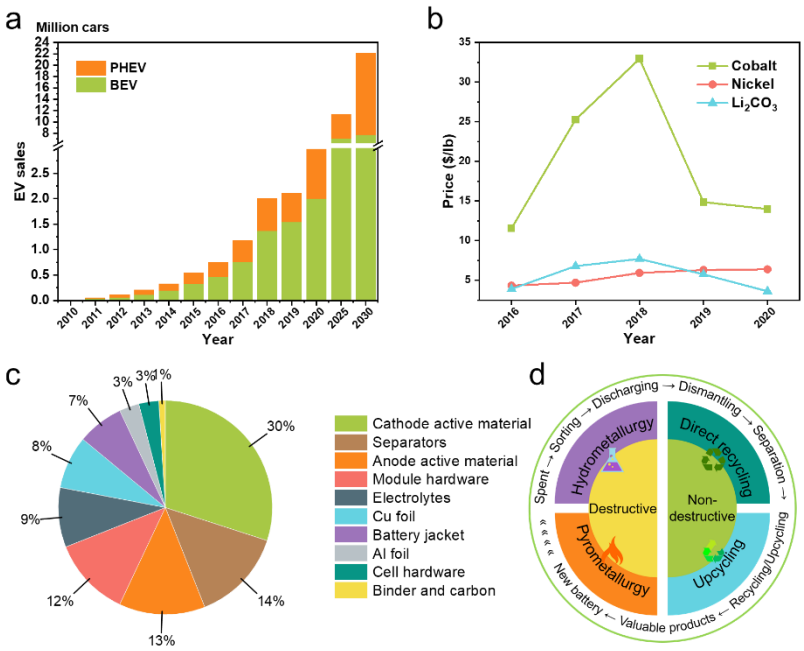

Figure 2 (a) Historical worldwide sales of plug-in hybrid EV (PHEV) and battery EV (BEV) from 2010 to 2020, and projections at 2025 and 2030. Based on data from IEA (2021) [3], all rights reserved; (b) Historical price for the three critical elements for LIBs: cobalt, nickel, and lithium. Based on data from ref. 4, in which the annual average price of Co and Ni from London Metal Exchange (LME), cash, is selected here. (c) The contribution of every component to the whole cost of LIBs. Based on data from ref. 7. (d) The four strategies dealing with spent LIB cathodes: the destructive pyro- and hydrometallurgical, and non-destructive direct recycling and upcycling methods.

As shown in Figure 2d, the strategies to recycle cathodes of spent LIBs include two categories: destructive methods, including pyrometallurgy and hydrometallurgy, and non-destructive methods, such as direct recycling and upcycling. The pyrometallurgy uses high-temperature treatment while the hydrometallurgy uses chemicals such as acids, ammoniacal agents [8], and even microorganisms [9-10], but both destructively destroy the chemical bonds within crystal lattices of cathode active materials. In practice, typical pyrometallurgy methods will transfer valuable transition metal into alloys or oxides, which require another step of hydrometallurgy to achieve the regeneration of cathode material [11]. Such processes are suitable for large-scale industrial applications but consume a lot of energy. On the other hand, hydrometallurgy, via

leaching with reductants like hydrogen peroxide and glucose [12], generate a mixture solution containing multi metal ions, such as Co^{2+}, Li^{+}, Ni^{2+}, Fe^{3+}, PO_4^{2-}, Mn^{2+} and etc., followed by purification and/or separation steps to obtain high purity products. Considering the efficiency of separation in pretreatment and the difficulty of keeping the single source of spent LIBs, the industrial scale of recycling spent LIBs makes it necessary to be able to recycle a mixture of various cathode materials, where pyro- and hydro-metallurgical recycling have the greatest capability in dealing with such situation. In lab scale, one of the most promising features of hydrometallurgy when dealing with NCM cathodes is that the ratio between triple metal ions keeps constant, enable the co-precipitation these metals.

Compared with aforementioned destructive methods, direct recycling is mainly achieved by recovery of degraded phases and re-lithiation of over-delithiated phase, in which major species still work normally. Direct recycling also avoided the inevitable regeneration step in hydrometallurgy and pyrometallurgy to calcinate precursors to fine cathode materials. Upcycling, also known as upgraded recycling, aims to recycle spent materials into upgraded compounds of better quality or potential for other applications. Although the ability of direct recycling and upcycling dealing with mixed cathodes (layered/spinel/phospho-olivine structured) remains to be explored, yet some fields, such as EVs and energy-storage stations, require a massive volume of LIBs with consistent chemistry, making it possible to find them applicable.

1.3. Pretreatment

Owing to the complex chemistry and dense structure of LIBs, pretreatment before recycling is inevitable to achieve a high efficiency. Typically, the extent of pretreatment depends on the LIB recycling methods, and also closely determines the recycling efficiency. Direct recycling (upcycling) typically requires the highest standards, i.e., a complete separation of active materials from other components. The pretreatment process can be divided into: i, sorting; ii, discharging; iii, dismantling; and iv, separation. The sorting process, often ignored in other literatures, yet is of great significance for hydrometallurgy and direct recycling methods. It is a process that identify and differentiate LIBs with different electrode materials in which the participation of the manufacturer shall make a big difference. The color codes introduced by manufacturers shall minimize the complexity and allow easier sorting of active materials [13]. Besides, sorting is no

longer needed when dealing with specific and constant sources of spent LIBs, e.g., recycle batteries from EVs. In fact, the 85-kWh battery pack, weighing 540 kg, of Tesla model S contains 7104 cylindrical cells in total (16 modules with six groups in series, each group contains 74 Panasonic 18650A cells in the chemistry of NCA) producing a nominal voltage of 345.6 V [14-15]. A constant source of spent LIBs means a steady chemistry in cells, making it much easier to control impurities and lower the cost.

In order to prevent short-circuit and self-ignition, spent LIBs need to be discharged first to remove residual energy. This step also concentrates Li^+ back to cathodes, leading to a decreased labor. One common method to complete discharging of spent LIBs is to immerse those cells into brine solutions (e.g., NaCl and Na_2SO_4 solution) [11, 16-23], known as electrolytic discharge, while some lab-scale reports electrically discharged them to certain levels (e.g., 2.0 V) [24-30]. It should be noted that discharging spent cells in salt solution leads to hydrogen evolution and other side reactions. For instance, discharging a typical 18650 cell with metal casing in NaCl solution shall induce iron and aluminum dissolution [31] and hydrogen evolution, the latter of which shall be noticed as safety hazards in industrial scale.

Typically, the lab-scale dismantling of spent LIBs is finished manually. Hence casings, cathode, anode, and separators can be retrieved efficiently yet not suitable for scaling up industrially. There are three methods popularly used to separate cathode materials from the binder, conductive agents, and Al current collector: (a) high-temperature treatment in the air to decompose the binder [32-39]; (b) solvent dissolution of binder (coupling sonication & centrifugation or filtration) [19, 24, 26, 29, 40-44]; (c) alkaline leaching of Al foil [12, 45-47]. Furthermore, some novel methods are also developed to separate active materials from Al current collector, such as by high-voltage pulsed discharge [48-49], and concentrated sulfuric acids [21]. For binder dissolution, N-methyl-2-pyrrolidone (NMP) is a popular solvent to dissolve PVDF-based binder yet is criticized because of the high cost. Alternative agents like dimethylformamide (DMF), DMC [23], formamide [19], molten salts [50], deep eutectic solvents [51] are also employed. In the end, another thermal calcination may also be introduced to remove further impurities.

Industrial process treating spent LIBs in the way of shredding, milling/thermal treatment and sieving [52-58], from which fine particles obtained are mainly composed of cathode and anode active materials, and then subjected to recycling processes. During such process, magnetic

separation can be employed to remove stainless steel casings, while further separation of cathode and anode active materials can be achieved by a flotation method due to their different densities [39, 59]. Coarse particles mainly include Al, Cu, and shall be sent to metal smelting facilities. Lee et al. developed a thermomechanical method that utilizes thermal treatment to remove binder, while active materials and current collector are separated mechanically by sieving to obtain NCM811 from cathode scrap [60]. Such strategy was also reported by Hanisch et al. [58], in which an air jet was employed to disengage active materials from Al foil, both were preheated to remove binder and separated by a fine sieve.

1.4. Pyrometallurgy

1.4.1. Conventional pyrometallurgy

Among all methods developed to recycle spent LIBs, the pyrometallurgy-dominated method is considered as a commercial choice due to its simplicity in the whole process, ease of scale-up, and flexibility or tolerance on battery types. A high-temperature is needed during smelting reduction of metals in spent LIBs. In a typical industrial pyrometallurgy-dominated process developed by *Umicore* Group, spent LIBs and Ni-hydride batteries are dealing like nature ores without any pretreatment, heated with carbon, slag formers, and metal-oxides simultaneously. Such treatment produces an alloy of Co-Ni-Cu-Fe, and a slag containing Li, Al, and Mn, while the graphite anode gets lost. Figure 3a shows the typical workflow of *Umicore* process.

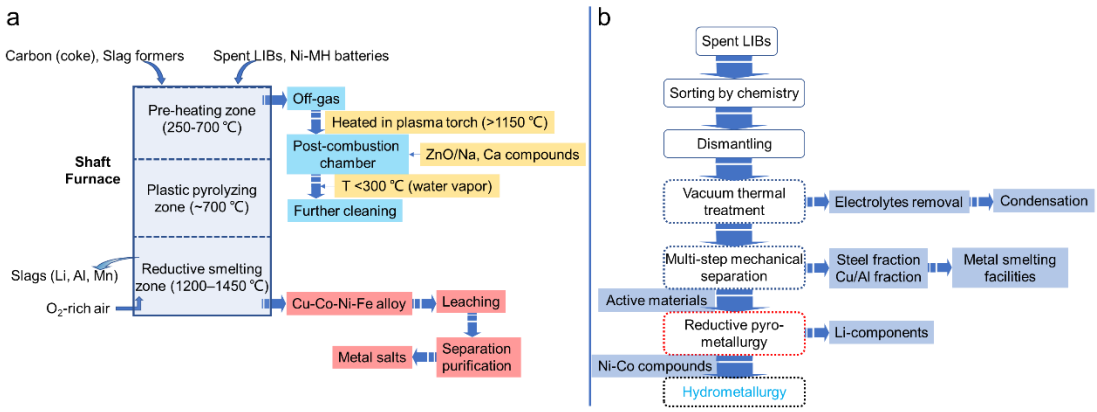

Figure 3 Workflow diagram of (a) *Umicore* process and (b) *Accurec* process.

As shown in Figure 3a, spent batteries was treated sequentially within three zones with different temperatures in shaft furnace, which are called pre-heating zone, plastic-pyrolyzing zone, and metal-smelting/reduction zone from top to bottom, respectively. Located at the top, the pre-heating zone possesses a lower temperature (< 300 ℃), where organic electrolytes (EC/DMC) are evaporated slowly to lower the explosion risk. In order to prevent the condensation of organic vapor and increase the collection efficiency, the top of the shaft furnace is maintained at a temperature between 250 and 700 ℃, which is preferably achieved by a plasma torch. The plastic-pyrolyzing zone, located in the middle of the furnace, is used to incinerate plastic components (PVDF/separator/composite can) in spent batteries. A medium temperature (~700 ℃) is needed here, and the heat produced by pyrolyzing organic components also helps reduce energy consumption. In the bottom zone where smelting/reduction of transition metals is achieved, oxygen-enriched gas is pumped into this part to oxidize carbon and aluminum, and metals including Cu, Co, Ni, Fe are reduced into alloys, as well as a slag containing Li, Al, Si, and part of Fe is formed. Heated by plasma torch to a temperature over 1150 ℃, evaporated toxic off-gas containing fluorine is sent into a post-combustion chamber, where injection of ZnO or calcium/sodium-based products removes fluorine from PVDF and $LiPF_6$ dissolved in electrolytes. Then, the temperature of the cleaned off-gas is rapidly decreased below 300 ℃ by injecting water vapor, which to prevent the formation of dioxines and furans, and recombination of organic compounds with fluorine.

As shown in Figure 3a, a typical *Umicore* process produces an alloy containing Co and Ni, both of which then need to be extracted hydrometallurgically for final recovery of Co- and Ni-salts, while Li and Mn are wasted in slags. The economic production of this process strongly depends on cobalt and nickel concentration in cathodes. The trend of lowering cobalt and nickel content to even free of them in LIBs not only decreases the cost of cathode but definitely also has a negative impact on the economic perspective on recycling spent LIBs. Lithium is another valuable element enriched in spent LIBs. Hence, in order to increase the profit of pyrometallurgical methods, Li wasted in slags should be avoided. Hu et al. pointed out that the high aluminum content in precursors is responsible for the Li loss in slags because Li_2O and Al_2O_3 can react to form the $LiAlO_2$ phase that is thermally and chemically stable [61]. Increasing carbon content can reduce the wasted lithium content in the slag through the formation of flue dust containing Li_2CO_3 which can be leached out by carbonated water. Despite of great simplicity and scalability, *Umicore* process

does not remove Al from casing and cathode current collector when treating spent LIBs, leading to a great Li^+ loss in slags. Besides, valuable graphite anode is also lost in the smelting process and incineration of plastic components increases the green-house gas (GHG) emissions.

1.4.2. Fine pyrometallurgy

Accurec Recycling GmbH in *Germany* developed a recycling process, as shown in Figure 3b, combining a mechanical pretreatment with hydro- and pyrometallurgical process steps dedicated to recycling both cobalt and lithium in portable LIBs [62-65]. Beginning from sorting, dismantling, thermal pretreatment (including electrolyte collection), and mechanical separation, this process yields valuable components, including steel fraction, Cu/Al fraction, and active materials fraction. The metal parts are sent to corresponding metal smelting facilities for metal recovery, while the active materials are forwarded to pyrometallurgical treatment following a hydrometallurgical extraction to a final recovery as metal salts. Lithium is recovered as metallic lithium through direct vacuum distillation recovery or lithium oxides volatilization using carrier gas [66].

Different from *Umicore* process dealing with spent LIBs like nature ores, *Accurec* recycling process treats pretreated materials in a pyrometallurgy-dominated process, classified as *fine pyrometallurgy*, which generally with a higher efficiency. Aluminum, copper, and steel remain in a high purity in outer-casing and current collectors, hence a pretreatment to separate them from active materials will definitely increase the efficiency. Hu et al. conducted a laboratory-scale experiment studying smelting and reduction of $LiCoO_2$ and cathode material (NCM) with carbon at 1550/1600 ℃ in a vertical furnace full of argon gas [61]. Without a slag-forming material, both, dealing with $LiCoO_2$ in chemical grade and NCM from spent LIBs, exhibited a nearly 100% recycling of transition metals and lithium, latter of which mainly concentrated in flue dust, a product of evaporated lithium oxide vapor reacts with carbon dioxide or halogens (come from the added CaF_2 or $CaCl_2$). Such high efficiency benefited from the absence of aluminum or silicon, which will confine lithium in slags.

In the following pilot-scale trial, Hu et al. demonstrated a pyrometallurgy-dominated recycling process (*Re-Lion process*) treating NCM622 in an electric arc furnace (EAF, >1500℃), which was developed at SWERIM (*Luleå, Sweden*) using a CaO-Al_2O_3 slag system, leading to

high recycling yields of 98.2%, 98.4%, 91.5% and 68.3% for Co, Ni, Mn and Li metals (in flue dust), respectively [52]. Anthracite (85.2% C) was used as reductant for smelting here. Metal alloy and slag obtained after smelting and reduction are expected to undergo a hydrometallurgy process to recycle critical metals and lithium simultaneously.

Fine pyrometallurgy in the presence of reducing agents, such as carbon [11, 36, 56, 67], methane [68], metallic Al [69] and even $(NH_4)_2SO_4$ [70], are proved feasible to destroy the structure of cathode active materials under lower temperature. For example, using activated carbon as the reducing agent, Maroufi et al. [36] reported a simple carbothermic reduction of $LiCoO_2$ cathode material (current collector was leached out using 2 M NaOH) in a temperature range between 600-800 ℃ in Ar. At 700 ℃, Li escaped from cathode material and was isolated in the form of Li_2CO_3, and LCO cathode was converted into cobalt oxides with partial metallic Co. After leaching treatment, around 36% of Li can be recovered.

Hu et al. [56] recovered Li, Ni, Co, and Mn from a $LiNi_xCo_yMn_zO_2$ cathode material (Al selectively leached by 1.5 M NaOH) roasted under 650 ℃ in Ar for 3 h with 19.9 wt.% carbon dosage. After roasting, the cathode was transformed into Li_2CO_3, Ni, Co, and MnO. Following that, a carbonation water leaching (solid-to-liquid ratio of 1:10) with CO_2 in 20 ml/min for 2 h was utilized to extract Li, and the filter residue was leached by 3.5 M H_2SO_4 at 85 ℃ for 3 h, resulting in 84.7% of Li and >99% of Ni-Co-Mn in the leachate.

Xiao et al. [11] reported a vacuum metallurgy method to treat spent LIBs in which under inclosed vacuum condition at 800 ℃ for 45 min, mixed electrode materials containing $LiMn_2O_4$ and graphite can be in situ carbothermally converted to MnO and Li_2CO_3. Subsequent water leaching with a solid-to-liquid ratio of 10 g/L yields 91.3% of Li and further air annealing filter residue yields Mn_3O_4 with a purity of 95.11%. A higher temperature shall lead to metallic products. With graphite as a reductant in oxygen-free roasting, metallic Co and Li salts shall form at 1000 ℃ for 30 mins [67]. The metallic Co can be separated through magnetic separation while Li salts (Li_2CO_3) are separated from graphite residue by the high solubility in water, leading to a recovery rate of 95.72%, 98.93%, and 91.05% for Co, Li, and graphite after a wet magnetic separation, respectively.

Similarly, Yang et al. [68] reported an improved reductive roasting approach with the methane as the reductant to treat spent $LiNi_xCo_yMn_zO_2$ cathode under the following conditions: temperature: 600 ℃, time: 0.5 h, methane flow rate: 500 ml/min. And it achieved a recovery rate about 88% of Li and over 98% of Mn, Ni, Co after treating the pyro-products with a carbonation water leaching and an acid leaching, respectively. They also pointed out that removal of Al by pre-alkali leaching helps to increase the recovery efficiency of Li from 70% to 88% by lowing the formation of water-insoluble $LiAlO_2$.

Metals can also serve as reductants in the metallurgical recycling of cathodes. A mechanochemical method was reported by Dolotko et al. [69] to separate metallic Co from $LiCoO_2$ cathodes by supplying Al as reductive agents. The presence of current collector (Al) minimized the amount of external Al needed. Tang et al.[70] demonstrated the feasibility of using $(NH_4)_2SO_4$, working as both sulfation and reducing agents, to covert spent NCM622 materials to corresponding metal sulfates. Under a temperature of 350 ℃ for 1.5 h and an $(NH_4)_2SO_4$-to-NCM622 mass ratio of four, 99.2% of Li, 99.4% of Ni, 98.8% of Co, and 98.5% of Mn were converted to water-soluble sulfates.

1.5. Hydrometallurgy

Compared with pyrometallurgy, hydrometallurgy, composed of leaching of cathodes and purification of metal ions, is of great promise for recycling spent LIBs due to its high selectivity, low energy consumption, high yield in a long term, and received much research attention. Hydrometallurgy is advantageous in recycling mixed cathode materials composed of Li, Co, Ni, Mn, Fe and impurities containing Al, Cu, etc. Increasing the tolerance over impurities and efficiency in separating critical elements can eliminate the need of sorting by different chemistries in pretreatment. However, this method also generates a large amount of chemical wastes containing excessive leachants, heavy metals, and salts.

Leaching is a process during which one or more solutes are extracted from a solid through the application of a liquid solvent. In the leaching process of meal oxides, reducing agents, like H_2O_2, $NaHSO_3$ [35], $C_6H_{12}O_6$ [12], etc., are also needed to enhance the leaching process. They work by reducing Co^{3+} to Co^{2+} and Mn^{4+} to Mn^{2+}, latter of which have weaker bonding with oxygen and hence are more readily dissolved into solution [71-73]. Then, various ions coexist in leachate solution,

and further purification and separation are needed. Typical purification is finished by adding chemicals, such as precipitation agents and solvent extraction agents, into the mixture solution. Usually, whole process holds a high efficiency in cathodes recycling. For instance, Zhu et al. reported leaching efficiencies 96.3 wt.% and 87.5 wt.% of Co and Li, respectively, by treating $LiCoO_2$ with 2 mol/L H_2SO_4 and 2.0 vol.% H_2O_2, and overall recovery efficiencies 94.7% of Co and 71.0% of Li respectively were achieved through precipitation of $CoC_2O_4 \cdot 2H_2O$ and Li_2CO_3 sequentially [74].

1.5.1. Leaching

Leaching of cathodes is usually achieved by acids including inorganic acids such as H_2SO_4 [54], HNO_3 [75], H_3PO_4 [16], HCl, and some mild organic acids such as citric acid [25], oxalic acid ($H_2C_2O_4$) [55], tartaric acid [17], etc., while chemicals like sodium persulfate ($Na_2S_2O_8$) [76] may also be employed. Dissolution reaction of metal oxides cathodes can be generally described as following:

$$LiNi_xCo_yMn_zO_2 + 6H^+ + (0.5y + z)H_2O_2 \rightarrow Li^+ + 2H_2O + xNi^{2+} + yCo^{2+} + zMn^{2+} + O_2 \ (x + y + z = 1) \quad (1)$$

$$2LiCoO_2 + 6H^+ + H_2O_2 \rightarrow 2Li^+ + 4H_2O + 2Co^{2+} + O_2 \ (y = 1) \quad (2)$$

Reductive leaching with inorganic acids

Traditionally, intensive hydrometallurgical recycling of cathodes focusses on strong inorganic acids including HCl, HNO_3, H_2SO_4 due to their capability of dissolving all cathode materials. For instance, Zhu et al. employed sulfuric acid to leach $LiCoO_2$ in which 96.3% of Co and 87.5% of Li can be leached into solution under the condition of 2 mol/L H_2SO_4 with 2.0 vol.% H_2O_2, 33 g/L solid-to-liquid (S:L) ratio, 2 h leaching time and a temperature of 60 °C [74]. To further enhance the metal dissolution, some other chemicals may also be used, including H_2O_2 [16-19, 25, 32, 34, 41, 54, 74-75, 77-79], $NaHSO_3$ [35], SO_2 [80], ethanol [81], ascorbic acid, citric acid [82], $Na_2S_2O_3$ [33], Na_2SO_3 [8] and $Na_2S_2O_8$ (for LFP) [76].

Generally, larger concentration of leachants, longer reaction time, higher temperature and smaller S:L ratio, will lead to a higher leaching efficiency. Higher concentration of reductants and leachants are helpful to promote leaching; however, it loses value-to-cost when the concentration reaches the optimal condition. Also, too high concentration may also prohibit the ion diffusion, hence external forces, such as ultrasonic treating [32], microwaving [40], stirring [55, 82] are also adopted to enhance the dissolution of metal oxides. Generally, during the leaching treatment, above parameters follows a priority order of time > reductants > acid > temperature > solid to liquid ratio [54]. Yet for the purpose of scaling up, industrial leaching of cathodes should be accomplished efficiently in a mild condition.

The focus of past studies was put on optimizing leaching parameters. Liu et al. studied the effect of various acids (H_3PO_4, HCl, HNO_3, and H_2SO_4) on the leaching efficiency of NCM622 without any reductant [83]. Among these acids, H_3PO_4, a weak acid, demonstrated the lowest performance over leaching of Li, Ni, CO, and Mn, and almost failed to extract Mn; sulfuric and nitric acids exhibited similar efficiencies in which the best leaching efficiencies are achieved on lithium due to the lower bond strength of Li-O comparing with transition metals. With strong reducing ability, HCl displayed the best leaching efficiency among all acids, and the performance drastically increased from 1 M, reached the maximum at 3 M, indicating the reducing role of hydrochloric acid. Liu's work demonstrated leaching efficiencies of 100% for Li, 99.7% for Ni, 99.3% for Co, and 99.7% for Mn, respectively, under a condition of 3 M HCl, 70 ℃, 400 rpm stirring speed, 20 g/L, and leaching time of 50 min [83]. However, corrosive gas Cl_2 will form as a result of the metal reduction in the case of using HCl, which enhances metal dissolving but also makes Cl_2 neutralization indispensable, leading to additional cost in safety and environmental protection.

Supplying reductants is one common method to enhance the dissolution of cathodes in hydrometallurgical recycling. H_2O_2 is the most convenient reductant, and hence is intensively utilized in this field (mechanism shown in eq 1-2) [16-18, 25, 32, 54, 74-75, 77-78]. Introduction of reductant is helpful to enhance the leaching efficiency. For instance, at 4 vol.% of H_2O_2, leaching efficiencies of Li, Mn, Co, Ni can reach 99.07, 99.31, 98.64, 99.31%, respectively, greatly improved comparing with 31.47, 30.44, 16.69, 29.59% in the absence of H_2O_2 under same conditions of 17 g/L S:L ratio, 2 M L-tartaric acid, 70 °C, and 30 min [78]. Notably, Porvali et al. [84] developed a redox

system ($2Fe^{3+} + Cu \rightarrow 2Fe^{2+}_{(reductant)} + Cu^{2+}$) to produce reductive agents Fe^{2+} enhancing the leaching of $LiCoO_2$. With a reduced product as HSO_4^-, $NaHSO_3$ is also promising to couple with sulfuric acid in hydrometallurgical leaching of cathodes. Meshram et al. demonstrated that with 1 M H_2SO_4 and 0.075 M $NaHSO_3$ as reducing agent, ~96.7% Li, 91.6% Co, 96.4% Ni, and 87.9% Mn were recovered in 4 h at 368 K and a pulp density of 20 g/L [35]. They also demonstrated the leaching of metals followed empirical logarithmic law controlled by surface layer diffusion [35].

Reductive leaching with organic acids

Inorganic acids used as leaching agents may generate toxic gases such as Cl_2, SO_3, and NO_x, and a lot of salts in the waste water. By contrast, organic acids are more environmentally benign for the leaching process due to their biocompatibility and biodegradability [41, 85]. Various organic acids have shown comparable ability than those strong inorganic acids to leach metals out from LIB cathodes, such as citric acid, oxalic acid, formic acid, ascorbic acid, etc. Typically, the leaching efficiency organic acids exhibited is directly related to their acidity (lower acid dissociation constant, pK_a, leads to stronger acidity). For example, citric acid is an organic acid with three carboxylic groups ($pK_{a1} = 3.13$, $pK_{a2} = 4.76$, $pK_{a3} = 6.40$) [85]. Using 1.25 M citric acid with 1.0 vol.% H_2O_2 with a S:L ratio of 20g/L, around 100% of Li and >90% of Co can be extracted from spent LCO in 30 min under 90 ℃ [41]. Compared with mineral acids, organic acids show small corrosivity or dissolution of metallic Al [45, 86]. Thereby, Al foil can be separated easily after leaching via organic acids, minimizing the work in pretreatment.

Meanwhile, some organic acids such as ascorbic acid and citric acid (H_3Cit) can also be used as effective reductants. For example, Zhang et al. utilized 0.2 M H_3PO_4 and 0.4 M H_3Cit in a S/L ratio of 20 g/L to leach NCM523 at 90 ℃ for 30 min, resulting in a leaching efficiency of ca. 100% for Li, 93.38% for Ni, 92.00% for Mn, and 91.63% for Co, where the H_3Cit worked as both leaching and reducing agent [82]. Li et al. studied the practicability of ascorbic acid to recycle $LiCoO_2$ [42]. 98.5% of Li and 94.8% of Co can be extracted in 20 min in a 1.25 M ascorbic acid with a 25 g/L S/L ratio, under 70 ℃. It was also demonstrated that biomass such as tea waste as well as powders of Phytolacca Americana (PA) branch also have the reducibility to enhance the leaching [87]. The H_3Cit/tea waste revealed similar leaching abilities compared with H_3Cit/H_2O_2 system (96% Co and 98% Li versus 98% Co and 99% Li), while H_3Cit/PA system with a slightly inferior leaching performance (83% Co and 96% Li).

Under some circumstances, several leaching agents can achieve leaching and precipitation simultaneously, such as oxalic acid [55], tartaric acid [17], and DL-malic acid [32], due to the insoluble chemicals composed of metal cations from spent cathodes and anions from the leaching agents.

Oxidative leaching of $LiFePO_4$

In the recycling of $LiFePO_4$, hydrogen peroxide is utilized as an oxidant to oxide Fe^{2+} to Fe^{3+} in a leaching mechanism shown in eq 3, in which Fe^{3+} will precipitate with PO_4^{3-} owing to a low solubility product constant (9.91×10^{-16}), minimizing the expense for the following separation. Yadav et al. used weak organic acids, such as methyl sulfonic acid (MSA) and p-toluene sulfonic acid (TSA), in the leaching of $LiFePO_4$ [20]. After leaching, they adjusted the pH value of the solution to ~4 by adding ammonium hydroxide, where $FePO_4 \cdot xH_2O$ precipitates will form. Applying a positive potential on $LiFePO_4$ can also extract valuable Li from it, and the deintercalated product $FePO_4$ will be obtained. For instance, Liu et al. used a $Li_{1-x}FePO_4$ electrode coated with TiO_2 to extract lithium ion from sea water [88]. Such electrochemical delithiation method is successfully demonstrated on leaching spent LFP cathode [89], achieving >96.74% of Li extracted in a current efficiency up to 85.81%. Notably, new methods treating $LiFePO_4$ directly with an oxidant are also feasible. Zhang et al. reported lithium recycling of $LiFePO_4$ by sodium persulfate oxidizer (as eq 4), with only 0.05 theoretical times excess of which 99.9% of lithium can be leached out in 20 mins at ambient temperature and a high S/L ratio of 300 g/L [76]. This value was achieved by dealing spent cathodes on Al foil, and leaching rates for Al, Fe, P are only 0.584%, 0.048%, and 0.387%, respectively. Gangaja et al. also used persulfate to achieve a full delithiation of $LiFePO_4$, forming $FePO_4$, which later reacts with LiI/NaI to (re)-fabricate LFP/$NaFePO_4$ [90].

$$2LiFePO_4 + 2H^+ + H_2O_2 \rightarrow 2Li^+ + 2H_2O + 2Fe^{3+} + 2PO_4^{3-} \quad (3)$$

$$LiFePO_4 + 0.5\,Na_2S_2O_8 \rightarrow FePO_4 + 0.5Li_2SO_4 + 0.5Na_2SO_4 \quad (4)$$

Similarly, $[FeCN_6]^{3-}$ can work as a redox mediator that can be instantaneously electrochemically regenerated in an oxygen flow cell to harvest Li^+ from $LiFePO_4$ in extraction efficiency of 99.8% in 50 min under ambient pressure and room temperature (RT), producing high purity LiOH (99.90 %) and $FePO_4$ (99.97 %) [91].

Leaching kinetics models

The leaching of metals from spent materials is a combination of mass transfer, diffusion and convection, and chemical reactions happen at the solid-liquid interfaces. Various kinetics models, including shrinking core, logarithmic rate law, and Avrami equation, are used to describe the leaching behaviors. Assuming solid particles are being consumed either by dissolution or reaction, shrinking core model includes situations that the leaching rate is controlled by liquid boundary layer mass transfer (eq 5), surface chemical reaction (eq 6), and residue layer diffusion (eq 7) [78, 92]. Most studies displayed data fits the shrinking core model well [8, 24, 78, 82, 92-93]. In some cases, the empirical logarithmic rate law (eq 8) controlled by the surface layer diffusion of the lixiviant or Avrami equation model (eq 9) describing the kinetics of phase transformation under the assumption of spatially random nucleation, opposite to leaching, better describes the leaching process [17, 22, 35, 94-96].

Shrinking core model

$$x = k \cdot t \quad (5)$$

$$1 - (1 - x)^{1/3} = k \cdot t \quad (6)$$

$$1 - 3(1 - x)^{2/3} + 2(1 - x) = k \cdot t \quad (7)$$

The logarithmic rate law model

$$(-ln(1 - x))^2 = k \cdot t \quad (8)$$

Avrami equation model

$$\ln[-ln(1 - x)] = lnk + n \cdot lnt \quad (9)$$

where the x is the leaching efficiency in time t, k is the reaction rate constant which can be calculated from the slope of fitting lines, n is a suitable parameter.

1.5.2. Separation

Impurities removal

After leaching, the hydrometallurgical method results in a mixture containing different types of ions/compounds, which needs the separation and purification process to get the final

products. Usually, impurities can be introduced from not only the manufacturing of pristine materials, i.e., doped elements and surface coating, but also the recycling processes, in which the pretreatment and leaching may bring some impurities, such as Al and Cu from the current collector, and Fe from mixed cathodes or casings. Those impurities, either in metallic or ionic forms, should be carefully controlled, especially for cathode regeneration purposes.

Zhang et al. studied the influence of Cu impurity in metallic or ionic forms on the NCM622 cathode materials [97]. The metallic Cu with content of 0.2, 1.0, or 5.0 at.% in NCM622 cathode all resulted in a sudden death situation, in which a Cu layer coated on Li metal anode with dendrites growth. Even this effect is negligible in the hydrometallurgical recycling, yet for direct recycling, the presence of metallic impurities should cause great concern. The ionic impurities, same with doping, can either improve or deteriorate the performance of regenerated cathodes. The NCM622 cathodes, prepared by Zhang et al., containing ionic Cu in contents of 0.2 and 1.0 at.% showed improved performances than the pure while the one containing 5.0 at.% ionic Cu impurity worsened, abiding by the general effect of ionic doping. Similarly, NCM622 cathode materials were demonstrated improved performance with 0.2 at.% Al ionic impurities and worse performance at 5 at.% [98]. Yet Kim et al. manifested different phenomena in NCM111 with only 0.05% of ionic Al impurity demonstrated close performance with that of the pure one, and higher impurity contents lead to deteriorated performance, indicating varied optimal contents for different foreign elements or cathode materials [99]. Iron is another element commonly occurred in the hydrometallurgical recycling process of cathodes, mainly from mixed $LiFePO_4$ and battery casings. Study revealed among three contents of Fe impurity, NCM111 cathode with 0.25% Fe showed relatively improved performance against the other two (0.05% and 1.0%) [100].

The above literatures studied the impurities effects on cathodes utilizing a simulation method that introduces one type of impurity into the common fabrication process of cathodes [97-101]. For the regeneration of $LiFePO_4$ though fewer studies focus on impurities, literatures studying $LiFePO_4$ doping effects[102-106] in different aims but equally work. Real cases for hydrometallurgical recycling can be more complicated when considering different type of impurities. Iron metallic powders have also been utilized to remove Cu^{2+} impurities in leachate [107]. This method eliminated one type of impurities, yet the amount is not changed. Impurities removal should start at the pretreatment step. For those spent cathode materials collected after crushing and screening,

impurities mainly present in the form of metallic particles, which can be removed by alkaline ($Al \rightarrow NaAlO_4$) or Fe^{3+} solution ($Cu/Fe \rightarrow M^{2+}$).

Impurity removal also matters for closed-loop regeneration of cathodes. Foreign elements for doping can be introduced the separation afterward, and separated elements shall be in high purity. Impurities such as Al^{3+}, Fe^{3+}, and Cu^{2+} can be removed by pH-controlling method. $Fe(OH)_3$ and $Al(OH)_3$ have quite small K_{sp} values leading to sparing solubility in aqueous solution, while Cu^{2+} may co-precipitate with Ni^{2+} and Co^{2+} owing to their close values in K_{sp} (Figure 4) [14, 108]. Meanwhile, although 100% of Al and Cu in the single metal system shall precipitate at pH = 7. However, about 50% of Co shall coprecipitate with Al and/or Cu hydroxides in the multi-metal system with the same initial concentrations (2×10^{-3} M) [109]. Coprecipitation is the precipitation of substances normally soluble under the conditions employed. There are three main mechanisms of coprecipitation: inclusion (critical metals occupied lattice sites of the precipitate), occlusion (physically trapped inside precipitate), and adsorption. Hydroxides coprecipitation of critical metals in impurities removal can be mitigated in a relatively lower concentration of impurities [46, 109-111]. For instance, in H_2O_2/H_2SO_4 leachate systems containing 13.54 g/L Ni^{2+}, 12.26 g/L Mn^{2+}, 12.32 g/L Co^{2+}, with/without 989.5 mg/L Cu^{2+}, Gratz et al. [46] tested the effect of Cu impurity removal on recovery efficiencies of Ni, Mn, Co. The synthetic system with Cu impurity possessed slightly lowered Ni, Co, Mn preservation rates that are 96, 99, 96%, respectively, at pH = 6.5 comparing with the system without Cu impurity (>99%). At even relatively lower concentrations of impurities (Al^{3+}: 830 mg/L, Cu^{2+}: 5.6 mg/L, Fe^{3+}:10.4 mg/L) in a leachate system containing Ni^{2+}: 18860 mg/L, Co^{2+}: 17740 mg/L, Mn^{2+}: 16700 mg/L, Li^{+}: 7020 mg/L, coprecipitation of

critical metals is nearly negligible at pH ~4.8 achieving ~100% impurities removal [111]. These results highlighted the importance of the pretreatment process.

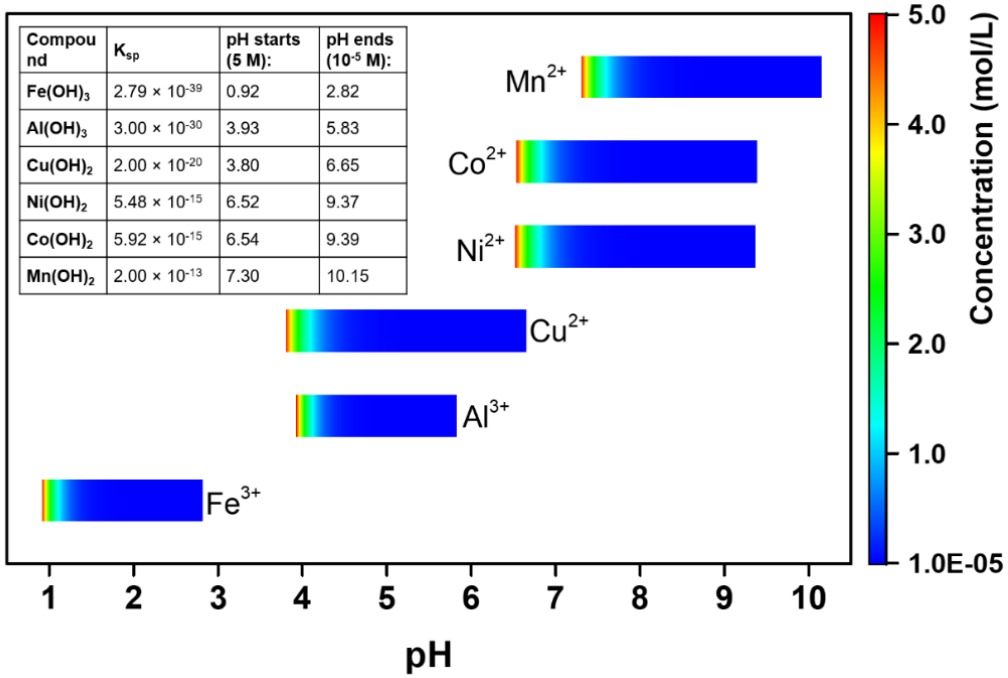

Figure 4 pH number of various metals start and end precipitation as hydroxides. Inset: The K_{sp} values [108, 112] of various metal hydroxides, and pH values when the precipitation starts and ends calculated from the definition of K_{sp} ($K_{sp} = [M][OH]^n$ for $M(OH)_n$). Note: the concentration range of metal ions is set between 10^{-5} - 5.0 M.

Chemical Precipitation

Precipitation is a chemical process transforming soluble substance into an insoluble solid, which typically requires the assistance of external precipitants such as hydroxides, carbonates, acetates, oxalates, etc. Relying on the sparing solubilities of various compounds formed on conditions employed, separation of them is thus realized. In the very beginning of hydrometallurgical recycling, it only involves separation of Co and Li, which can be easily achieved by adding precipitant such as $(NH_4)_2C_2O_4$ (Co^{2+}) and Na_2CO_3 (Li^+) [74]. However, market focuses of LIBs shifted to NCM and NCA cathodes, resulted in a more complicated leachate composition.

Selective precipitation though generates pure metal compounds but is hard to achieve through ordinary precipitation, and avoid co-precipitates. As a matter of fact, even without consideration of impurities, Ni^{2+} and Co^{2+} are very hard to be separated through hydroxides precipitation (pH control) as they have very close K_{sp} values (as shown in Figure 4). Hence, in some studies, Co, Ni, and Mn are co-precipitated to directly resynthesize ternary cathode materials, yet determining the composition is still inevitable [21, 79, 113].

Generally, selective precipitation of Ni^{2+} and Co^{2+} is achieved by different precipitants. Meshram et al. recovered Co^{2+} firstly as $CoC_2O_4 \cdot 2H_2O$ from the sulfates leachate (6.56 g/L Co, 1 g/L Li, 2 g/L Ni, 2 g/L Mn; pH 1.4) [35]. Under the optimal condition (1 M oxalic acid, equilibrium pH 1.5, temperature 323 K and time 2 h), 98.93% of Co can be extracted as cobalt oxalate with a purity of 95.91%, in which 3.81% Ni and 0.28% Mn serve as impurities. Then, Mn and Ni remaining in the raffinate are precipitated as their carbonates at pH 7.5, and 9.0, respectively. ~92% of Mn and ~89% of Ni are extracted in this step. Li_2CO_3 (~98% purity) is precipitated by the addition of Na_2CO_3 in the filtrate, which is condensed to increase the recovery rate.

Furthermore, Co^{2+} can be separated from mixture by an oxidative precipitation (eq 10) to form $Co_2O_3 \cdot 3H_2O$ [114-116]. As respectively shown in eq 11-13, selective separation of Ni^{2+} can be achieved by formation of 2:1 nickel dimethylglyoxime (Ni^{2+}:DMG) red solid complex with the DMG ($C_4H_8N_2O_2$) react with $[Ni(NH_3)_6]^{2-}$ in basic conditions, while Mn^{2+} can be extracted from solution oxidized by $KMnO_4$ or O_3 to form MnO_2 [116-117].

$$2Co^{2+} + ClO^- + 5H_2O \rightarrow Co_2O_3 \cdot 3H_2O + Cl^- + 4H^+ \quad (10)$$

$$2Ni^{2+} + 2OH^- + 2C_4H_8N_2O_2 \rightarrow Ni \cdot (C_4H_8N_2O_2)_2\ (s) + 2H_2O \quad (11)$$

$$Ni \cdot (C_4H_8N_2O_2)_2\ (s) + 2HCl \rightarrow NiCl_2 + 2C_4H_8N_2O_2 \quad \text{metal stripping} \quad (12)$$

$$3Mn^{2+} + 2MnO_4^- + 2H_2O \rightarrow 5MnO_2\ (s) + 4H^+ \quad (13)$$

In such scheme, Wang et al. revealed a stepwise extraction of Mn, Ni, Co, and Li from a HCl leachate system [116]. Mn^{2+} was selectively extracted as MnO_2 and manganese hydroxides by reaction with $KMnO_4$. A Mn powder of 98.23% purity was thus obtained under the optimal condition (Mn^{2+}:$KMnO_4$ = 2, 40 °C, pH = 2). The optimal separation of Ni from the raffinate was achieved by DMG with a molar ratio of 2 as the pH value to be 9, and Co thus could be extracted

via a simple chemical precipitation as $Co(OH)_2$ at pH = 11. Li was recovered as Li_2CO_3, in purity of 96.97%, while Ni and Co were 96.94, 98.23%, respectively.

Solvent extraction

Solvent extraction is another common method to separate metals, typically working by their different solubilities in two different immiscible solvents, usually aqueous (leachate) and organic (solvent extractants) phases. The abilities of extractants, especially the selectivity over various metals, determine the efficiency of extraction. Popular solvent extractants such as 2-ethylhexyl hydrogen-2-ethylhexylphosphonate (PC-88A)[54, 109-110, 118], di(2-ethylhexyl)phosphoric acid (D2EHPA)[54, 118-119], bis(2,4,4-triethylpentyl)phosphinic acid (Cyanex 727), di-(2-ethylhexyl) phosphinic acid (P277) are employed to the extraction of metals. Typically, the separation ability of cobalt and nickel increases in the order phosphinic > phosphonic > phosphoric acid due to the increasing stabilization of tetrahedral coordination cobalt compounds with the extractant in the organic phase, because tetrahedral compounds are more lipophilic than octahedral compounds [54]. For a liquid-liquid solvent extraction process, the extractant agents are diluted in an organic nonpolar diluent, immiscible with water, with a phase modifier that aids their miscibility. The extractants work by a mechanism of forming coordination complexes with metal ions. After the solvent extraction, metal ions are concentrated in the organic phase, and usually are stripped out with strong acids and then physically collected by forming precipitates, while the extractants are recycled. It is important to maintain a high selectivity over one metal for an extractant, and usually control pH of the solution as well as saponification of extractants are necessary to achieve this.

Based on a cation exchange mechanism, extractants in acid form, HA, are usually saponified to their sodium salts, NaA, by alkaline as eq 14 [14].

$$Na^+_{aq.} + 1/2\,(HA)_{2\,(org.)} \rightarrow NaA_{org.} + H^+_{aq.} \quad (14)$$

During the extraction, metals (M^{2+} and Li^+) will form complexes with saponified extractants in routes shown in eq 15 and eq 16, respectively [120-123].

$$M^+_{aq.} + A^-_{aq.} + 2(HA)_{2\,(org.)} \rightleftharpoons MA_2 \cdot 3HA_{org.} + H^+_{aq.} \quad (15)$$

$$Li^+_{aq.} + A^-_{aq.} + (HA)_{2\,(org.)} \rightleftharpoons LiA \cdots 2HA_{org.} \quad (16)$$

The equilibrium constant of eq 15, M^{2+} extraction, can be written as:

$$K = \frac{[\mathrm{M}A_2 \cdot 3HA]_{org.}\,[H^+]_{aq.}}{[M^{2+}]_{aq.}\,[A^-]_{org.}\,[(HA)_2]^2_{org.}} \quad (17)$$

$$K = \frac{D_{M^{2+}} \cdot [H^+]_{aq.}}{[A^-]_{org.} \cdot [(HA)_2]^2_{org.}} \text{ with } D_{M^{2+}} = \frac{[\mathrm{M}A_2 \cdot 3HA]_{org.}}{[M^{2+}]_{aq.}} \quad (18)$$

(Distribution coefficient, *D*: metal ratio between that in organic phase against aqueous phase, i.e., extraction efficiency). Taking logarithms of both sides, eq 18 can be re-arranged into eq 19 with the relation pH = -log $[H^+]$:

$$logD_{M^{2+}} = log\ K + pH + log[A^-]_{org.} + 2log[(HA)_2]_{org.} \quad (19)$$

Similarly, the relationship between extraction efficiency of Li^+ and various parameters can be written as:

$$logD_{Li^+} = log\ K + log[A^-]_{org.} + log[(HA)_2]_{org.} \quad (20)$$

The relationship between extraction efficiency of M^{2+}/Li^+, pH, degree of saponification, and the concentration of extractants are modeled in eq 19 and 20, respectively. Typically, the M^{2+} extraction efficiency of one extractant increases with increasing concentration, and pH value, yet the pH has no effect on the extraction efficiency of Li^+ as indicated in eq 20 [121]. Furthermore, other parameters like organic/aqueous (O:A) ratio, temperature, time, and chemical structure of extractants play key roles in determining extraction efficiency. For instance, D2EHPA was reported by Yang et al. in co-extraction of Ni-Mn-Co with great Li loss from a H_2SO_4/H_2O_2 leachate [34]. Prior to solvent extraction of critical elements, impurities were removed by using 4 M NaOH at pH = 4.8 firstly, and followed with a deep solvent extraction with 10% D2EHPA in sulfonated kerosene, O:A ratio of 1:2, pH = 2, and extraction time of 1.5 min. Under the optimal conditions: a three-stage solvent extraction with 40% D2EHPA (60% saponified) in diluent sulfonated kerosene, pH at 3.5, O:A ratio of 3:1, almost 100% Mn, 99% Co and 85% Ni can be co-extracted under a sacrifice that nearly 30.0% of Li lost into the organic phase.

After the solvent extraction, acid stripping and co-precipitation after adjusting metals ratio are necessary for the regeneration of cathode materials. For ternary cathode materials, co-extraction with equivalent contents of critical elements gets rid of the final ratio adjustment of Ni, Mn, Co ions, and is thus of great promise. Liu et al. demonstrated an equivalent co-extraction of Ni (2053.5 ppm), Co (2054 ppm) and Mn (2027 ppm) by a 0.8 M P227 in n-heptane, under conditions of O:A of 1:1, 20 min mixing, 298 K and pH at 2.5 from a leaching liquor of NMC622 leached by 3 M HCl [83]. Subsequently, lithium and remaining Ni need to be separated in another step.

Selective solvent extraction requires extractants with high selectivity against specific metal ions, and also multi-steps in general. Wang et al. [54] reported a stepwise separation of cobalt from a H_2SO_4-H_2O_2 leaching system containing Co^{2+}, Ni^{2+}, Mn^{2+}, Cu^{2+}. The solvent extraction processes were finished in the following stages: (i) Ni and Mn extraction for 15 min and in O:A ratio of 1:1, with an organic phase mixing the diluent, which is composed of 30 vol.% D2EHPA (saponified by 20 mol.% of 10 M NaOH solution) and 70 vol.% sulfated kerosene, with 5 vol.% tri-n-butylphosphate (phase modifier), repeated twice under controlled pH of the aqueous solution at 2.70 and 2.60, respectively; and (ii) 80.13% of $Co^{2+}_{org.}$ was separated from $Ni^{2+}_{aq.}$ with 30 mol% saponified PC-88A dispersed in the same condition with the pH at 4.25; (iii) chemical depositing of Co^{2+} was finished with 0.5 M oxalic acid, finally resulting in CoC_2O_4 with a purity of 99.50%. Suzuki et al.[109] demonstrated a solvent extraction circuits that can effectively separate Al, Co, Cu, and Li from a synthetic sulfate system containing 2 M of these critical metals: (i) copper extraction with 5-nonyl-2-hydroxy-benzaldoxime (Acorga M5640) within the pH range of 1.5–2.0, (ii) aluminum extraction with PC-88A within the pH range of 2.5–3.0, and (iii) cobalt extraction in an efficiency of 90% and an 1170 separation factor against Li with PC-88A (10 vol.%)/tri-n-octylamine (TOA, 5 vol.%) within the pH range of pH 5.5–6.0. Additionally, high metal stripping efficiencies (Cu: 98.7%, Al: 100%, Co: 98.9%) from the organic phases were obtained using a 3.0 mol/L H_2SO_4 solution.

Mn and Co can be stepwise extracted from a NMC111 leachate (after de-aluminum) in 4N H_2SO_4/H_2O_2 system using extractants P-204 and P-507 (both 60% saponified by NaOH), respectively, in conditions of 20 vol.% in the organic diluent, O:A ratio of 1 and shaken for 30 min, where Mn extraction is finished in three-stage and solvent extraction of Ni is complexation-

assisted by a complexation agent, ammonium thiolate, to achieve a larger separation factor (D_{Co}/D_{Ni} = 372) between Ni and Co than that (D_{Co}/D_{Ni} = 72) of conventional [124]. For one-stage solvent extraction, complexation-assisted one achieved superiority both in extraction efficiency and purity (stripped out by 1N H_2SO_4) than those of conventional (85 % in 98% versus 70% in 70%), comparable with 6-stages (95% in purity of 94%).

ILs can also work as extractants. Viet Nhan Hoa Nguyen and Man Seung Lee developed an extraction process that efficiently separated various metals in high purity from a synthetic 2 M H_2SO_4 solution containing Co(II), Ni(II), Mn(II), and Li(I) in concentrations of 2590.0, 2610.0, 1400.0, and 800.0 mg/L, respectively [125]. The separation process was finished in multi-stages: (i) 0.3 mol L^{-1} ALi-SCN (IL, synthesized from equal moles of N-methyl-N,N,N-trioctylammonium chloride, Aliquat 336, with NH_4SCN) with kerosene as diluent was employed to preferentially extract Co^{2+} at O:A = 1, achieving a 92.0% recovery efficiency with equal volume of 5% NH_3 solution as stripping agent; (ii) Cyanex 301 (bis(2,4,4-trimethylpentyl)dithiophosphinic acid) and Alamine 336 (tri-octyl/decylamine) was used to extract Ni^{2+} at pH = 2, leading to a 99.9% extraction efficiency, after which equal volume of 75% aqua regia was utilized for Ni^{2+} stripping, leading to a 99.9% recovery of Ni in the purity of 98.2%; (iii) then, 99.9% of Mn can be recovered at pH = 2 by an ionic liquid, Ali-CY (obtained from the reaction of equimolar concentration of Aliquat 336 with Cyanex 272 in kerosene, which latter was added with 0.5 M $HaHCO_3$), then Mn^{2+} stripping (efficiency: >99.9%) was finished with 1 M HCl solution. (iv) 99.9% of Li^+ left in raffinate can be recovered.

Schaeffer et al. [117] reported an aqueous separation of Co(II), Mn(II) from a concentrated Ni(II) solution. Mn(II) was selectively precipitated by oxidation in the form of MnO_2 using O_3, and Co(II) was separated from Ni(II) through a thermo- and acid-responsive aqueous biphasic system (ABS) based on an IL, tributyltetradecylphosphonium chloride ($[P_{44414}]Cl$), with a $\alpha_{Co/Ni}$ of 484. Ni(II) was collected as $NiCO_3$ precipitate with Na_2CO_3 addition, and subsequently IL was recovered with Na_2CO_3 as precipitant, allowing a closed-loop process.

1.6. Direct recycling

1.6.1. Degradation mechanism in $LiMO_2$ cathodes

Spent cells or end-of-life (EOL) cells are defined as batteries only possessing 80% of its initial capacity or with an internal resistance increased 30%. There are many factors considered working in the failure/degradation of the whole system, including dendrite formation, active Li^+ consumption, electrolyte consumption, electrode materials failure, etc. As the nature of active materials determines the performance of cells, interfacial stability is the key factor deciding the cycling performance [126]. Performance degradation of LIBs mainly includes two parts (as shown in Figure 5a): the irreversible capacity loss (active materials fade) and voltage loss (internal resistance increased, *iR*). Hence, for the cathode materials separated from a spent cell, they still retained the majority of the initial capacity, pyro- and hydro-metallurgy methods atomically destroyed bonds within them and regenerated them (re-crystallization) with high-temperature treatment not only wasted a great amount of energy but also increased complexity of batteries recycling. Direct recycling using mild conditions to heal/repair the structure of cathode materials is thereby more economical and environmentally benign than pyro- and hydrometallurgy methods.

Direct recycling is regarded as the most efficient method in cathode recycling as it keeps the core structure of cathode materials and eliminates stored energy lost, and most importantly, it gets rid of the complex chemical processes commonly exist in the smelting part in pyro-, and leaching and separation parts in the hydrometallurgical recycling process. Generally, active cathode materials of discharged spent LIBs are separated and concentrated via pretreatment methods introduced in Section 3 in order to maximize efficiency. In addition, the main aim of direct recycling is to heal the defects evolved during the operation of LIBs, which account of the most responsibility of cathodes capacity degrading. Understanding the degrading mechanism of cathode materials not only helps to improve them, but also determines the way how they should be treated in direct recycling. As layered transition metal oxides $LiMO_2$ have been greatly chosen as cathode materials for commercial LIBs, spinel-structured LiM_2O_4 and phospho-olivine based (e.g., $LiFePO_4$) materials are also attracting increasing attention.

$LiCoO_2$ is well-known for its high theoretical specific capacity of 274 mAh/g in an α-$NaFeO_2$ structure with Li^+ and $Co^{3+}O_2^-$ layers ordered in alternating (111) planes, but it also suffers

from the high cost of cobalt and intrinsic instability under elevated temperature in a delithiated state. $LiCoO_2$ is thermodynamically metastable [127], and such phenomenon is even worse in a Li^+ deficient state, and the layered structure will transfer into the spinel phase (LiM_2O_4), in which transition metal ions migrated into Li layer, blocking Li^+ diffusion and leading to increased independence. In practice, $LiCoO_2$ is avoided to be overcharged, keeping x in Li_xCoO_2 from getting too small in the charging processes. The charging voltage of $LiCoO_2$ is restricted to 4.2 V to avoid irreversible phase transformation, leading to only half of the theoretical capacity in practice. Besides, high temperature is another factor inducing the degradation of cathode material. As a matter of fact, pristine layered $LiCoO_2$ materials is quite stable under high temperature, e.g., 900 °C, yet charged particles with partial lithium extracted start to release oxygen above 250 °C [128].

$LiNiO_2$ is another promising cathode candidate, as a substitute to LCO, yet generally suffers for terrible cyclability. Comparing with LCO, LNO is more cost-effective, less toxic, and with higher reversible capacity. However, due to the unpaired e_{2g} electron and Jahn-Teller distortion, $LiNiO_2$ is much more thermodynamically unstable than $LiCoO_2$, implying oxygen releases easier. The presence of Ni^{2+} (0.069 nm) with similar ion radius to Li^+ (0.076 nm) lowers the activation energy for misordering, leading to increased difficulty in preparing stoichiometric $LiNiO_2$. Doping is one effective method to improve the cyclability and simplicity-in-preparing, such as $LiNi_{1-x-y}Mn_xCo_yO_2$ and $LiNi_{1-x-y}Co_xAl_yO_2$ were developed and commercialized. Generally, Ni contributes to a higher capacity with sacrificed safety and ease-in-processing, and Co guarantees the rate performance, while Mn and Al showing no activity for redox reaction mainly work to stabilize the structure. With an increasing amount of Ni, the onset temperature for both phase transitions and oxygen release shall decrease, e.g., 245 °C for NCM433 comparing with 130 °C for NCM811 [129], as shown in Figure 5e. During deintercalation of Li from Ni-rich layered NMC or NCA covalence of Ni-O will increase, where higher M-O covalence leads to electrons delocalization, decrease in M-O bond length, and concomitant oxygen release with valence state decreasing. Generally, it is believed that the instability of Ni-rich cathode exponentially aggravated with Ni-content increased [130]. Such phenomena can be blamed to the problematic Ni^{4+} in NCM or NCA cathodes, where the amount of high-valence Ni ions (i.e., Ni^{3+}, Ni^{4+}) increases being increasingly rich in Ni. Ni^{4+} is known to be unstable and shall be reduced to its most stable state Ni^{2+}. Besides, Ni^{4+}-e_g is a very low lying LUMO that can easily accept electrons from the

electrolyte, leading to side-reactions. It is experimentally demonstrated that $LiNiO_2$ displays better cyclability than NMC811 under the same degree of delithiation, while even the latter possesses better lattice stability, indicating the significance of interfacial stability [126].

For layered $LiMO_2$ cathode materials, the extraction of lithium ions plays one important role in the phase transition, which also closely determines their degradation behaviors. With the extraction of lithium ions from transition-metal-oxides, phase transition as a function of lithium content is undesirable as it follows with irreversibilities and large volume change inducing cracks. As shown in Figure 5b, with a cutoff potential limited at 4.2 V, transition metal oxides will experience a reversible phase transition from the original hexagonal phase (H1), to the second (H2) and third (H3) hexagonal phases upon Li deintercalation [131-133]. The phase transitions are accompanied by anisotropic lattice changes, leading to a large volume change and further inducing both interparticle and intraparticle microcracks [131, 134-135]. For instance, the *c* lattice parameter gradually increases at the initial charging process due to the increased electrostatic repulsion between the negatively charged oxygen planes, resulted from the loss of compensation effect from Li^+ ions (O^{2-}-Li^+-O^{2-}), and then the lattice shrinks with more than 0.5 Li^+ ions extracted as the repulsion effect is weakened due to increased valence of O^{2-} with donated electrons from partial Li ions and the pillaring effect of lithium ions decreases at low Li concentrations [134-136]. Such property shall induce great intraparticle stress with inhomogeneous delithiation states within particles: from surface to interior, leading to particle fracture [137]. Kikkawa et al. [138] found the microcracks formed in 60% charged primary LCO particles extended in the direction perpendicular to stacking layers via selected area electron diffraction (SAED), which is correlated with the abrupt lattice change along *c*-direction. Introduction of a protective layer, e.g., Li_2BO_3 [139], Al_2O_3, is effective to mitigate lattice expansion during phase transition from H2 – H3, thus improving cyclability. Furthermore, such change in lattice parameters also results in great interparticle stress between particles aggregated with different orientations, which may give rise to spallation (intergranular cracks along grain boundaries), leading to reduced conductivity and capacity.

The phase transition behaviors of transition metal oxides at high delithiated states were also studied. The change from the O3 (H3) phase to H1-3 phase (~ 4.55 V) and then to O1 phase (single layered MO_2, ~ 4.63 V) was reported in Li_xCoO_2 with upper cutoff voltage greater than 4.7

V, leading to a layered cubic close packing (ABCABC) to the hexagonal closed packing (ABAB) in O1, where nearly all lithium ions extracted [140-141]. Generally, the upper working potential for commercial LIBs is limited at 4.2 V, in order to achieve an admirable cyclability (>500 cycles). Oxygen evolution and irreversible phase transformation occur as charging potential increased above 4.2 V for $LiCoO_2$ due to the overlapping between t_{2g} band of Co^{3+}:$t_{2g}^6e_g^0$ and the top of O-2p band, leading to a constancy of cobalt oxidation state for lithium content less than 0.5 where the extraction of lithium ions is compensated by oxidation of O^{2-} ions by removal of electrons from O-2p band [142-144]. Similarly, the extraction of electrons is accompanied with electrons removal from e_g band of Ni (Ni^{3+}:$t_{2g}^6e_g^1$) in LiNiO2 system, while e_g band of $Ni^{3+/4+}$ lies above O^{2-} 2p band, allowing a higher reversible capacity [143]. H1-3 phase is a hybrid phase of O3 and O1 phases, in which the CoO_2 layers in O1 phase are separated by weak Van der Waals force leading to a lower stability than that of O3 stacking [145]. Face sharing octahedra in the O1 phase offers a path for cation mixing, where H1-3 is thought as the key intermediate for phase transitions to the spinel phase [146]. Typically, cycling between 3.0-4.5 V, layered cathode materials suffer from an irreversible phase transition enriched on the surface with the main composition of spinel phase and a trace of rock salt formation [147]. These degraded phases increase the resistance of Li^+ transfer, and result in capacity fading.

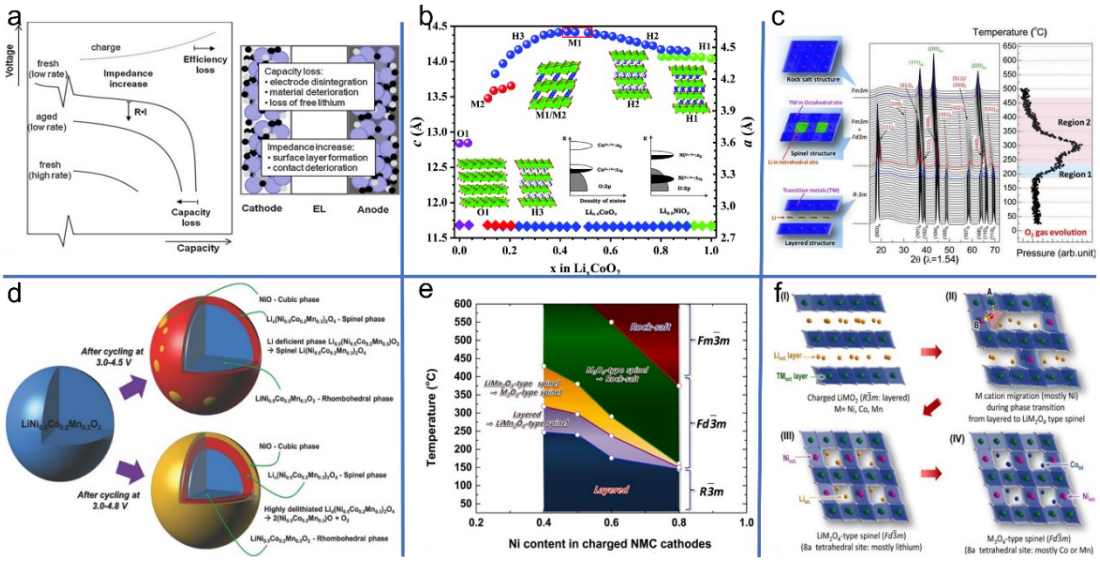

Figure 5 (a) Degradation mechanism of LIBs as shown in the discharging curve (left) and two main factors(right). Reprinted from ref. 127, copyright 2015 Elsevier. (b) The variations in *c*, and *a* lattice parameters, and corresponding phase transitions during Li^+ deintercalation. Adapted from ref. 148, copyright 2018 Royal Society of Chemistry. Inset: comparison between energy diagrams of $Li_{0.5}CoO_2$ and $Li_{0.5}NiO_2$. Reprinted from ref. 143 with permission, copyright 2001 Elsevier. **(c)** Time-resolved (TR) XRD patterns (middle) and trace oxygen gas release results (right) from simultaneously measured mass spectroscopy (MS) from the overcharged $Li_{0.33}Ni_{0.8}Co_{0.15}Al_{0.05}O_2$ during heating up to 500 °C. Reprinted from ref. 149, copyright 2013 Wiley. (d) The degraded structure of NCM523 cycled under different voltage windows. Reprinted with permission from ref. 147, copyright 2014 Wiley. (e) The effect of Ni content on the temperature inducing irreversible phase transformations. (f) Schematic illustration of one transition metal migration route inducing irreversible phase transformations. e-f: reprinted from ref. 129 with permission, copyright 2014 American Chemical Society.

Migration of transition metal ions from their octahedral sites into the Li octahedral sites of the alternate layers is thought as the initial step of structural degradation of layered cathode materials. In layered oxides cathodes ($R\bar{3}m$) subjected to extensive (dis)charge cycling, such migration, sometimes known as cation mixing, triggers a phase transformation into $LiMn_2O_4$-type spinel ($Fd\bar{3}m$) structure [129, 146, 150], promoted by a high extent of delithiation state (increased

content of Li vacancies) [151] and/or elevated temperature [152-153]. For migration of transition metal from the octahedral sites $O_{h,\,M}$ in their layer to the octahedral sites in adjacent Li layer $O_{h,\,Li}$, there are two pathways: one travels straight through the edge shared by neighboring octahedra, i.e., $O_{h,\,M} \rightarrow O_{h,\,Li}$, known as the most direct path, while another travels through a nearest tetrahedral site via the face-shared neighboring octahedra, i.e., $O_{h,\,M} \rightarrow T_d$ (tetrahedral sites)$\rightarrow O_{h,\,Li}$, known as more energetically favorable owing to lower energy barrier (Figure 5f) [142, 154-155]. Upon continued migration, a spinel M_3O_4 phase formed with an increased partial transition metal occupancy at the 8a tetrahedral sites, yet Ni is unstable at the tetrahedral sites giving rise to a MO rock-salt ($Fm\bar{3}m$) structure.

Therefore, a two-step irreversible phase transformation (eq 21 and 22) of layered oxides is proposed as following:

$$Li_xMO_2\ (\text{layered}) \rightarrow LiMO_2\ (\text{layered}) + Li_aM_{3-a}O_4\ (\text{spinel}) + \alpha O_2 \qquad (21)$$

$$\rightarrow LiMO_2\ (\text{layered}) + Li_bM_{3-b}O_4\ (\text{spinel}) + Li_cM_{1-c}O\ (\text{rock salt}) + \beta O_2 \qquad (22)$$

Higher degree of Li^+ extraction (higher cutoff potential) promotes the irreversible phase transformation, with oxygen evolution, leading to severer capacity fading. Upon completely delithiated state, O1 phase of $LiNiO_2$ was directly observed by Wang et al. to preferentially transform into rock-salt phase with oxygen loss [156]. Subjected to long cycling, $LiMO_2$ cathode materials in many works were reported with impurity phases emerged and oxygen evolution as shown in Figure 5c. Extensive release of oxygen leads to severe resistance increase, capacity fading, and challenges the safety of batteries by triggering thermal run-away. The high extent of delithiation promotes the glide of partial dislocations, and provides a pathway for transition metal migration to lithium octahedral sites leading to a mis-ordering of transition metal ions in lithium layers, serving as the main reason for increased resistance of lithium diffusion, and formation of spinel phase [146, 155]. Surface of layered $LiMO_2$ particles tends to degrade first due to the inhomogeneous Li distribution under the charged state. Kikkawa et al. conducted quantitative Li mapping and EELS analysis for Co and O, and they found a gradually increased Li/Co ratio from the surface to the interior of partially-lithiated $LiCoO_2$ particles [138]. At and around the surface of 60% Li^+ extracted particles, their characterization results illustrated a chemical structure of Co_3O_4, and Li-inserted Co_3O_4 spinel phases lie outer on Li_xCoO_2 ($x \geq 0.05$, layered $R\bar{3}m$) with CoO rock-

salt phase at the topmost. As shown in Figure 5d, the degradation process for layered $LiMO_2$ cathode materials (M includes Ni) can be described as following equation [147]:

$$LiMO_2(\text{layered}) \rightarrow Li_{1-x}MO_2(\text{layered}) + xLi^+ \quad (23)$$

$\rightarrow$ Stage I: $Li_{1-x}MO_2$(layered core)-[LiM_2O_4 (spinel surface)+MO(trace cubic surface)]

$\rightarrow$ Stage II: $Li_{1-x}MO_2$(layered core)-LiM_2O_4 (spinel sublayer)-MO(cubic surface)

where the spinel phase LiM_2O_4 shall decompose into layered $LiMO_2$, cubic MO/spinel M_3O_4 and oxygen via simple heat treatment [127, 157].

1.6.2. Direct recycling methods

Direct recycling, also known as a nondestructive crystal repair technology, is a process that recovers the electrochemical activity of spent cathodes under mild condition. Given that the destructive methods (pyro- and hydrometallurgy) that extract elements with high-temperature calcination or reductive leaching also need to regenerate cathodes through common synthesis procedures, direct recycling maintains most of the crystal structure reduces the recycling cost and maximizes the efficiency, achieving a closed-loop utilization on the cathodes. In order to do so, recovering the lithium content back to normal stoichiometry and repairing degraded structure are the two main prerequisites for direct recycling to perfectly regenerate cathode materials. In general, direct recycling contains two parts: relithiation and structure re-ordering, where commonly studied methods include solid-state sintering directly with lithium salts, and combined hydrothermal with short annealing. In addition to the self-saturation relithiation derived by solid-state sintering and hydrothermal treatment, relithiation can also be achieved by electrochemical process [158], redox mediator [90, 159], eutectic molten salts [26, 44, 160] and ionic liquids (ionothermal) [161], and structure re-ordering is generally finished by high temperature while some reductive methods, such as fed with reducing agent as well as extra electrons injection, can also promote the structure reordering of LFP cathode.

Solid-state sintering

Solid-state sintering with lithium salts is one common method for relithiation of degraded cathode materials. In a typical regeneration process using solid-state sintering, the lithium content

in the degraded cathode materials should be quantified in order to lower the waste of lithium and to increase the purity of the final product. In general, composition determination is performed by inductively coupled plasma mass spectrometry (ICP−MS), but involves tedious procedures and error-prone preparation. Chunmei Ban Group developed a facile thermalgravimetric analysis (TGA) method to achieve a fast determination of lithium content by a linear relationship between lithium loss (%) and mass loss determined by TGA [162]. After that, stoichiometric amount of lithium salts (LiOH/Li_2CO_3, etc.) is quantitively mixed with the degraded cathode, and hereafter both go through a solid-state treatment. It has been demonstrated by Chen et al. that the amount of degraded phase, Co_3O_4, decreased dramatically according to XRD, XPS, and Raman characterizations after solid-state sintering with Li_2CO_3, in which the amount of Co^{3+} increased from 83% in spent to >95% in the recycled $LiCoO_2$ [163]. Such strategy has been verified to be feasible on the regeneration of $LiCoO_2$ [29, 163], NCM523 [164], $LiFePO_4$ [27-28] but also it can be finished in the current LIBs industry without further requirements and hence is easy for scale-up. For solid-state sintering of degraded cathode materials with enough lithium salts, the following reactions (eq 24-25) occur as a healing process transforming degraded phases back to layered oxides [29, 163]:

$$Co_3O_4 + Li_2CO_3 + \frac{1}{2}O_2 \rightarrow CO_2 + LiCoO_2 \quad (24)$$

$$MO_x + Li_2CO_3 + \frac{1}{2}O_2 \rightarrow CO_2 + LiMO_2 \ (M = Ni, Co, Mn) \quad (25)$$

As a matter of fact, during the initial stage of high-temperature treatment, the partially delithiated $Li_{1-x}CoO_2$ region is thermodynamically unstable (eq 26), and shall start release oxygen and phase transformation by the following reaction at around 220 ℃.

$$Li_{1-x}CoO_2 \rightarrow \frac{x}{3}Co_3O_4 + (1-x)LiCoO_2 + \frac{x}{3}O_2 \quad (26)$$

Combined hydrothermal treatment with short annealing

Solid-state direct recycling typically requires harsh conditions such as long time high-temperature treatment [23, 27-28, 163-164]; hence it is desirable to develop direct recycling methods consuming less energy. Hydrothermal methods have been demonstrated effective in recovering the lithium content of spent cathode materials. Typically, spent cathode material is immersed in Li^+ enriched solution and sealed in an autoclave, which is generally heated to a temperature below

250 ℃. After the hydrothermal treating, the lithium content of spent cathode materials shall reach an admirable level. With a 4 M LiOH solution as Li^+ ions fed source, Shi et al. demonstrated that the Li/M ratio could reach >0.95 for various cathode materials including LCO, NCM111, and NCM523 after being hydrothermally treated in 180 ℃ for 24 h while higher temperature shortened the time required (>0.98 at 220 ℃ for 4 h) [165]. Yet spent cathode materials experienced only the hydrothermal treatment showed poorer cycling stability than the pristine due to the limited effectiveness of hydrothermal treatment against recovering phases of cation mixing [29]. This is because the lower temperature of hydrothermal methods offers insufficient energy for phase transformation from spinel back to layered structure, and relithiation is a self-saturation process [26, 165] and the focus of direct recycling also include how to heal those irreversible degradations. Typically, well-ordered layered cathode materials are synthesized under high temperature above 600 ℃, and $LiCoO_2$ processed under 400 ℃ shows a disordered structure differing with the conventional hexagonal layered structure [142, 166-168]. Thereby, a short annealing to high temperature after hydrothermal treatment is necessary to increase crystallinity of recycled materials. In case of lithium evaporation under high temperature, excess lithium salts (~ 5 mol.%) are typically employed for compensation. For a typical hydrothermal treatment followed by a short annealing, following reactions (eq 27-28) occur:

$$Li_{1-x}CoO_2 + xLiOH \rightarrow \frac{x}{2}H_2O + LiCoO_2 + \frac{x}{4}O_2 \ \ Hydrothermal \quad (27)$$

$$Co_3O_4 + Li_2CO_3 + \frac{1}{4}O_2 \rightarrow CO_2 + LiCoO_2 \ \ Annealing \quad (28)$$

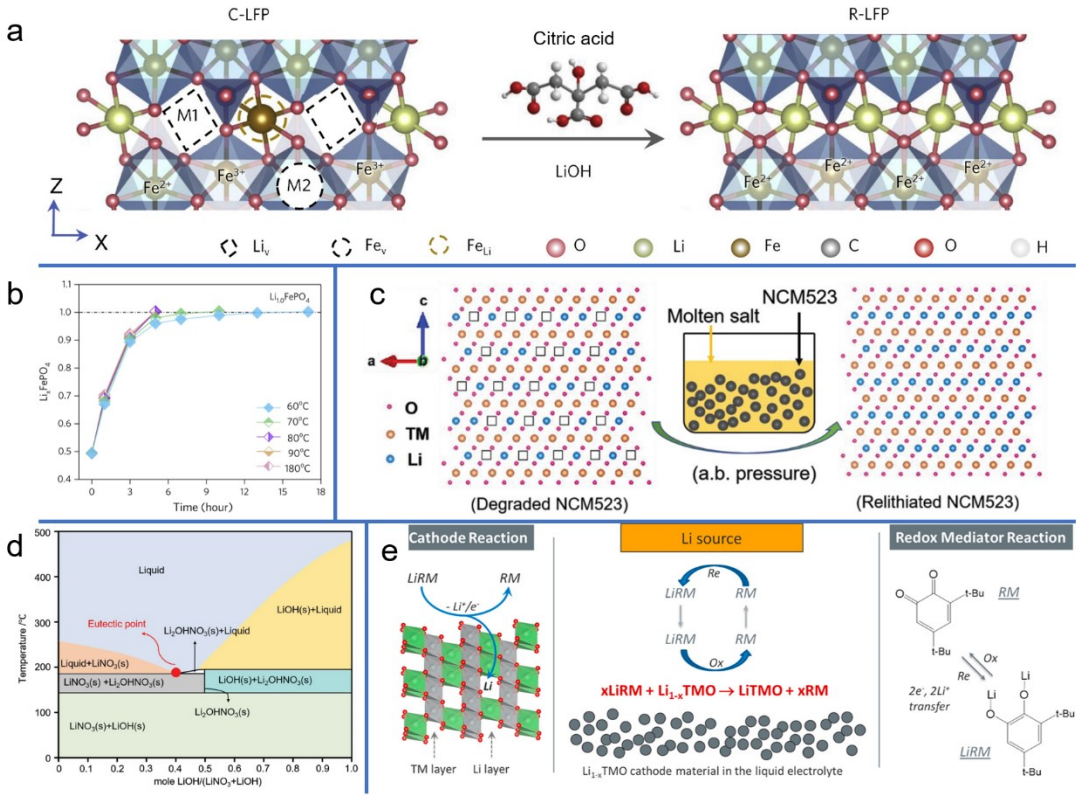

Figure 6 (a) Schematic illustration of hydrothermal relithiation method, where Fe^{3+} cations disordered in Li sites are reduced by with presence of citric acid in LiOH solution. (b) The evolution of LFP composition during relithiation at different temperatures. a-b: reprinted with permission from ref. 169, copyright 2020 Elsevier. (c) Illustration for recovering Li composition of degraded cathodes by eutectic molten salts relithiation approach. (d) Phase diagram of $LiNO_3$:LiOH system. c-d: reprinted with permission from ref. 26, copyright 2019 Wiley. (e) Reaction scheme for relithiation of the EOL cathode materials via redox mediation: Li-deficient transition-metal oxide ($Li_{1-x}MO_2$) is relithiated via shuttling of quinone molecules, the redox mediator (RM). Left: relithiation process; Middle: whole process; Left: regeneration of LiRM from the reaction of 3,5-di-tert-butyl-o-benzoquinone (DTBQ), the RM, with metallic Li. Reprinted with permission from ref. 159, copyright 2021 American Chemical Society.

Shi et al. used a hydrothermal treatment (220 ℃ for 4 h in 4 M LiOH solution) followed a short annealing (850 ℃ for 4 h) to direct recycle NCM111 and NCM523 [165]. It was found hydrothermal combined short annealing method generated less cation mixing (higher I_{003}/I_{104} ratio) than solid sintering method (850 ℃ for 12 h). They also demonstrated that higher nickel content

leads to larger cation mixing, higher Ni^{2+} content of cycled NCM111 (55.14%) than NCM523 (72.56%) in XPS measurement, which is implied by different cation mixing degrees of solid sintered NCM523 in oxygen and air while NCM111 reached similar level. NCM111 and NCM523 both showed the similar electrochemical performance to the pristine materials after hydrothermal combined short annealing treatment, while solid sintering in oxygen behaved with slightly worse performance. Xu et al. optimized such direct recycling process by replacing 4 M LiOH solution with a mixture of 3.9 M KOH and 0.1 M LiOH or recycling the concentrated LiOH solution in the hydrothermal treatment, and the temperature of solid sintering can be decreased to 750 ℃ using LiOH [170].

Reductive methods promoting structure reordering of LFP

Except for heat-treatment, structure re-ordering of spent $LiFePO_4$ can also be promoted by some reductive methods. As illustrated in Figure 6a, Zheng Chen's group also demonstrated that adding a reducing agent, citric acid, into Li^+ containing solution during the hydrothermal process is helpful in reducing Fe^{3+}, and subsequently lowering the activation barrier for migration of Fe^{2+} ions out the 1D lithium diffusion channel [169]. The XRD peaks of $FePO_4$ and Fe_2O_3 gradually disappeared after hydrothermally treated under 80 ℃ for 5 h, implying a conversion of $FePO_4$ to $LiFePO_4$ and dissolution of Fe_2O_3. The relithiated $LiFePO_4$ after hydrothermal treatment of 80 ℃ for 5 h as shown in Figure 6b, enabling this process conducted at safer pressure, exhibited an initial capacity of 159 mAh/g at 0.5 C which is comparable with 161 mAh/g of fresh $LiFePO_4$, yet only 93.7% of capacity retention after 100 cycles is achieved on relithiated material probably due to the proton/Li^+ exchange from the weak acidity of citric acid. A short annealing with excess 4% Li_2CO_3 at 600 ℃ for 2 h enabled the recycled $LiFePO_4$ to deliver a 159 mAh/g capacity with < 1% loss after 100 cycles. Besides, Park et al. [171] demonstrated a great Fe_{Li}-defect annihilation in defective $Li_{0.9}FePO_4$ (prepared by a chemical delithiation followed by heating at 380 ℃ for 4 h), which is electrochemically subjected to a deep discharge below general cutoff voltage (reduction with extra electrons injection), leading to a defect-less $LiFePO_4$. As such, the electrochemical activity of $LiFePO_4$ can be greatly enhanced, and density function theory calculation suggests that the vacancies near Fe_{Li} defects and the extra electrons offered by the over-discharging lower the energy barrier for defect annihilation [171].

Electrochemical relithiation

Direct relithiation can also be achieved by an electric field. Yang et al. [158] utilized an electrochemical method to achieve lithiation of $Li_{1-x}CoO_2$ in an aqueous electrolyte (1.5 M Li_2SO_4, 0.5 M LiOH) with oxygen evolution on the counter electrode, and the recycled $LiCoO_2$ showed comparable capacity and stability in 100 cycles than commercials. Besides, the relithiation level is controlled by electrode potential and hence is rid of Li content determination prior to recycling. Their work also illustrated a trace amount of Co_3O_4 in recycled $LiCoO_2$ by XRD and Raman spectra after the electrochemical intercalation of Li^+ and a post-sintering at 700 ℃ for 6 h in air, which is possibly due to the lack of lithium salts in sintering. Chemical reduction of Li^+-deficient cathode is another type of relithiation method via an electric field. Gangaja et al. demonstrated $LiFePO_4$ could be directly regenerated by reduction of $FePO_4$ via iodide salt[90], implying chemical reduction of delithiated cathode materials also works. Such strategy is demonstrated in Figure 6e, where Park et al. have demonstrated that some quinone-based redox mediators, especially DTBQ, can shuttle electrons and lithium ions between lithium metal and chemically delithiated NCM111 cathode [159].

Relithiation in molten salts and ILs

Molten salts is a class of homogeneous system contains abundant molten salts at high temperature, and is applied in the fabrication of single-crystal cathodes [135]. Molten salts behave like a solution, and hence can have a lower melting point (at eutectic point, as shown in Figure 6d) than that of any component salt at a certain ratio. The eutectic salts can both serve as solvents and lithium sources with lower melting temperature under ambient pressure, as shown in Figure 6c. In 2019, Shi et al. adopted a $LiOH:LiNO_3$ eutectic molten salts system in a molar ratio of 2:3 to relithiate spent NCM532 (~ 40% Li loss) at 300 ℃, and lithium content of the treated LCO can reach a level near the stoichiometry [26]. After the relithiation by low-temperature eutectic molten salts, a 4 h annealing in oxygen at 850 ℃ is also employed, and the regenerated NCM532 shows an initial capacity of 149.3 mAh/g and maintains at 134.6 mAh/g after 100 cycles at a current density of 150 mAh/g, while the capacity values of pristine are 146.6 and 130.4 mAh g^{-1}, respectively. Increasing the temperature of molten salts can both realize relithiation and structure reordering simultaneously. Yang et al. utilized a eutectic system composed of $LiOH\text{-}KOH\text{-}Li_2CO_3$ at a molar ratio of 7 : 3 : 0.5 at 500 ℃ to regenerate spent $LiCoO_2$, where LiOH-KOH served as

an oxidizing flux to remove conductive agents/binder, and Li_2CO_3 is added as lithium source due to the greater reactivity than LiOH [44]. The regenerated $LiCoO_2$ material treated at 500 ℃ possesses an increased I_{003}/I_{104} ratio than degraded one even comparable with commercial LCO, meaning less disordering and improved layered structure, and exhibited a 92.5 % capacity retention with an initial of 144.5 mAh/g at 0.2 C (1 C = 150 mAh/g).

However, such molten salts strategy of direct recycling requires excess Li salts as the solution (i.e., 50 g LiOH-KOH-L_2CO_3 for regenerating 1 g spent $LiCoO_2$ demonstrated by Yang et al. [44]), leaving doubts of wasting costly Li salts and on the economic feasibility of molten salts direct recycling. Ma et al. illustrated the viability utilizing much less Li eutectic salts, LiOH:$LiNO_3$ = 3:2, on the regeneration of spent NCM523 cathode [160]. With 1.1 molar times of NCM523 (Li salts/NCM) calcined at 320 ℃ for 4 h and 850 ℃ for 4 h, the water-washed cathode finally annealed at 600 ℃ for another 6 h demonstrated delivered a capacity of 152.5 mAh/g at 0.2 C rate with a capacity retention of 86% after 100 cycles. Furthermore, it is proven by Wang et al. that the reliathiation of NCM111, which is chemically delithiated by NO_2BF_4 oxidizer, through ILs, a family of nonconventional molten salts, ([C_2mim][NTf_2]) with lithium halide salts as Li^+ source is also feasible, where the major cost-contributing ionic liquids can be efficiently recycled (98.7%), lowering total cost of ionic liquids relithiation method [161].

1.7. Upcycling

Upcycling is another recycling process that differs from direct recycling, it aims to develop non-destructive methods on recycling spent cathodes to be of better performance, or explore different applications. Not limited to LIBs, reuse of spent cathodes can be extended to other fields, a common example is developing electrocatalysts owing to the layered structure of $LiMO_2$ species cathodes. In this field, it is quite promising to develop much more value-added products from spent cathodes.

While for regeneration purposes, direct recycling regenerates the performance of the spent cathodes to a level comparable with pristine ones, while upcycling tends to transform spent cathodes to renewed ones perceived to be of greater activity and quality. As such, upcycling offers one route to recycle those batteries with the chemistry of previous generations, with which direct recycling strategy fails to deal in such fast-changing market. Furthermore, the upgraded

regeneration of cathodes after hydrometallurgical leaching, e.g., regeneration of $Li_{1.2}[Mn_{0.56}Ni_{0.16}Co_{0.08}]O_2$ from spent $LiMn_2O_4$ [75], cannot be categorized as upcycling since such process involves a complete breakage of the crystal structure of the spent cathode materials.

1.7.1. Upcycling towards greater performance

Surface engineering

Surface engineering is one common and effective strategy developed to fabricate high-performance cathodes, achieved by either doping or surface coating methods. By employing a protective surface, the cyclability of fabricated cathodes is greatly improved owing to mitigated degradation behaviors. Similar to the direct recycling of spent cathodes, relithiation and structure re-ordering are both necessary for upcycling process, while a process to fabricate the protective layer is also required to improve the stability and electrochemical performance. Typically, upcycling by surface engineering can be realized by methods either coating-forming or doping. Both have been proven effective in studies on the LIB cathodes field. The coating layer, in either metallic compounds (e.g., ZrO_2 [172], Al_2O_3 [173], B_2O_3 [174], etc.) or lithium compounds ($LiAlO_2$ [145], $Li_{1.02}Ni_{0.5}Mn_{1.5}O_4$ [175], $LiMn_{0.75}Ni_{0.25}O_2$ [176], etc.), is helpful separating bulk materials from the electrolytes, and thus side-reactions can be alleviated, while doping works to decrease cations disordering, and thus to increase the cyclability.

(i) Coating-forming upcycling

Such strategy, employing a protective coating on the surface of spent cathode materials, has been demonstrated feasible in regeneration and promotion of spent cathode materials, i.e., the upcycling. Meng et al. [177] uses NH_4VO_3 recovered from vanadium-bearing slag to fabricate a V_2O_5 coated NCM111 cathode material via spray drying and sintering (350 ℃ × 4 h). With a V_2O_5 coating thickness of 45.9 nm, NCM111-5%V_2O_5 delivered a capacity of 156.3 mAh/g after 100 cycles at 0.1 C (1 C = 278 mAh/g) with a capacity retention of 90.6% cycling between 2.5 V - 4.3 V (versus Li^+/Li). Similarly, Zhang et al. reported a lithium-rich material ($Li_{1.20}Mn_{0.54}Ni_{0.13}Co_{0.13}O_2$) coated spent NCM622, whilst the relithiation/structure reordering of spent NCM622 and coating of $Li_{1.20}Mn_{0.54}Ni_{0.13}Co_{0.13}O_2$ are finished in different steps, making such route less promising [178].

Upcycling method via surface coating was also employed on degraded Ni-rich cathode materials. By forming a Li_2TiO_3 coating layer on air-exposed $LiNi_{0.8}Co_{0.15}Al_{0.05}O_2$ (NCA80), Wu et al. reported such restored NCA80 material can retain 82% of initial capacity after 200 cycles under 1 C at RT, and 87% and 55% after 100 and 500 cycles under 1 C at 55 ℃, whilst fresh NCA80 only preserved 68% after 200 cycles [179]. A similar upcycling method achieving both Mg^{2+} surface doping and Li_3PO_4 coating was demonstrated by Chen et al. [180] on Ni-rich NCA80 material, which was exposed in air for a month. The upcycling process was finished by mixing degraded NCA80 with 0.015 mol $MgHPO_4 \cdot 3H_2O$, and annealing at 750 ℃ for 5 h in an oxygen flow. Via this process, the regenerated cathode exhibited a $1^{st}/200^{th}$ discharge capacities of 168.5/142.6 mAh/g with a capacity retention of 84.6% under 2 C, respectively, during which the $1^{st}/200^{th}$ discharge capacities for fresh NCA80 material are 169.7/121.4 mAh/g in a retention of 71.5%, respectively. What need to emphasize here is that the Ni-rich cathodes these routes delt with were induced to degrade by exposing them into air, and their degradation mechanisms are far different with those cycling in cells. It remained to be explored for the direct recycling/upcycling of Ni-rich cathodes subjected to electrochemical cycling.

(ii) Doping

Typically, the doping-directed upcycling process is finished by incorporating a protective layer in the same chemistry with the precursors (spent cathodes) but doped to increase stability, which shall benefit from the following factors: (1) lattice coherent coating leading to an improved wettability; (2) easiness for another recycling owing to the least possible foreign elements, especially for hydrometallurgical regeneration.

Fan et al. [181] constructed a PO_4^{3-}-doped layer on spent NCM523 cathode by calcinating a precursor containing spent NCM523, LiOH, NiO, MnO_2, and $NH_4H_2PO_4$ with a stoichiometric ratio of 1.05 *Li*: 0.5 *Ni*: 0.2 *Co*: 0.3 *Mn*: 0.01-0.05 PO_4^{3-}. As such, a lattice-coherent coating layer (NCM523) that is doped with PO_4^{3-} was fabricated on the surface of spent NCM523 material. The PO_4^{3-} doping enlarges the Li^+ diffusion channel, and stabilizes the surface of regenerated cathodes, where 0.02 M PO_4^{3-} doped cathode (RNCMP-2) shows a specific discharge capacity of 189.8 mAh/g at 0.1 C rate between 2.7-4.3 V. The regenerated NCM without PO_4^{3-} doped (RNCM) showed a capacity of 142.9 mAh/g after 300 cycles with a capacity retention of 65.4%, whilst

RNCMP-2 maintained 83.2% under the same conditions (1 C, 25 ℃). At higher temperature (55 ℃), the capacity retention after 200 cycles of RNCMP-2 is as high as 85.3% at 1 C; meanwhile, RNCM died after 157 cycles. The rate performance of the regenerated cathode was also improved, where RNCMP-2, whose discharge capacities reached 189.8 (0.1 C), 184.9 (0.2 C), 178.1 (0.5 C), 170.7 (1 C), 160.7 (2 C), and 135.1 (5 C) mAh/g, was better than that of commercial NCM. Xu et al. demonstrated a facile upcycling process to prepare (1-x)$LiFePO_4$@x$Li_3V_2(PO_4)_3$ cathode via mechanochemical activation assisted V^{5+} doping [182]. The cathode was prepared by planetary milling raw-materials including spent LFP, $NH_4H_2PO_4$, Li_2CO_3, and V_2O_5, latter sintered at 450 ℃ for 4 h and 700 ℃ for 6 h in Ar. The regenerated cathode material with x = 0.01 showed a single-olivine-structured LFP phase without the presence of $Li_3V_2(PO_4)_3$ phase (not detected until x = 0.03), and V^{5+} ions occupied Fe^{2+} sites. The optimal discharge capacities of 154.3 and 142.6 mAh/g at 0.1 and 1 C rates, respectively, with a very stable cyclability (nearly 100% after 100 cycles) were achieved with x = 0.01.

Wu et al. [183] demonstrated a similar work by introducing Li_2CO_3/Na_2CO_3 into the solid-state sintering (850 ℃ × 12 h) of degraded LCO materials, forming a Na^+-doped layer. The regenerated material NLCO0.01, $Li_{0.99}Na_{0.01}CoO_2$, demonstrated an initial discharge capacity of 151.5 mAh/g at 1 C rate (150 mA/g) between 3.0-4.3 V, where RLCO, the regenerated material without Na^+-doping, and CLCO, the commercial LCO, showed initial capacities of 149.4 and 152 mAh/g, respectively. With a capacity of 143.9 mAh/g after 100 cycles at 1 C, corresponding to a capacity retention of 95.0%, NLCO0.01 displayed a much higher stability compared with RLCO and CLCO. Na^+-doped cathode material, NLCO0.01, also demonstrated much better performances at high rates and high cut-off potential than CLCO. The capacity retention after 100 cycles of NLCO0.01 at the rate of 10 C is as high as 87.6%, superior to the 63.2 and 54.2% retention of RLCO and CLCO, respectively. It held 80.1% of capacity even after 200 cycles. When increasing the upper cut-off voltage from 4.3 V to 4.5 V, the capacity retention of RLCO and NLCO0.01 were 93.8 and 94.1 % after 100 cycles, respectively, while that of CLCO was only 66.9%.

Even with much improved performance, upcycling via surface engineering is only suitable to those cathode materials without any surface passivation, and the feasibility for direct recycling of such surface-passivated cathodes remains to be studied.

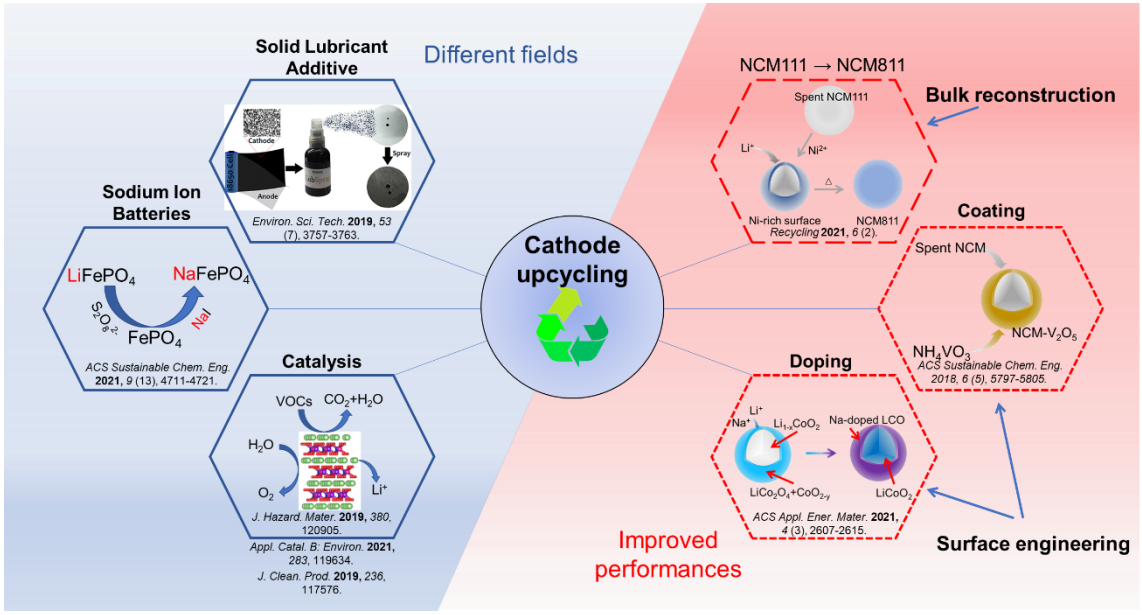

Figure 7 Upcycling strategies for spent cathodes, achieving different applications or with improved performance. Upper left: reprinted from ref. 184 with permission. Copyright 2019 American Chemical Society.

Surface reconstruction

Researchers from *ReCell Center*, set by U.S. Department of Energy (DOE), are also considering another type of upcycling that upgrading a cathode material by chemically changing its composition to reflect the stoichiometry of more desirable cathode formulations, e.g., changing NCM111 to NCM622 [5]. As reported, NMC111 materials shifting to higher nickel content typically used a coating layer of $Ni(OH)_2$ annealing with a stoichiometric amount of LiOH, leading to a binary mixture of $LiNiO_2$ and NMC111, which on annealing in oxygen can be equilibrated to more uniform NMC622 [5]. However, it remained to be explored on how to control the homogeneity of the upcycled cathode materials, where a formation of undesired binary metal oxides should be avoided. In general, this process requires metal cation diffusion, which is favored at high temperatures, longer sintering time, and lower oxidation states. The feasibility of such upcycling strategy remains to be explored yet is quite promising.

In summary, upcycling strategies through either surface engineering or bulk reconstruction (Figure 7) offered one way to deal with those cathode materials developed in past decades, for which direct recycling cannot tune them competitive enough for the current market.

1.7.2. Upcycling towards new applications

The recycled materials/chemicals obtained during or after pyrometallurgical and hydrometallurgical processes are not restricted to regenerate new electrode materials, but also can be extended to new fields, in which the values of new products and the size of the market should be carefully evaluated.

Parikh and co-workers [184] found applications of spent LCO as a solid lubricant additive, mixed with graphene and Aremco binder in an excess volatile organic solvent, leading to an excellent solid lubricant spray (Figure 8a). Zhang et al. also demonstrated the ability of spent LFP and LMO cathodes as adsorbents toward heavy metals in water, where spent LFP showed adsorption capacities of 44.28, 39.54, 25.63, and 27.34 mg g^{-1} for Cu^{2+}, Pb^{2+}, $Cd^{2+,}$ and Zn^{2+}, respectively, while spent LMO achieved lower adsorption capacities (32.51, 31.83, 26.24 and 25.25 mg g^{-1}, respectively) [185]. Furthermore, Liu et al. utilized a delithiated Li_xFePO_4 (x = 0) electrode coating with TiO_2 to achieve efficient Li^+ extraction from seawater with high selectivity (Li^+ over Na^+) through intercalation chemistry [88]. The 0.17 V potential difference of Na^+ and Li^+ insertion/extraction in Me_xFePO_4 (Me = Na/Li) matrix, and faster Li^+ insertion kinetics in the $FePO_4$ host and TiO_2 coating both lead to a 10-cycle stable Li extraction from seawater with 1:1 Li/Na recovery, which is equivalent to the high selectivity of 1.8×10^4. From another perspective, such achievement using intercalation chemistry of Li^+ into traditional cathode materials for Li^+ extraction from seawater makes it promising to explore another upcycling field for spent LIB cathodes.

As shown in Figure 8d, Lv et al. [186] demonstrated the layered transition oxides obtained from DC electric field driven delithiated NCM523 exhibited excellent electrocatalytic oxygen evolution reaction (OER) performance. As shown in Figure 8e, the obtained delithiated product $Li_{0.4}Ni_{0.5}Co_{0.2}Mn_{0.3}O_2$ achieves a small overpotential of 236 mV at 20 mA cm^{-2}, a low Tafel slope of 66 mV dec^{-1} (lower than those reported for novel electrocatalysts, 90 mV dec^{-1} for RuO_2 and 85 mV dec^{-1} for IrO_2), and extraordinary long-term electrolysis durability for over 80 h, while the extracted lithium can be recovered as Li_3PO_4. The activity comes from: (i) increased surface area (19.76 m^2/g of $Li_{0.4}Ni_{0.5}Co_{0.2}Mn_{0.3}O_2$ versus 0.54 m^2/g of original) due to the lamellar morphological structure (Figure 8d) coming from exfoliation effect during the delithiation of

layered cathode materials; (ii) increased lattice oxygen content, leading to larger covalence of Ni-O, Mn-O, Co-O bonds; (iii) increased oxidation state of Ni after delithiation, and changed electronic structure, leading to a more electrophilic nature of the obtained catalyst which promoting the adsorption of OH^- group and thus leading to improved activity. Similarly, Yang et al. [187] reported a mechanochemical activation method for selective recycling of lithium and recovery of $M(OH)_2$ (M: $Ni_{0.5}Co_{0.2}Mn_{0.3}$) from spent NCM523 batteries. As shown in Figure 8c, spent NCM523 material was ball milled with the co-grinding agent, Na_2S, at a rotation speed of 600 rpm for 15 min, during which the following reaction (eq 29) occurs:

$$6LiNi_{0.5}Co_{0.2}Mn_{0.3}O_2 + Na_2S \cdot 9H_2O \rightarrow 6Ni_{0.5}Co_{0.2}Mn_{0.3}(OH)_2 + Na_2SO_3 + 6LiOH \quad (29)$$

Finally, a lithium leaching efficiency and selectivity of 95.10% and 100% were achieved, respectively, leading to final Li_2CO_3 with a purity of 99.96%. As shown in Figure 8f, the resultant $M(OH)_2$ requires an overpotential of about 0.28 V (1.51 V vs. RHE) for catalyzing OER at a current density 10 mA cm^{-2}, whereas the spent $LiNi_{0.5}Mn_{0.3}Co_{0.2}O_2$ and commercial IrO_2 catalysts require overpotentials of 0.41 and 0.29 V, respectively.

Chemicals/materials yielded during the recycling process of LIB cathodes can be more value-added. Guo et al. demonstrated a route to transform transition metal ions from leachate of spent ternary cathodes treated by citric acid and glucose to multi-oxides as high-efficient catalysts for volatile organic compounds (VOCs) oxidation [188]. The catalysis mechanism is demonstrated in Figure 8b. Given that a slag phase in pyrometallurgy is necessary to prevent metal oxidation for refining purposes, and inhibit thermal radiation from increasing heating efficiency, Hu et al.[52] suggest that a $CaO\text{-}Al_2O_3$ system can improve the economic viability of the smelting recycling process as $CaO\text{-}Al_2O_3$ is a potential salable mineral for applications such as synthetic slag in ladle metallurgy operations and high-performance cement.

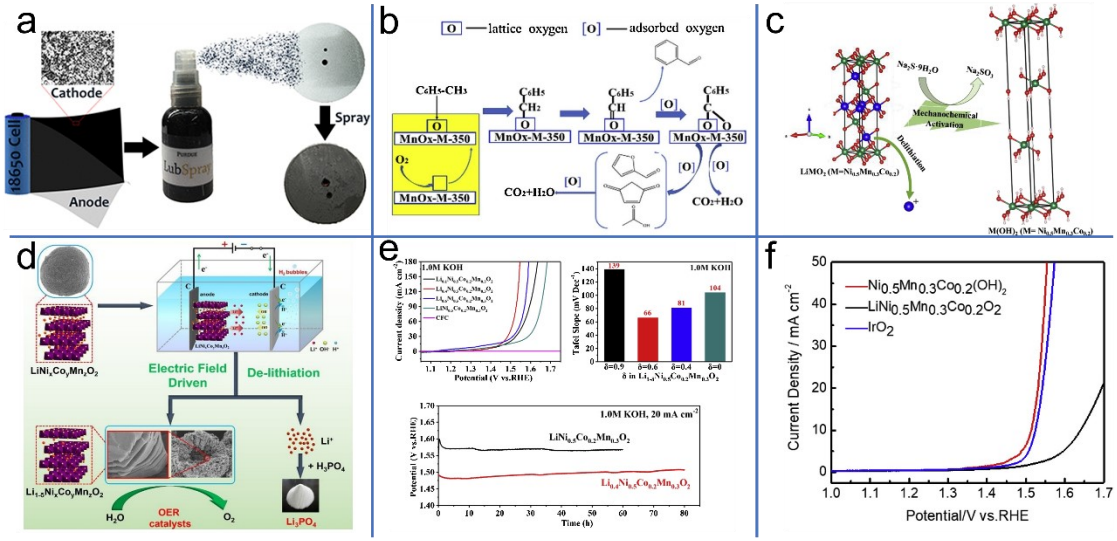

Figure 8 (a) Illustration on the application of spent LCO as lubricate additive. Reprinted from ref. 184 with permission. Copyright 2019 American Chemical Society. (b) Catalysis mechanism of toluene oxidation over upcycled MnO_x. Adapted with permission from ref. 188. Copyright 2019 Elsevier. (c) Schematic illustration of the mechanochemical process of spent NCM523 with $Na_2S{\cdot}9H_2O$. Reprinted with permission from ref. 187, copyright 2019 Elsevier. (d) Schematic diagram of upcycling process transforming spent NCM523 into OER catalysts with Li salts extracted electrochemically. (e) The polarization curves (top left), and Tafel slopes (top right) at 20 mA/cm^2 of the delithiated $Li_{1-\delta}Ni_{0.5}Co_{0.2}Mn_{0.3}O_2$ (δ = 0.9, 0.6, 0.4, 0) samples, and the long-term chrono-potentiometric stability (bottom) of $Li_{0.4}Ni_{0.5}Co_{0.2}Mn_{0.3}O_2$ and $LiNi_{0.5}Co_{0.2}Mn_{0.3}O_2$ at 20 mA/cm^2. d-e: reprinted/adapted with permission from ref. 186. Copyright 2019 Elsevier. (f) Polarization curves of $M(OH)_2$ (M: $Ni_{0.5}Co_{0.2}Mn_{0.3}$), $LiNi_{0.5}Co_{0.2}Mn_{0.3}O_2$, and IrO_2. Reprinted with permission from ref. 187, copyright 2019 Elsevier.

1.8. Conclusions and perspectives

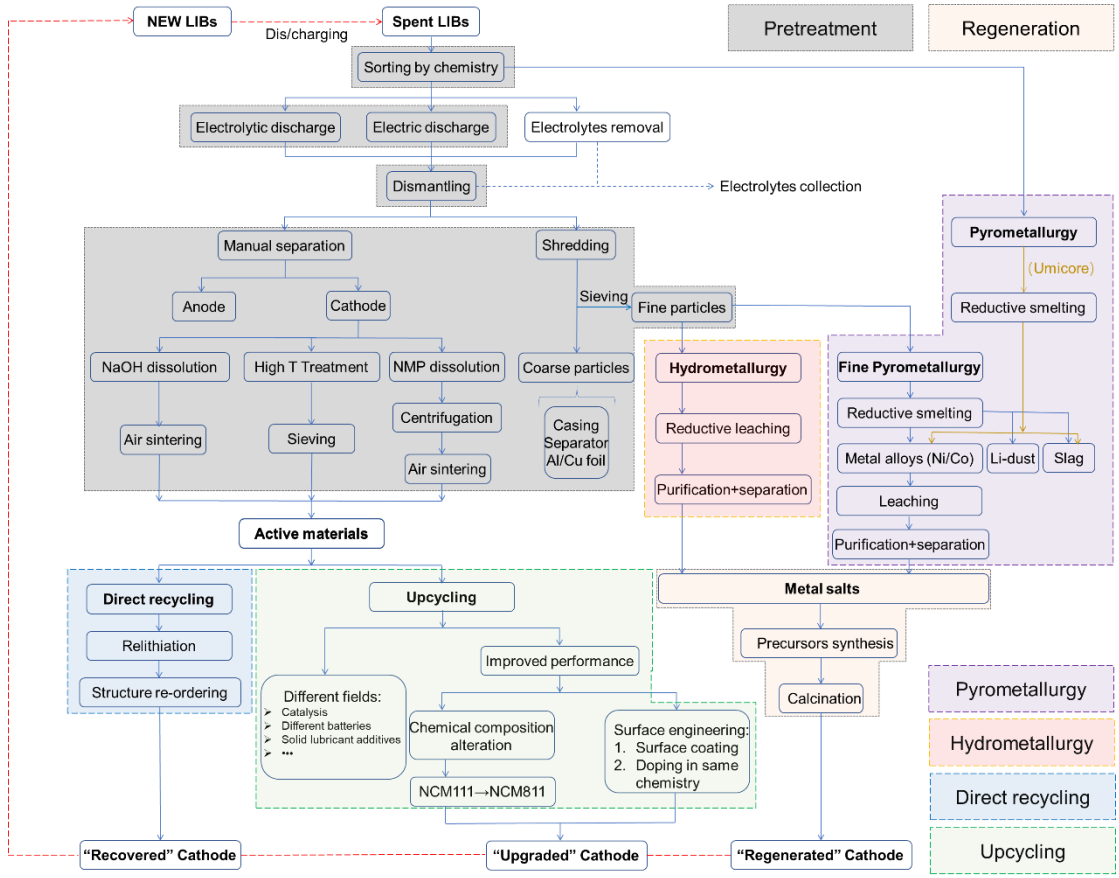

Figure 9 Process workflows for pyrometallurgical, hydrometallurgical, direct recycling, and upcycling processes.

Green and sustainable energy storage remain one of the top topics in today's academic and industrial fields. With increasing demand and market of LIBs powering EVs and portable electronics, the shrinking natural reserve, government regulations on spent LIBs treatment, profit of recycling critical metals will drive more researches and tries on recycling. There is no doubt that recycled materials will play a critical role in the supply chain of LIBs. As shown in Figure 9, the current four recycling processes from spent LIBs are summarized as follows:

a) The main purpose of pyrometallurgical methods is to produce metals or metal alloys, enabling a simultaneous processing with other types of batteries, e.g., Ni-MH battery in *Umicore* process, and ores. As such, treating spent LIBs like ores leads to a decreased requirement on pretreatment, even charged batteries can be directly fed into furnace. Besides the need of further hydrometallurgical processing for refining valuable metals, the toxic gasses emission which mainly comes from electrolytes and polymers (binder, separator, and casings) requires off-gas treatment. Most importantly, the profitability of such process largely relies on the price of cobalt and nickel as most Li is slagged and wasted, and the tendency of EVs market is shifting to Co-poor and Co-free chemistry, making pyrometallurgical routes less suitable for recycling spent LIBs from EVs. However, LCO still dominates the market for consumer electronics, where pyrometallurgical recycling should focus. Besides, fine pyrometallurgical recycling (e.g., *Accurec* and *Re-Lion processes*) should be promoted for a more sustainable recycling of lithium.

b) Accompanied with a pretreatment, hydrometallurgical recycling routes maintain the highest recycling efficiencies against lithium and other valuable metals in cathodes, as well as other batteries components. Among the current four LIBs recycling routes, another advantage of hydrometallurgical methods is the highest tolerance over cathodes composition, no matter in cobalt-rich or -poor or even in mixed chemistries. Great efforts have been made to study reductive acid leaching, including inorganic and organic acids. Given that the corrosive Cl_2 formation with HCl and oxidation effect from HNO_3 in leaching, H_2SO_4 is currently the most promising acid for industrial plants due to the low cost and effectiveness. Organic acids, although with promising merits of biocompatibility and biodegradability, yet are criticized for high cost for large-scale applications. Lab-scale studies have already proven the feasibility of yielding separate compounds of Li, Ni, Co, and Mn with high purity and efficiency from complex leachate systems, yet typically in many steps. Hence, the reliability of such route remains to be improved. Although the direct resynthesis from leachate through co-precipitation and sol-gel methods is so promising in fewer steps, a careful control on the composition (metal ratio) and impurities (such as Cu, Al, Fe) is necessary.

c) Direct recycling, which remains in lab-study, aims to recover cathode materials in a non-destructive method, and comparing with metallurgical methods, direct recycling holds a lower cost, and less GHG emissions. Solid-state sintering, and combined hydrothermal treatment with

short annealing are two common strategies in direct recycling spent cathodes, however, it remained to study their feasibility in pilot-scale tests. The viability of direct recycling on mixed cathode materials remains to be studied. More importantly, current super-increasing EVs market offers direct recycling great opportunity since one battery pack of EV generally has thousands of LIBs in the same chemistry. EVs manufacturers also should cooperate with recycling facilities to increase the automation degree of disassembly lines for battery packs.

d) As talked in *Section 7*, upcycling, as one alternative method for direct recycling, also focuses on developing non-destructive methods on recycling spent cathodes to be of better performance, or exploring different applications where the value of new products is the key factor. For upgradedly regenerating spent cathodes back to fresh LIBs, the surface-engineering and chemical composition alteration strategies are still developing, and their feasibility requires more effort to be studied.

e) More importantly, due to advantages including (i) sorting spent LIBs by different cathode chemistry in order to be sent to different routes, (ii) economies of scale, (iii) collection of valuable components including current collectors, metal casing and electrolytes, (iv) lower costs from the transportation of cathodes against that of spent LIBs with safety hazards[5], pretreatment facilities are also profitable to be set at upstream of spent LIBs recycling chain. However, spent LIBs recycling facilities treat spent batteries without knowing the chemistry of EOL cells, leading to a decreased efficiency. This requires LIBs manufacturers to disclose necessary information on casings, leading to less effort in sorting. Comparing with LIBs market for portable electronics, currently, LIBs from EVs and energy stations are more benign for recycling chain due to a single source of chemistry in one battery pack.

Chapter 2: Surface coating enabled upcycling of spent lithium-cobalt oxide cathodes

2.1. Introduction

The emerging popularity of electrical vehicles, regarding as green alternatives to replace fossil fuel vehicles, has drawn great need for lithium-ion batteries (LIBs) owing to its unique properties like high energy density, high working voltage, no memory effect and long life-span. It is projected that the LIBs market shall expand in an annual grow rate of 12.3% from US$ 41.1 billion in 2021 to US$ 116.6 billion by 2026.[189] However, such exigency not only stresses the supply chain from ore suppliers to manufacturers, but also generates a booming demand to treat retired LIBs. Recycling them is thought as an effective solution. Except the benefit to eliminate the safety and environmental hazards which though may as regulated by governments as well, recycling spent LIBs can also support a more secure and resilient supply chain that leads to more competitive and sustainable cells.

Intensive efforts have been paid on recovery of metals from cathode materials due to their highest value comparing with the other components.[7] The pyrometallurgical and hydrometallurgical recycling have been demonstrated commercial promise in recycling metals such as nickel (Ni) and cobalt (Co) yet their costs to refabricate new cathodes shows no significant advantages than that of primary manufacturing from ores.[5] Pyrometallurgical methods smelt spent cathodes under high temperature (> 1200 ℃) to produce Ni- and Co-bearing alloys, making refining necessary. The advantages of pyrometallurgy lie in its simpleness and high tolerance in status, composition, and size of the spent cells, yet it is also criticized of low recovery efficiency of Li and graphite, high energy consumption, high greenhouse gas emission, and low purity of final product. Due to the high-purity product, high yield, and low operation temperature, hydrometallurgy is regarded as the most viable option. It is generally finished in aqueous chemistry, via leaching followed with purification as well as separation processes. Inorganic acids are widely studied as leaching agents in hydrometallurgy, resulting in an emission of toxic gases such as Cl_2, SO_3, and NO_x, and waste water containing salts and excessive acids. Organic leachants though are environmentally benign but not suits for industrial application due to their high cost.

Moreover, pyro- and hydrometallurgy are both destructive methods that completely destroy the crystal structure, leading to another labor to re-create the structure.

Recently, extensive works have been paid on developing mild recycling methods, i.e., the direct recycling[29, 44, 159-161, 164-165, 169], to recover stoichiometry composition and desired crystal structure. Many studies have demonstrated cathode in cycling degraded mainly due to loss of active Li^+ as well as irreversible phase transitions from layered structure, as the former deteriorated the reversible capacity while the latter one increased resistance leading to voltage loss (*iR*).[138, 147, 156] Solid-state sintering and hydrothermal treatment coupling with short annealing are the two direct recycling methods that have been demonstrated effective to convert failed cathodes back to the pristine state. Direct recycling via solid-state sintering uses a single-step high temperature calcination of a mixture of Li salts with spent cathodes, and is thus promising for its simplicity. Many lab-scale studies have proven solid-state sintered direct recycling is able to recover the electrochemical performance of degraded cathodes, including $LiCoO_2$, NCM111, NCM523[38, 164-165], LiFePO4[28, 190], etc. However, the Li/Co ratio in cathodes should be pre-determined to accurate the addition amount of lithium salts, making it inferior for large-scale applications. To solve this issue, combined hydrothermal treatment with short annealing is adopted. The hydrothermal treatment is a self-saturation process of the degraded cathodes in a Li^+-abundant solution, leading to uniform products (relithiation); the degraded phases are hard to be recovered at relatively low-temperature (< 220 ℃), thus requiring a short annealing process (re-ordering). Nonetheless, direct recycling can only regenerate spent cathodes to their original performance, remaining insufficient to recycle antiquated cathodes. Thereby, an upcycling strategy, i.e., upgraded recycling, is developed to recycle spent cathodes into materials with enhanced functionality either in performance or for alternated applications.

The LIBs market is rapidly shifting toward cathodes with high energy density, high nickel content. It makes less favorable to direct recycle those cathodes used many years ago. Thereby, the bulk reconstruction is developed to convert outdated cathodes into enhanced ones with different composition. Initial upcycling targeted the transformation of NCM111 to NCM622 with Ni fed into the crystal structure, but it remains to be optimized to achieve a good homogeneity.[5] The second upcycling approach is the surface engineering, including coating and doping. It has been widely utilized to prepare high-performance cathodes with a more stabilized surface.

Herein, we developed a new method to prepare upcycled $LiCoO_2$ cathodes through a urea-assisted coating formation in hydrothermal treatment coupled with a short annealing. The coating formation on the degraded LCO cathodes is finished simultaneously with the hydrothermal relithiation, latter the short annealing transfers the coating and degraded phases into layered lithium transition metal oxides. Through a series of materials and electrochemical characterizations, we prove such strategy fabricating a coating layer while hydrothermal relithiation process is effective on upcycling of spent cathodes.

2.2. Experimental

Materials and reagents

All reagents were obtained from commercial sources without any purification. Manganese (II) acetate tetrahydrate was purchased from Sigma-Aldrich Co., Ltd. Urea, lithium hydroxide, potassium hydroxide, nickel (II) acetate tetrahydrate of reagent grade were purchased from Thermo Fisher Scientific Co., Ltd. Cylindrical 18650 LIBs (Toshiba A&TB, LGR18650P, 3.6 V, 1650 mAh) were purchased from electronic market.

Commercial LIBs cycling and cathode harvesting

The LCO cathode are harvested from commercial cylindrical LIBs (LGR18650P) which were cycled between 3.0 – 4.2 V with a charge/discharge current of 825 mA (0.5 C) for 500 cycles. The cycling stability is shown in Figure S1. Before dismantling, the cycled batteries were immersed in a potassium sulfate solution for 24 hours to completely discharged state due to safety concerns. After a manual dismantling, the cathode was separated from anode, separators, steel casing, plastic package. The cathode strips were soaked in N,N-Dimethylformamide (DMF) for 24 hours. Then, LCO powders, binder and conductive agent were removed from Al plate by manually scraping. The mixture was washed with DMF for three times, and then subjected into tube furnace under 550 ℃ for 1 hour in air to obtain LCO powders, denoted as DLCO.

For comparison, direct recycling through solid sintering with excess LiOH was also prepared. After a calcination at 900 for 8 hours and deionized (DI) water washing, the obtained sample was denoted as SolidS. Meanwhile, fresh LCO powders were obtained in same route from

the cell without cycling. After that, pristine LCO powders were treated with excess LiOH at 900 ℃ for 4 hours. After DI water washing, the as-obtained powder was denoted as LCO-pri.

Upcycling process of spent cathode materials

In a typical upcycling process, spent cathode materials were regenerated in two steps: hydrothermal relithiation with urea-assisted coating, and short annealing. In the hydrothermal treatment, 1 g DLCO was added into a 50 mL Teflon-lined stainless-steel autoclave, and mixed with stoichiometric amount of nickel and manganese acetates (Mn: Ni = 3:1) in 10 mL DI water. Urea was introduced as one precipitation agent. After mixing above compounds for 30 min, 20 mL solution containing 3 M LiOH and 3 M KOH was added and mixed well. Then, the autoclaves were hydrothermally treated at 190 ℃ for 16 hours. The treated powders were collected via a centrifugation, and sintered with excess amount of LiOH at 900 ℃ for 4 hours in air. The recycled cathode materials were washed with DI water before cathode preparation. Finally, the upcycled cathode materials after DI water washing with coating contents of 3%, 5%, and 10% were defined as NM-DLCO-x% (x = 3, 5, 10).

Electrochemical characterization

The cathode materials were mixed with PVDF (NMP, 25 mg/mL), Super P with a mass ratio of 8:1:1 to prepare a fine slurry. The slurry was cast onto a carbon-coated Al foil with a doctor blade, and dried in vacuum at 80 ℃. The mass loading was controlled at ~3.0 mg/cm^2. Before half-cell assembly, the disc electrodes were compressed. The electrochemical tests were performed in 2032-type coin cell with Li metal as anode and Celgard 2500 as separator in an electrolyte of 1 M $LiPF_6$ in EC: DMC (1:1 of volume ratio). The cycle and capability tests were carried out on Neware battery testing system under different parameters. Cyclic voltammetry (CV) with a scan rate of 0.1 mV/s in a voltage range from 3.0 V to 4.5 V and electrochemical impedance spectroscopy (EIS) tests at a charged state in a frequency range of 10^6 Hz to 10^{-2} Hz with a signal amplitude of 10 mV were performed on Bio-Logic SAS VMP-3 potentiostats.

Characterization of the cathode materials

The composition and structure of the samples were tested on an Ultima IV (Rigaku) X-ray diffractometer equipped with a Cu Kα X-ray source (λ = 1.5418 Å). The morphology of the

cathode materials was observed on a field-emission scanning electron microscope (FE-SEM, Zeiss Sigma) equipped with an energy dispersive X-ray detector (EDX, Oxford). X-ray photoelectron spectroscopy (XPS) measurements were carried out on Kratos AXIS Ultra spectrometer to get electronic structure of the as-prepared samples.

2.3. Results and Discussion

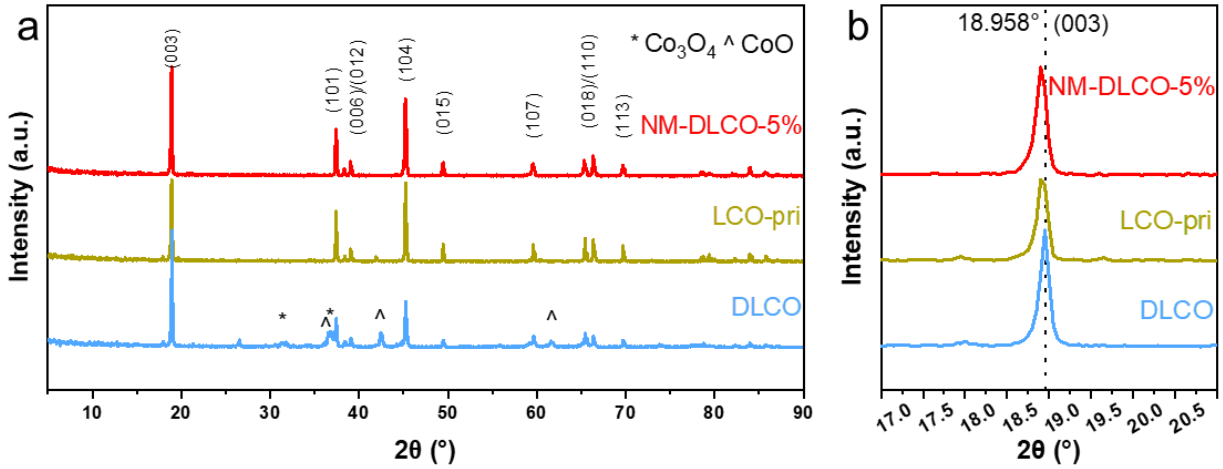

Figure 10 (a) XRD patterns of DLCO, LCO-pri, and NM-DLCO-5%, and the (b) enlarged view.

The XRD patterns of LCO samples are shown in Figure 10 and Figure S2. All samples exhibit a typical pattern of α-$NaFeO_2$ layered structure with the space group of R-3m. For the layered cathode materials, the value of $I_{(003)}/I_{(104)}$ ratio is popularly combined with the degree of cation disordering.[191] The smaller this ratio is, the larger the structure deviated from hexagonal to cubic symmetry. The cation disordering is regarded minor when this value is above 1.2. The DLCO sample obtained from cycled cell shows a higher $I_{(003)}/I_{(104)}$ ratio comparing with other samples, as shown in Table 1. This phenomenon is also reported by some literatures, which may stem from the preferred orientation of certain facets after microstructure changes during cycling.[26] However, hydrothermally treated samples all present $I_{(003)}/I_{(104)}$ ratios higher than 1.2, while this value is found to be 0.66 and 1.04 for samples SolidS and LCO-pri that were treated only by solid-state sintering. This result shows the preeminence of HT-SA approach in regenerating spent cathode materials, which was also showed by Shi et al.[165]

Characteristic peaks of metallic oxides are found in XRD pattens of DLCO, where peaks located at 31.30°, 36.85° are indexed as Co_3O_4 (PDF# 42-1467), and 36.50°, 42.40°, and 61.50° are indexed as CoO (PDF# 48-1719). After treatment, the peaks of Co_3O_4 and CoO disappear in all recycled cathode materials, meaning a successful restoration of layered structure. Benefited to the completely discharged state before disassembly, the (003) peak of DLCO shows no shift to lower angles (Figure 10b), indicating a well reservation of Li. The coated sample shows no peaks other than that of characteristic $LiCoO_2$, indicates coating layer has similar structure with α-$NaFeO_2$ type $LiCoO_2$ core.

Sample	**$I_{(003)}/I_{(104)}$**
DLCO	2.57
SolidS	0.66
LCO-pri	1.04
NM-DLCO-0%	1.42
NM-DLCO-3%	2.12
NM-DLCO-5%	1.41
NM-DLCO-10%	1.35

Table 1 $I_{(003)}/I_{(104)}$ ratios of spent cathode materials and treated cathode materials.

SEM and EDX mapping images showing morphology and composition of the precursor and coating samples are presented in Figure 11. It can be found in Figure 11a that the DLCO precursor is made of single crystal particles with irregular sizes. As shown in Figure 11b, the flocculent materials attached on the particle surface is the residual carbon of the binder and conductive agents, owing to an incomplete calcination of pretreatment at 550 ℃ in air. After a short annealing at 900 ℃ in air for 4 hours, the surface of LCO particles become smooth as shown in Figure 11e. The high temperature treatment not only removes impurities, but also recovers cubic phases back to the normal hexagonal structure and creates a homogeneous coating layer. The EDX mapping images further prove an even distribution of Mn and Ni in NM-DLCO-5% (Figure 11g-11h), demonstrating the hydrothermal coating treatment combined with a short annealing can effectively prepare a well-coated structure. The EDX mapping results also further confirmed that around 5% of $LiMn_{0.75}Ni_{0.25}O_2$ is contained in NM-DLCO-5%

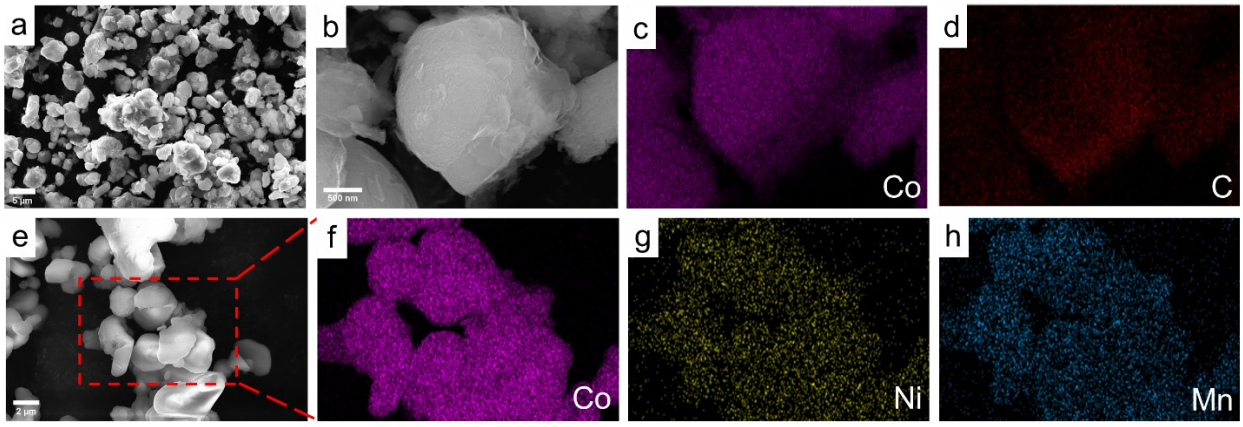

Figure 11 SEM images and corresponding EDX mapping images of DLCO (a-d), and NM-DLCO-5% (e-h).

Galvanostatic discharge/charge tests are finished to evaluate the electrochemical performance of LCO samples, and the cycling stabillity and rate capability performance are shown in Figure 12. Initial three cycles are employed here to study the performance of samples under moderate parameters, and the charge-discharge curves are plotted in Figure 13a and 13c. Owing to the efforts to form stablized interfaces, all samples shows slightly lower dischage capacities in the first cycle.[192] As shown in Figure 13b and 13d, the first cycles of NM-DLCO-5%, and LCO-pri present an elevetaed charging voltage plateu and lower discharging capacity comparing with the other two. Upon stablization, NM-DLCO-5% shows the highest discharge capacity of 138.5 mAh/g, much larger than that of LCO-pri (111.5 mAh/g). Then, the upper cut-off voltage and discharging rate are increased to 4.35 V and 1 C, respectively, to test the cycling stability. As such, the disharge capacities of NM-DLCO-5%, and LCO are increased to 160.23, 124.05 mAh/g, respectively, while the capacity retention at 100th cycle are 91.2%, 89.5%, respectively. For comparision, DLCO sample though exhibits a discharge capacity of 117.90 mAh/g yet dies rapidly at ~ 70th cycle. Meanwhile, the conventional direct recycling methods, solid-state sintering and HT-SA, successfully regenerate the elelctrochemical performance of degraded LCO to 151.08 and

158.19 mAh/g, but both degrade rapidly in cycling, indicating the superiority of proposed hydrothermal coating treatment with a short annealing.

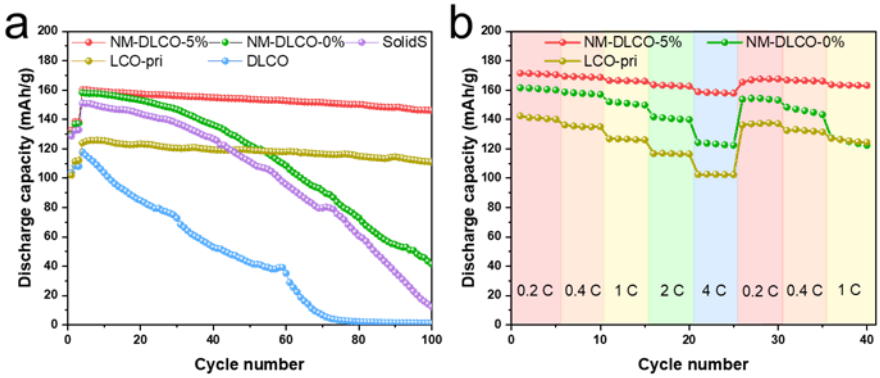

Figure 12 (a) Cycling performance of degraded, pristine, and regenerated cathode materials. (Initial three cycles: 0.4 C (1 C = 140 mAh/g) from 3.0 to 4.2 V; the following cycles: 1 C from 3.0 to 4.35 V). (b) Rate capability of the regenerated and pristine cathode materials with a cut-off voltage of 4.35 V.

NM-DLCO-5% also shows the best rate capabilities of 171.07, 169.02, 166.29, 163.10, and 158.28 mAh/g at rates of 0.2, 0.4, 1, 2, and 4 C, respectively. The NM-DLCO-5% still retains capacities of 166.97, 166.44, 163.36 mAh/g when dischage rate returns to 0.2, 0.4, and 1 C, respectively. For comparison, LCO-pri shows capacities of 141.05, and 102.49 mAh/g at 0.2 and 4 C, respectively, while those of NM-DLCO-0% are 160.82 (0.2 C) and 123.28 mAh/g (4 C). In another way, NM-DLCO-5% demonstrated a rate retention of 92.5% (calculated in $Q_{4\ C}/Q_{0.2\ C}$), while LCO-pri and NM-DLCO-0% show retention rates of 72.7 and 76.7%, respectively. This result further demonstrates the benefit introducing coating layers in upcycling process.

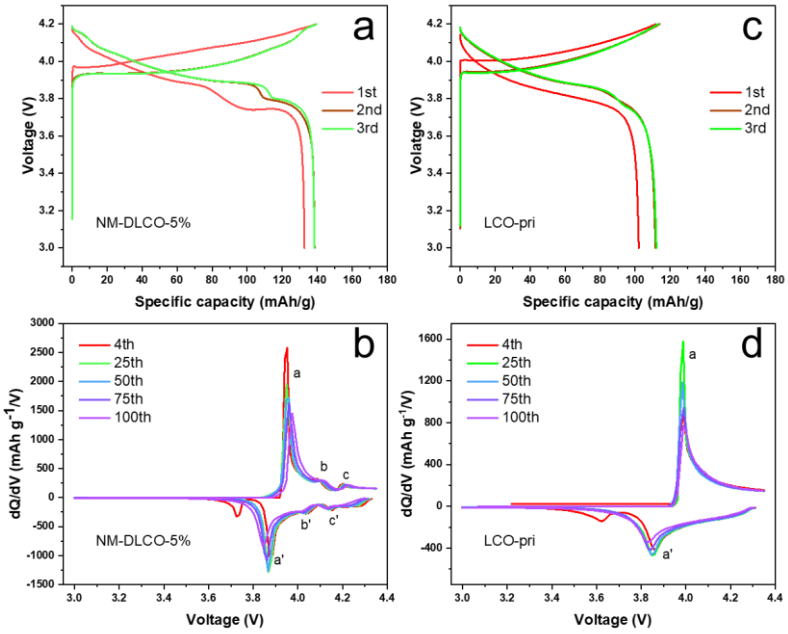

Figure 13 Voltage profiles of the regenerated (a), and pristine (c) cathode materials at the initial three cycles at 0.4 C in the volatage range of 3.0 – 4.20 V. The differential specific capacity vs. voltage (dQ/dV) curves for the regenerated (b), and pristine (d) cathode materials.

As shown in Figure S4, CV curves of coated-LCO samples denote in similar elelctrochemical behaviors. The 1st cycle of coated sample shows distinct anodic peaks than next two cycles, owing to the formation of solid-electrolyete interface (SEI) layer. From 2nd cycle, the coated sample shows three pairs of redox peaks located at around 4.02/3.85, 4.07/4.04, and 4.19/4.16 V, while only a pair of broad peaks at 4.10/3.82 V is found in LCO-pri. Upcycled samples with coating show smaller voltage differences (~0.17 V) between main peaks, which are much smaller that of 0.28 V in LCO-pri, suggesting better reversibility and smaller polarization in upcycled samples. The dQ/dV plots of upcycled and pristien samples derived from charge/dishcarge curves at different cycles in cycling are shown in Figure 13b, and 13d, in which the charge/discharge plateaus are represented as peaks in dQ/dV plots. Similar with CV curves, Figure 13b shows that coated LCO samples have one pair of sharp peaks locate at 3.96/3.86 V, and two pairs of minor peaks locate at 4.07/4.05 V, and 4.20/4.16 V, respectively. The sharp peaks correspond to the first-order metal-insulator transition, while the following two pairs correspond to the order-disorder transition in composition near $Li_{0.5}CoO_2$.[141] Only one pair of peaks at 3.99/3.86 V is found in LCO-pri since it demonstrates a specific capacity of only 111.5 mAh/g.

After cycling, all samples show peak shifts and increases in voltage differences, indicating increased polarizations along with decreases in capacities. Yet smaller voatge differences are found in the upcycled sample than that of LCO-pri, indicating improved polarization owing to the coating layer.

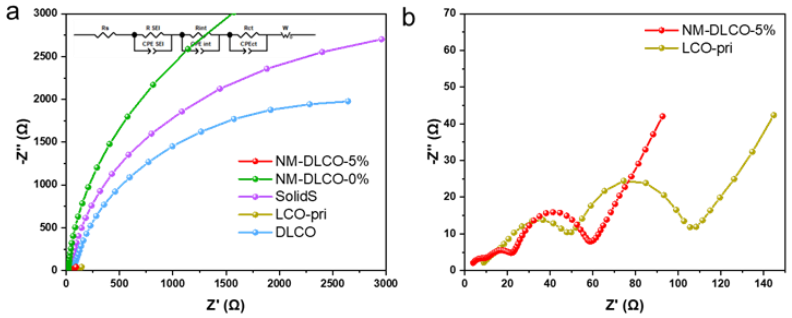

Figure 14 (a) Nyquist plots of regenerated, pristine, and degraded LCO samples after 100 cycles, equivalent circuit (inset), and (b) enlarged view of NM-DLCO-5% and LCO-pri.

To understand the effect of coating layer on electrochemical performance, EIS is employed. Before the EIS tests, the half-cells are charged to 4.35 V and relaxed for 2 hours. Figure 14 shows the Nyquist plots of the regenerated, pristine, and degraded LCO samples after cycling. Plots are fitted according the equivalent circuit shown in Figure 5a, and the fitted results are shown in Table S3. As shown in Figure 14b, a typical Nyquist plot contains three semicircles and one inclined strait line. Three semicircles are attributed to the Li^+ diffusion resistance (R_{SEI}) through SEI layer, interface contact resistance (R_{int}), and charge-transfer resistance (R_{ct}), while the inclined line reflects the diffusion in solid state. According to the fitting results, NM-DLCO-5% shows the smallest R_{ct} of 31.05 Ω as compared DLCO (R_{ct}: 41.65 Ω), while the continuing third semicircles at the low-frequency region of NM-DLCO-0%, SolidS, and DLCO indicate completely destructed crystal structures due to cycling. This results further prove the positive effect of coating to inhibit structure degradation and to regenerate more stable cathode materials.

2.4. Conclusions

Achieving relithiation and coating formation simultaneously, we designed an improved hydrothermal treatment coupled with short annealing process to upcycle degraded LCO cathode materials. Urea is here utilized to facilitate the coating formation. The regenerated LCO with 5% $LiMn_{0.75}Ni_{0.25}O_2$ coating layer delivers a discharge capacity of 160.23 mAh/g, with a capacity

retention of > 91% after 100 cycles under 1 C. The improved hydrothermal relithiation with urea-assisted coating formation, following a short annealing is effective to regenerate outdated LCO cathode to meet current market. We also believe the efficient strategy introduced above can be extended to upcycle other cathode materials.

2.5. Supplementary Information

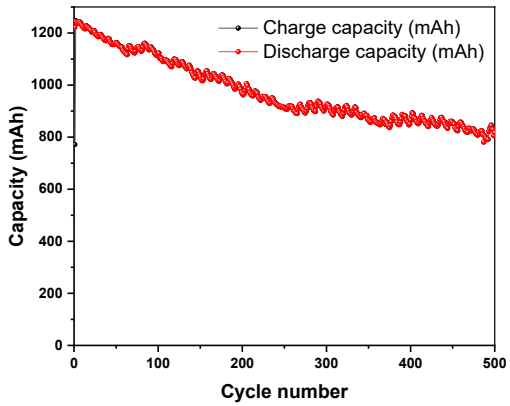

Figure S1 Cycling performance of the LCO commercial cylindrical cell which was cycled in a voltage range of 3.0 - 4.2 V at 825 mA (total capacity: 1650 mAh).

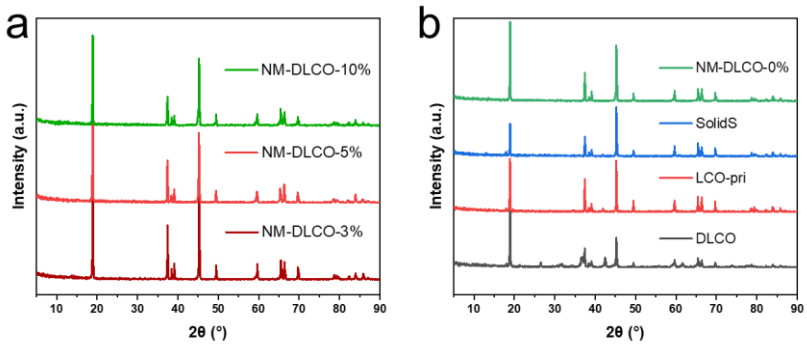

Figure S2 XRD patterns of all LCO samples.

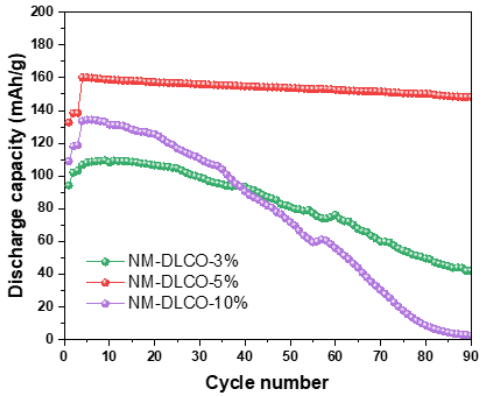

Figure S3 Cycling performance of upcycled cathode materials with different coating contents. (Initial three cycles: 0.4 C (1 C = 140 mAh/g) from 3.0 to 4.2 V; the following cycles: 1 C from 3.0 to 4.35 V).

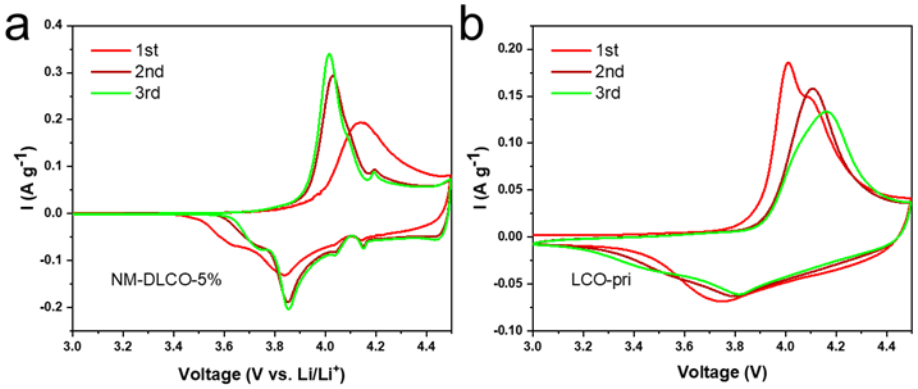

Figure S4 CV curves of NM-DLCO-5%, and LCO-pri samples in a scan rate of 0.1 mV/s from 3.0 V to 4.5 V.

Sample	Cycle	Main anodic peak	Main cathodic peak	ΔV
NM-DLCO-5%	1st	4.14	3.84	0.30
	2nd	4.02	3.85	0.17
	3rd	4.02	3.85	0.17
LCO-pri	1st	4.01	3.75	0.26
	2nd	4.11	3.80	0.31
	3rd	4.17	3.92	0.25

Table S1 Potential change of redox peaks in CV curves of coated, and pristine LCO samples.

Sample	Cycle	a	a'	ΔV
NM-DLCO-5%	4th	3.9524	3.8730	0.08
	100th	3.9739	3.8428	0.13
LCO-pri	4th	3.9895	3.8612	0.13
	100th	3.9882	3.8286	0.16

Table S2 Potential of main peaks, and their voltage differences at 4th, and 100th cycle in dQ/dV plots.

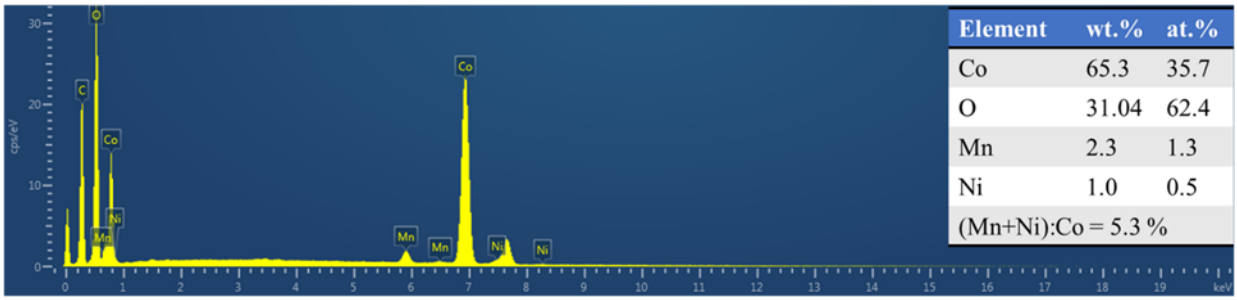

Element	wt.%	at.%
Co	65.3	35.7
O	31.04	62.4
Mn	2.3	1.3
Ni	1.0	0.5
(Mn+Ni):Co = 5.3 %		

Figure S5 EDX-ray spectrometry analysis, and content of various elements.

Sample	R_s	R_{SEI}	R_{int}	R_{ct}
NM-DLCO-5%	2.27	7.97	13.3	31.05
LCO-pri	5.24	41.3	14.3	41.65

Table S3 Resistance values of various samples obtained after fitting Nyquist plots.

Chapter 3. Conclusions and future work

Since LIBs are becoming increasingly vital for energy storage markets, including portable electronics, electrical vehicles, and stationary grid-energy storage, the market size of LIBs is also rapidly expanding. However, due to the limited reserve, recycling critical metals from spent cells or regenerating spent cathodes is thus more and more important to increase the sustainability, competitiveness and security of LIBs market. This thesis offers with a deeper understanding to the recycling strategies being studied or utilized in industrial- and lab-scale. Comparing with those destructive metallurgical methods (pyro- and hydro-metallurgy), direct recycling is still the most promising strategies with the lowest stress on environment, the lowest energy consumption and the lowest cost. It is critical for direct recycling to prove its feasibility in larger scale since publications have proven its superiority in lab-scale. Another drawback of direct recycling is the less practicality of directly recycling outdated cathodes since direct recycling only aims to recover the performance of spent cathodes to a level reach that of pristine one. Upcycling is hence developed. As a new emerging field, strategies developed for upcycling are systemically discussed in this thesis.

This thesis also includes our experimental attempt on upcycling, through an improved hydrothermal treatment with short annealing, after which a $LiMn_{0.75}Ni_{0.25}O_2$ layer is evenly coated on the spent LCO cathodes, the layered structure is recovered, and the electrochemical performance of product is greatly enhanced comparing with pristine cathodes. We also believe this work can be extended to other cathode materials, such as NCM111, and $LiFePO_4$. As a continuation of the current work, a high-resolution transition electrons microscopy imaging is planned. By so, a more detailed micro-structure information can be obtained.

Finally, more efforts need to be put to evaluate the feasibility of upcycling method to treat outdated cathodes, comparing with the route extracting critical metals in metallurgical methods from economic view.

References

1. Whittingham, M. S.; Gamble, F. R., The lithium intercalates of the transition metal dichalcogenides. *Mater. Res. Bull.* **1975,** *10* (5), 363-371.
2. Battery Pack Prices Cited Below $100/kWh for the First Time in 2020, While Market Average Sits at $137/kWh. https://about.bnef.com/blog/battery-pack-prices-cited-below-100-kwh-for-the-first-time-in-2020-while-market-average-sits-at-137-kwh/ (accessed 29 September).
3. International Energy Agency (IEA) Global EV Data Explorer. https://www.iea.org/articles/global-ev-data-explorer (accessed 30 September).
4. U. S. Geological Survey *Mineral commodity summaries 2021*; Reston, VA, 2021; p 200.
5. Gaines, L.; Dai, Q.; Vaughey, J. T.; Gillard, S., Direct Recycling R&D at the ReCell Center. *Recycling* **2021,** *6* (2).
6. Vehicle Technologies Office, National Blueprint for Lithium Batteries. U.S. Department of Energy, Ed. Office of Energy Efficiency & Renewable Energy,: 2021.
7. Gallagher, K. G.; Nelson, P. A., 6 - Manufacturing Costs of Batteries for Electric Vehicles. In *Lithium-Ion Batteries*, Pistoia, G., Ed. Elsevier: Amsterdam, 2014; pp 97-126.
8. Zheng, X.; Gao, W.; Zhang, X.; He, M.; Lin, X.; Cao, H.; Zhang, Y.; Sun, Z., Spent lithium-ion battery recycling – Reductive ammonia leaching of metals from cathode scrap by sodium sulphite. *Waste Manag.* **2017,** *60*, 680-688.
9. Bahaloo-Horeh, N.; Mousavi, S. M., Enhanced recovery of valuable metals from spent lithium-ion batteries through optimization of organic acids produced by Aspergillus niger. *Waste Manag.* **2017,** *60*, 666-679.
10. Xin, Y.; Guo, X.; Chen, S.; Wang, J.; Wu, F.; Xin, B., Bioleaching of valuable metals Li, Co, Ni and Mn from spent electric vehicle Li-ion batteries for the purpose of recovery. *J. Clean. Prod.* **2016,** *116*, 249-258.
11. Xiao, J.; Li, J.; Xu, Z., Recycling metals from lithium ion battery by mechanical separation and vacuum metallurgy. *J. Hazard. Mater.* **2017,** *338*, 124-131.
12. Meng, Q.; Zhang, Y.; Dong, P., A combined process for cobalt recovering and cathode material regeneration from spent $LiCoO_2$ batteries: Process optimization and kinetics aspects. *Waste Manag.* **2018,** *71*, 372-380.
13. Natarajan, S.; Aravindan, V., An Urgent Call to Spent LIB Recycling: Whys and Wherefores for Graphite Recovery. *Adv. Energy Mater.* **2020,** *10* (37), 2002238.
14. Or, T.; Gourley, S. W. D.; Kaliyappan, K.; Yu, A.; Chen, Z., Recycling of mixed cathode lithium-ion batteries for electric vehicles: Current status and future outlook. *Carbon Energy* **2020,** *2* (1), 6-43.
15. Roper, L. D. Tesla Model S. http://roperld.com/science/TeslaModelS.htm (accessed 27 August).
16. Chen, X.; Ma, H.; Luo, C.; Zhou, T., Recovery of valuable metals from waste cathode materials of spent lithium-ion batteries using mild phosphoric acid. *J. Hazard. Mater.* **2017,** *326*, 77-86.
17. Chen, X.; Kang, D.; Cao, L.; Li, J.; Zhou, T.; Ma, H., Separation and recovery of valuable metals from spent lithium ion batteries: Simultaneous recovery of Li and Co in a single step. *Sep. Purif. Technol.* **2019,** *210*, 690-697.
18. Wang, G.; Wu, T.; Liu, B.; Gong, S.; Huang, Q.; Su, Y.; Wu, F.; Kelly, R. M., Gradient-Regeneration of $Li(Ni_{0.9}Co_{0.05}Mn_{0.05})O_2$ from Spent $LiCoO_2$ lithium-Ion Battery. *J. Electrochem. Soc.* **2021,** *167* (16), 160557.

19. Fu, Y.; He, Y.; Qu, L.; Feng, Y.; Li, J.; Liu, J.; Zhang, G.; Xie, W., Enhancement in leaching process of lithium and cobalt from spent lithium-ion batteries using benzenesulfonic acid system. *Waste Manag.* **2019,** *88*, 191-199.
20. Yadav, P.; Jie, C. J.; Tan, S.; Srinivasan, M., Recycling of cathode from spent lithium iron phosphate batteries. *J. Hazard. Mater.* **2020,** *399*, 123068.
21. Fan, X.; Song, C.; Lu, X.; Shi, Y.; Yang, S.; Zheng, F.; Huang, Y.; Liu, K.; Wang, H.; Li, Q., Separation and recovery of valuable metals from spent lithium-ion batteries via concentrated sulfuric acid leaching and regeneration of $LiNi_{1/3}Co_{1/3}Mn_{1/3}O_2$. *J. Alloys Compd.* **2021,** *863*, 158775.
22. Meng, Q.; Zhang, Y.; Dong, P.; Liang, F., A novel process for leaching of metals from $LiNi_{1/3}Co_{1/3}Mn_{1/3}O_2$ material of spent lithium ion batteries: Process optimization and kinetics aspects. *J. Ind. Eng. Chem.* **2018,** *61*, 133-141.
23. Jiang, G.; Zhang, Y.; Meng, Q.; Zhang, Y.; Dong, P.; Zhang, M.; Yang, X., Direct Regeneration of $LiNi_{0.5}Co_{0.2}Mn_{0.3}O_2$ Cathode from Spent Lithium-Ion Batteries by the Molten Salts Method. *ACS Sustain. Chem. Eng.* **2020,** *8* (49), 18138-18147.
24. Meng, Q.; Zhang, Y.; Dong, P., Use of electrochemical cathode-reduction method for leaching of cobalt from spent lithium-ion batteries. *J. Clean. Prod.* **2018,** *180*, 64-70.
25. dos Santos, C. S.; Alves, J. C.; da Silva, S. P.; Evangelista Sita, L.; da Silva, P. R. C.; de Almeida, L. C.; Scarminio, J., A closed-loop process to recover Li and Co compounds and to resynthesize $LiCoO_2$ from spent mobile phone batteries. *J. Hazard. Mater.* **2019,** *362*, 458-466.
26. Shi, Y.; Zhang, M.; Meng, Y. S.; Chen, Z., Ambient-Pressure Relithiation of Degraded $Li_xNi_{0.5}Co_{0.2}Mn_{0.3}O_2$ ($0 < x < 1$) via Eutectic Solutions for Direct Regeneration of Lithium-Ion Battery Cathodes. *Adv. Energy Mater.* **2019,** *9* (20), 1900454.
27. Song, X.; Hu, T.; Liang, C.; Long, H. L.; Zhou, L.; Song, W.; You, L.; Wu, Z. S.; Liu, J. W., Direct regeneration of cathode materials from spent lithium iron phosphate batteries using a solid phase sintering method. *RSC Adv.* **2017,** *7* (8), 4783-4790.
28. Li, X.; Zhang, J.; Song, D.; Song, J.; Zhang, L., Direct regeneration of recycled cathode material mixture from scrapped $LiFePO_4$ batteries. *J. Power Sources* **2017,** *345*, 78-84.
29. Shi, Y.; Chen, G.; Chen, Z., Effective regeneration of $LiCoO_2$ from spent lithium-ion batteries: a direct approach towards high-performance active particles. *Green Chem.* **2018,** *20* (4), 851-862.
30. Gao, H.; Yan, Q.; Xu, P.; Liu, H.; Li, M.; Liu, P.; Luo, J.; Chen, Z., Efficient Direct Recycling of Degraded $LiMn_2O_4$ Cathodes by One-Step Hydrothermal Relithiation. *ACS Appl. Mater. Interfaces* **2020,** *12* (46), 51546-51554.
31. Xiao, J.; Guo, J.; Zhan, L.; Xu, Z., A cleaner approach to the discharge process of spent lithium ion batteries in different solutions. *J. Clean. Prod.* **2020,** *255*, 120064.
32. Zhou, S.; Zhang, Y.; Meng, Q.; Dong, P.; Fei, Z.; Li, Q., Recycling of $LiCoO_2$ cathode material from spent lithium ion batteries by ultrasonic enhanced leaching and one-step regeneration. *J. Environ. Manag.* **2021,** *277*, 111426.
33. Gao, G.; He, X.; Lou, X.; Jiao, Z.; Guo, Y.; Chen, S.; Luo, X.; Sun, S.; Guan, J.; Yuan, H., A Citric Acid/$Na_2S_2O_3$ System for the Efficient Leaching of Valuable Metals from Spent Lithium-Ion Batteries. *JOM* **2019,** *71* (10), 3673-3681.
34. Yang, Y.; Xu, S.; He, Y., Lithium recycling and cathode material regeneration from acid leach liquor of spent lithium-ion battery via facile co-extraction and co-precipitation processes. *Waste Manag.* **2017,** *64*, 219-227.
35. Meshram, P.; Pandey, B. D.; Mankhand, T. R., Hydrometallurgical processing of spent

lithium ion batteries (LIBs) in the presence of a reducing agent with emphasis on kinetics of leaching. *Chem. Eng. J.* **2015,** *281*, 418-427.
36. Maroufi, S.; Assefi, M.; Khayyam Nekouei, R.; Sahajwalla, V., Recovery of lithium and cobalt from waste lithium-ion batteries through a selective isolation-suspension approach. *SM&T* **2020,** *23*, e00139.
37. Lombardo, G.; Ebin, B.; Steenari, B.-M.; Alemrajabi, M.; Karlsson, I.; Petranikova, M., Comparison of the effects of incineration, vacuum pyrolysis and dynamic pyrolysis on the composition of NMC-lithium battery cathode-material production scraps and separation of the current collector. *Resour. Conserv. Recycl.* **2021,** *164*, 105142.
38. Han, Y.; You, Y.; Hou, C.; Xiao, X.; Xing, Y.; Zhao, Y., Regeneration of Single-Crystal $LiNi_{0.5}Co_{0.2}Mn_{0.3}O_2$ Cathode Materials from Spent Power Lithium-Ion Batteries. *J. Electrochem. Soc.* **2021,** *168* (4), 040525.
39. Zhu, X.; Zhang, C.; Feng, P.; Yang, X.; Yang, X., A novel pulsated pneumatic separation with variable-diameter structure and its application in the recycling spent lithium-ion batteries. *Waste Manag.* **2021,** *131*, 20-30.
40. Shih, Y.-J.; Chien, S.-K.; Jhang, S.-R.; Lin, Y.-C., Chemical leaching, precipitation and solvent extraction for sequential separation of valuable metals in cathode material of spent lithium ion batteries. *J. Taiwan. Inst. Chem. Eng.* **2019,** *100*, 151-159.
41. Li, L.; Ge, J.; Wu, F.; Chen, R.; Chen, S.; Wu, B., Recovery of cobalt and lithium from spent lithium ion batteries using organic citric acid as leachant. *J. Hazard. Mater.* **2010,** *176* (1), 288-293.
42. Li, L.; Lu, J.; Ren, Y.; Zhang, X. X.; Chen, R. J.; Wu, F.; Amine, K., Ascorbic-acid-assisted recovery of cobalt and lithium from spent Li-ion batteries. *J. Power Sources* **2012,** *218*, 21-27.
43. Liu, D.; Su, Z.; Wang, L., Pyrometallurgically regenerated $LiMn_2O_4$ cathode scrap material and its electrochemical properties. *Ceram. Int.* **2021,** *47* (1), 42-47.
44. Yang, J.; Wang, W.; Yang, H.; Wang, D., One-pot compositional and structural regeneration of degraded $LiCoO_2$ for directly reusing it as a high-performance lithium-ion battery cathode. *Green Chem.* **2020,** *22* (19), 6489-6496.
45. Zhou, S.; Zhang, Y.; Meng, Q.; Dong, P.; Yang, X.; Liu, P.; Li, Q.; Fei, Z., Recycling of spent $LiCoO_2$ materials by electrolytic leaching of cathode electrode plate. *J. Environ. Chem. Eng.* **2021,** *9* (1), 104789.
46. Gratz, E.; Sa, Q.; Apelian, D.; Wang, Y., A closed loop process for recycling spent lithium ion batteries. *J. Power Sources* **2014,** *262*, 255-262.
47. Muzayanha, S. U.; Yudha, C. S.; Nur, A.; Widiyandari, H.; Haerudin, H.; Nilasary, H.; Fathoni, F.; Purwanto, A., A Fast Metals Recovery Method for the Synthesis of Lithium Nickel Cobalt Aluminum Oxide Material from Cathode Waste. *Metals* **2019,** *9* (5).
48. Tokoro, C.; Lim, S.; Teruya, K.; Kondo, M.; Mochidzuki, K.; Namihira, T.; Kikuchi, Y., Separation of cathode particles and aluminum current foil in Lithium-Ion battery by high-voltage pulsed discharge Part I: Experimental investigation. *Waste Manag.* **2021,** *125*, 58-66.
49. Kikuchi, Y.; Suwa, I.; Heiho, A.; Dou, Y.; Lim, S.; Namihira, T.; Mochidzuki, K.; Koita, T.; Tokoro, C., Separation of cathode particles and aluminum current foil in lithium-ion battery by high-voltage pulsed discharge Part II: Prospective life cycle assessment based on experimental data. *Waste Manag.* **2021,** *132*, 86-95.
50. Wang, M.; Tan, Q.; Liu, L.; Li, J., Efficient Separation of Aluminum Foil and Cathode Materials from Spent Lithium-Ion Batteries Using a Low-Temperature Molten Salt. *ACS Sustain. Chem. Eng.* **2019,** *7* (9), 8287-8294.

51. Wang, M.; Tan, Q.; Liu, L.; Li, J., A low-toxicity and high-efficiency deep eutectic solvent for the separation of aluminum foil and cathode materials from spent lithium-ion batteries. *J. Hazard. Mater.* **2019,** *380*, 120846.
52. Hu, X.; Mousa, E.; Ye, G., Recovery of Co, Ni, Mn, and Li from Li-ion batteries by smelting reduction - Part II: A pilot-scale demonstration. *J. Power Sources* **2021,** *483*, 229089.
53. Boxall, N. J.; Adamek, N.; Cheng, K. Y.; Haque, N.; Bruckard, W.; Kaksonen, A. H., Multistage leaching of metals from spent lithium ion battery waste using electrochemically generated acidic lixiviant. *Waste Manag.* **2018,** *74*, 435-445.
54. Wang, F.; Sun, R.; Xu, J.; Chen, Z.; Kang, M., Recovery of cobalt from spent lithium ion batteries using sulphuric acid leaching followed by solid–liquid separation and solvent extraction. *RSC Adv.* **2016,** *6* (88), 85303-85311.
55. Zeng, X.; Li, J.; Shen, B., Novel approach to recover cobalt and lithium from spent lithium-ion battery using oxalic acid. *J. Hazard. Mater.* **2015,** *295*, 112-118.
56. Hu, J.; Zhang, J.; Li, H.; Chen, Y.; Wang, C., A promising approach for the recovery of high value-added metals from spent lithium-ion batteries. *J. Power Sources* **2017,** *351*, 192-199.
57. Qiu, R.; Huang, Z.; Zheng, J.; Song, Q.; Ruan, J.; Tang, Y.; Qiu, R., Energy models and the process of fluid-magnetic separation for recovering cobalt micro-particles from vacuum reduction products of spent lithium ion batteries. *J. Clean. Prod.* **2021,** *279*, 123230.
58. Hanisch, C.; Loellhoeffel, T.; Diekmann, J.; Markley, K. J.; Haselrieder, W.; Kwade, A., Recycling of lithium-ion batteries: a novel method to separate coating and foil of electrodes. *J. Clean. Prod.* **2015,** *108*, 301-311.
59. Yu, J.; He, Y.; Ge, Z.; Li, H.; Xie, W.; Wang, S., A promising physical method for recovery of $LiCoO_2$ and graphite from spent lithium-ion batteries: Grinding flotation. *Sep. Purif. Technol.* **2018,** *190*, 45-52.
60. Lee, S.-H.; Kim, H.-S.; Jin, B.-S., Recycling of Ni-rich $Li(Ni_{0.8}Co_{0.1}Mn_{0.1})O_2$ cathode materials by a thermomechanical method. *J. Alloys Compd.* **2019,** *803*, 1032-1036.
61. Hu, X.; Mousa, E.; Tian, Y.; Ye, G., Recovery of Co, Ni, Mn, and Li from Li-ion batteries by smelting reduction - Part I: A laboratory-scale study. *J. Power Sources* **2021,** *483*, 228936.
62. Georgi-Maschler, T.; Friedrich, B.; Weyhe, R.; Heegn, H.; Rutz, M., Development of a recycling process for Li-ion batteries. *J. Power Sources* **2012,** *207*, 173-182.
63. Pinegar, H.; Smith, Y. R., Recycling of End-of-Life Lithium Ion Batteries, Part I: Commercial Processes. *J. Sustain. Met.* **2019,** *5* (3), 402-416.
64. Velázquez, M.; Valio; Santasalo, A.; Reuter; Serna, G., A Critical Review of Lithium-Ion Battery Recycling Processes from a Circular Economy Perspective. *Batteries* **2019,** *5* (4), 68.
65. Sojka, R.; Pan, Q.; Billmann, L., Comparative study of Li-ion battery recycling processes. In *Proceedings of the 25th International Congress for Battery Recycling ICBR*, Salzburg, Austria, 16–18 September 2020.
66. Friedrich, B.; Weyhe, R.; Träger, T., Optimizing the efficiency of recycling of lithium batteries through flexible process design. In *5. Fachtagung Kraftwerk Batterie*, Aachen, Germany, 2013.
67. Li, J.; Wang, G.; Xu, Z., Environmentally-friendly oxygen-free roasting/wet magnetic separation technology for in situ recycling cobalt, lithium carbonate and graphite from spent $LiCoO_2$/graphite lithium batteries. *J. Hazard. Mater.* **2016,** *302*, 97-104.
68. Yang, C.; Zhang, J.; Yu, B.; Huang, H.; Chen, Y.; Wang, C., Recovery of valuable metals from spent $LiNi_xCo_yMn_zO_2$ cathode material via phase transformation and stepwise leaching. *Sep. Purif. Technol.* **2021,** *267*, 118609.

69. Dolotko, O.; Hlova, I. Z.; Mudryk, Y.; Gupta, S.; Balema, V. P., Mechanochemical recovery of Co and Li from LCO cathode of lithium-ion battery. *J. Alloys Compd.* **2020,** *824*, 153876.
70. Tang, Y.; Qu, X.; Zhang, B.; Zhao, Y.; Xie, H.; Zhao, J.; Ning, Z.; Xing, P.; Yin, H., Recycling of spent lithium nickel cobalt manganese oxides via a low-temperature ammonium sulfation roasting approach. *J. Clean. Prod.* **2021,** *279*, 123633.
71. Pinegar, H.; Smith, Y. R., Recycling of End-of-Life Lithium-Ion Batteries, Part II: Laboratory-Scale Research Developments in Mechanical, Thermal, and Leaching Treatments. *J. Sustain. Met.* **2020,** *6* (1), 142-160.
72. Zeng, X.; Li, J.; Singh, N., Recycling of Spent Lithium-Ion Battery: A Critical Review. *Crit. Rev. Environ. Sci. Technol.* **2014,** *44* (10), 1129-1165.
73. Chagnes, A.; Pospiech, B., A brief review on hydrometallurgical technologies for recycling spent lithium-ion batteries. *J. Chem. Technol. Biotechnol.* **2013,** *88* (7), 1191-1199.
74. Zhu, S.-g.; He, W.-z.; Li, G.-m.; Zhou, X.; Zhang, X.-j.; Huang, J.-w., Recovery of Co and Li from spent lithium-ion batteries by combination method of acid leaching and chemical precipitation. *T. Nonferr. Metal. Soc.* **2012,** *22* (9), 2274-2281.
75. Zhang, Y.; Zhang, Y.; Zhang, Y.; Dong, P.; Meng, Q.; Xu, M., Novel efficient regeneration of high-performance $Li_{1.2}[Mn_{0.56}Ni_{0.16}Co_{0.08}]O_2$ cathode materials from spent $LiMn_2O_4$ batteries. *J. Alloys Compd.* **2019,** *783*, 357-362.
76. Zhang, J.; Hu, J.; Liu, Y.; Jing, Q.; Yang, C.; Chen, Y.; Wang, C., Sustainable and Facile Method for the Selective Recovery of Lithium from Cathode Scrap of Spent $LiFePO_4$ Batteries. *ACS Sustain. Chem. Eng.* **2019,** *7* (6), 5626-5631.
77. Chen, W.-S.; Ho, H.-J., Recovery of Valuable Metals from Lithium-Ion Batteries NMC Cathode Waste Materials by Hydrometallurgical Methods. *Metals* **2018,** *8* (5).
78. He, L.-P.; Sun, S.-Y.; Mu, Y.-Y.; Song, X.-F.; Yu, J.-G., Recovery of Lithium, Nickel, Cobalt, and Manganese from Spent Lithium-Ion Batteries Using l-Tartaric Acid as a Leachant. *ACS Sustain. Chem. Eng.* **2017,** *5* (1), 714-721.
79. He, L.-P.; Sun, S.-Y.; Yu, J.-G., Performance of $LiNi_{1/3}Co_{1/3}Mn_{1/3}O_2$ prepared from spent lithium-ion batteries by a carbonate co-precipitation method. *Ceram. Int.* **2018,** *44* (1), 351-357.
80. Chow, N.; Jung, J. C.-Y.; Nacu, A. M.; Warkentin, D. D. Processing of cobaltous sulpha/dithionate liquors derived from cobalt resource. U.S. Patent 10308523 B1, Jun. 4, 2019.
81. Zhao, J.; Zhang, B.; Xie, H.; Qu, J.; Qu, X.; Xing, P.; Yin, H., Hydrometallurgical recovery of spent cobalt-based lithium-ion battery cathodes using ethanol as the reducing agent. *Environ. Res.* **2020,** *181*, 108803.
82. Zhuang, L.; Sun, C.; Zhou, T.; Li, H.; Dai, A., Recovery of valuable metals from $LiNi_{0.5}Co_{0.2}Mn_{0.3}O_2$ cathode materials of spent Li-ion batteries using mild mixed acid as leachant. *Waste Manag.* **2019,** *85*, 175-185.
83. Liu, T.; Chen, J.; Shen, X.; Li, H., Regulating and regenerating the valuable metals from the cathode materials in lithium-ion batteries by nickel-cobalt-manganese co-extraction. *Sep. Purif. Technol.* **2021,** *259*, 118088.
84. Porvali, A.; Shukla, S.; Lundström, M., Low-acid leaching of lithium-ion battery active materials in Fe-catalyzed Cu-H_2SO_4 system. *Hydrometallurgy* **2020,** *195*, 105408.
85. Fan, E.; Li, L.; Wang, Z.; Lin, J.; Huang, Y.; Yao, Y.; Chen, R.; Wu, F., Sustainable Recycling Technology for Li-Ion Batteries and Beyond: Challenges and Future Prospects. *Chem. Rev.* **2020,** *120* (14), 7020-7063.
86. Zhang, X.; Xie, Y.; Cao, H.; Nawaz, F.; Zhang, Y., A novel process for recycling and resynthesizing $LiNi_{1/3}Co_{1/3}Mn_{1/3}O_2$ from the cathode scraps intended for lithium-ion batteries.

Waste Manag. **2014,** *34* (9), 1715-1724.
87. Chen, X.; Luo, C.; Zhang, J.; Kong, J.; Zhou, T., Sustainable Recovery of Metals from Spent Lithium-Ion Batteries: A Green Process. *ACS Sustain. Chem. Eng.* **2015,** *3* (12), 3104-3113.
88. Liu, C.; Li, Y.; Lin, D.; Hsu, P.-C.; Liu, B.; Yan, G.; Wu, T.; Cui, Y.; Chu, S., Lithium Extraction from Seawater through Pulsed Electrochemical Intercalation. *Joule* **2020,** *4* (7), 1459-1469.
89. Li, Z.; He, L.; Zhu, Y.; Yang, C., A Green and Cost-Effective Method for Production of LiOH from Spent $LiFePO_4$. *ACS Sustain. Chem. Eng.* **2020,** *8* (42), 15915-15926.
90. Gangaja, B.; Nair, S.; Santhanagopalan, D., Reuse, Recycle, and Regeneration of $LiFePO_4$ Cathode from Spent Lithium-Ion Batteries for Rechargeable Lithium- and Sodium-Ion Batteries. *ACS Sustain. Chem. Eng.* **2021,** *9* (13), 4711-4721.
91. Yu, J.; Wang, X.; Zhou, M.; Wang, Q., A redox targeting-based material recycling strategy for spent lithium ion batteries. *Energy Environ. Sci.* **2019,** *12* (9), 2672-2677.
92. Liu, P.; Xiao, L.; Chen, Y.; Tang, Y.; Wu, J.; Chen, H., Recovering valuable metals from $LiNi_xCo_yMn_{1-x-y}O_2$ cathode materials of spent lithium ion batteries via a combination of reduction roasting and stepwise leaching. *J. Alloys Compd.* **2019,** *783*, 743-752.
93. Gao, R.; Sun, C.; Zhou, T.; Zhuang, L.; Xie, H., Recycling of $LiNi_{0.5}Co_{0.2}Mn_{0.3}O_2$ Material from Spent Lithium-ion Batteries Using Mixed Organic Acid Leaching and Sol-gel Method. *ChemistrySelect* **2020,** *5* (21), 6482-6490.
94. Meshram, P.; Pandey, B. D.; Mankhand, T. R., Recovery of valuable metals from cathodic active material of spent lithium ion batteries: Leaching and kinetic aspects. *Waste Manag.* **2015,** *45*, 306-313.
95. Farjas, J.; Roura, P., Modification of the Kolmogorov–Johnson–Mehl–Avrami rate equation for non-isothermal experiments and its analytical solution. *Acta Mater.* **2006,** *54* (20), 5573-5579.
96. Muzayanha, S.; Yudha, C.; Hasanah, L.; Gupita, L.; Widiyandari, H.; Purwanto, A., Comparative Study of Various Kinetic Models on Leaching of NCA Cathode Material. *Indones. J. Chem.* **2020,** *20*, 1291.
97. Zhang, R.; Meng, Z.; Ma, X.; Chen, M.; Chen, B.; Zheng, Y.; Yao, Z.; Vanaphuti, P.; Bong, S.; Yang, Z.; Wang, Y., Understanding fundamental effects of Cu impurity in different forms for recovered $LiNi_{0.6}Co_{0.2}Mn_{0.2}O_2$ cathode materials. *Nano Energy* **2020,** *78*, 105214.
98. Zhang, R.; Zheng, Y.; Yao, Z.; Vanaphuti, P.; Ma, X.; Bong, S.; Chen, M.; Liu, Y.; Cheng, F.; Yang, Z.; Wang, Y., Systematic Study of Al Impurity for NCM622 Cathode Materials. *ACS Sustain. Chem. Eng.* **2020,** *8* (26), 9875-9884.
99. Kim, S.; Park, S.; Jo, M.; Beak, M.; Park, J.; Jeong, G.; Yu, J.-S.; Kwon, K., Electrochemical effects of residual Al in the resynthesis of $Li[Ni_{1/3}Mn_{1/3}Co_{1/3}]O_2$ cathode materials. *J. Alloys Compd.* **2021,** *857*, 157581.
100. Park, S.; Kim, D.; Ku, H.; Jo, M.; Kim, S.; Song, J.; Yu, J.; Kwon, K., The effect of Fe as an impurity element for sustainable resynthesis of $Li[Ni_{1/3}Co_{1/3}Mn_{1/3}]O_2$ cathode material from spent lithium-ion batteries. *Electrochim. Acta* **2019,** *296*, 814-822.
101. Jeong, S.; Park, S.; Beak, M.; Park, J.; Sohn, J.-S.; Kwon, K., Effect of Residual Trace Amounts of Fe and Al in $Li[Ni_{1/3}Mn_{1/3}Co_{1/3}]O_2$ Cathode Active Material for the Sustainable Recycling of Lithium-Ion Batteries. *Materials* **2021,** *14* (9).
102. Liu, Y.; Gu, Y.-J.; Luo, G.-Y.; Chen, Z.-L.; Wu, F.-Z.; Dai, X.-Y.; Mai, Y.; Li, J.-Q., Ni-doped $LiFePO_4$/C as high-performance cathode composites for Li-ion batteries. *Ceram. Int.* **2020,** *46* (10, Part A), 14857-14863.

103. Čech, O.; Thomas, J. E.; Visintin, A.; Sedlarikova, M.; Vondrák, J.; Moreno, S., Cobalt Doped $LiFePO_4$/C Composite Material for Li-Ion Cathodes. *ECS Trans.* **2019,** *40* (1), 93-98.
104. Wang, Y.; Zhang, D.; Yu, X.; Cai, R.; Shao, Z.; Liao, X.-Z.; Ma, Z.-F., Mechanoactivation-assisted synthesis and electrochemical characterization of manganese lightly doped $LiFePO_4$. *J. Alloys Compd.* **2010,** *492* (1), 675-680.
105. Chang, Z.-R.; Lv, H.-J.; Tang, H.; Yuan, X.-Z.; Wang, H., Synthesis and performance of high tap density $LiFePO_4$/C cathode materials doped with copper ions. *J. Alloys Compd.* **2010,** *501* (1), 14-17.
106. Amin, R.; Lin, C.; Maier, J., Aluminium-doped $LiFePO_4$ single crystals Part II. Ionic conductivity, diffusivity and defect model. *Phys. Chem. Chem. Phys.* **2008,** *10* (24), 3524-3529.
107. Wang, H.; Friedrich, B., Development of a Highly Efficient Hydrometallurgical Recycling Process for Automotive Li–Ion Batteries. *J. Sustain. Met.* **2015,** *1* (2), 168-178.
108. Zou, H.; Gratz, E.; Apelian, D.; Wang, Y., A novel method to recycle mixed cathode materials for lithium ion batteries. *Green Chem.* **2013,** *15* (5), 1183-1191.
109. Suzuki, T.; Nakamura, T.; Inoue, Y.; Niinae, M.; Shibata, J., A hydrometallurgical process for the separation of aluminum, cobalt, copper and lithium in acidic sulfate media. *Sep. Purif. Technol.* **2012,** *98*, 396-401.
110. Kang, J.; Senanayake, G.; Sohn, J.; Shin, S. M., Recovery of cobalt sulfate from spent lithium ion batteries by reductive leaching and solvent extraction with Cyanex 272. *Hydrometallurgy* **2010,** *100* (3), 168-171.
111. Joo, S.-H.; Shin, D. j.; Oh, C.; Wang, J.-P.; Senanayake, G.; Shin, S. M., Selective extraction and separation of nickel from cobalt, manganese and lithium in pre-treated leach liquors of ternary cathode material of spent lithium-ion batteries using synergism caused by Versatic 10 acid and LIX 84-I. *Hydrometallurgy* **2016,** *159*, 65-74.
112. Lide, D. R., *CRC handbook of chemistry and physics, 2003-2004*. CRC Press: Boca Raton, Florida, 2003.
113. Gao, R.; Sun, C.; Xu, L.; Zhou, T.; Zhuang, L.; Xie, H., Recycling $LiNi_{0.5}Co_{0.2}Mn_{0.3}O_2$ material from spent lithium-ion batteries by oxalate co-precipitation. *Vacuum* **2020,** *173*, 109181.
114. Joulié, M.; Laucournet, R.; Billy, E., Hydrometallurgical process for the recovery of high value metals from spent lithium nickel cobalt aluminum oxide based lithium-ion batteries. *J. Power Sources* **2014,** *247*, 551-555.
115. Li, Q.; Fung, K. Y.; Ng, K. M., Hydrometallurgy process for the recovery of valuable metals from $LiNi_{0.8}Co_{0.15}Al_{0.05}O_2$ cathode materials. *SN Appl. Sci.* **2019,** *1* (7), 690.
116. Wang, R.-C.; Lin, Y.-C.; Wu, S.-H., A novel recovery process of metal values from the cathode active materials of the lithium-ion secondary batteries. *Hydrometallurgy* **2009,** *99* (3), 194-201.
117. Schaeffer, N.; Passos, H.; Gras, M.; Rodriguez Vargas, S. J.; Neves, M. C.; Svecova, L.; Papaiconomou, N.; Coutinho, J. A. P., Selective Separation of Manganese, Cobalt, and Nickel in a Fully Aqueous System. *ACS Sustain. Chem. Eng.* **2020,** *8* (32), 12260-12269.
118. Zhang, P.; Yokoyama, T.; Itabashi, O.; Suzuki, T. M.; Inoue, K., Hydrometallurgical process for recovery of metal values from spent lithium-ion secondary batteries. *Hydrometallurgy* **1998,** *47* (2), 259-271.
119. Chen, X.; Chen, Y.; Zhou, T.; Liu, D.; Hu, H.; Fan, S., Hydrometallurgical recovery of metal values from sulfuric acid leaching liquor of spent lithium-ion batteries. *Waste Manag.* **2015,** *38*, 349-356.
120. Nayl, A. A.; Hamed, M. M.; Rizk, S. E., Selective extraction and separation of metal values

from leach liquor of mixed spent Li-ion batteries. *J. Taiwan. Inst. Chem. Eng.* **2015,** *55*, 119-125.
121. Swain, B.; Jeong, J.; Lee, J.; Lee, G.-H., Separation of cobalt and lithium from mixed sulphate solution using Na-Cyanex 272. *Hydrometallurgy* **2006,** *84* (3), 130-138.
122. Sarangi, K.; Reddy, B. R.; Das, R. P., Extraction studies of cobalt (II) and nickel (II) from chloride solutions using Na-Cyanex 272.: Separation of Co(II)/Ni(II) by the sodium salts of D2EHPA, PC88A and Cyanex 272 and their mixtures. *Hydrometallurgy* **1999,** *52* (3), 253-265.
123. Devi, N. B.; Nathsarma, K. C.; Chakravortty, V., Separation and recovery of cobalt(II) and nickel(II) from sulphate solutions using sodium salts of D2EHPA, PC 88A and Cyanex 272. *Hydrometallurgy* **1998,** *49* (1), 47-61.
124. Wang, W.-Y.; Yang, H.-C.; Xu, R.-B., High-Performance Recovery of Cobalt and Nickel from the Cathode Materials of NMC Type Li-Ion Battery by Complexation-Assisted Solvent Extraction. *Minerals* **2020,** *10* (8).
125. Nguyen, V. N. H.; Lee, M. S., Separation of Co(II), Ni(II), Mn(II) and Li(I) from synthetic sulfuric acid leaching solution of spent lithium ion batteries by solvent extraction. *J. Chem. Technol. Biotechnol.* **2021,** *96* (5), 1205-1217.
126. Xie, Q.; Cui, Z.; Manthiram, A., Unveiling the Stabilities of Nickel-Based Layered Oxide Cathodes at an Identical Degree of Delithiation in Lithium-Based Batteries. *Adv. Mater.* **2021,** *n/a* (n/a), 2100804.
127. Hausbrand, R.; Cherkashinin, G.; Ehrenberg, H.; Gröting, M.; Albe, K.; Hess, C.; Jaegermann, W., Fundamental degradation mechanisms of layered oxide Li-ion battery cathode materials: Methodology, insights and novel approaches. *Mater. Sci. Eng., B* **2015,** *192*, 3-25.
128. Furushima, Y.; Yanagisawa, C.; Nakagawa, T.; Aoki, Y.; Muraki, N., Thermal stability and kinetics of delithiated $LiCoO_2$. *J. Power Sources* **2011,** *196* (4), 2260-2263.
129. Bak, S.-M.; Hu, E.; Zhou, Y.; Yu, X.; Senanayake, S. D.; Cho, S.-J.; Kim, K.-B.; Chung, K. Y.; Yang, X.-Q.; Nam, K.-W., Structural Changes and Thermal Stability of Charged $LiNi_xMn_yCo_zO_2$ Cathode Materials Studied by Combined In Situ Time-Resolved XRD and Mass Spectroscopy. *ACS Appl. Mater. Interfaces* **2014,** *6* (24), 22594-22601.
130. Xia, Y.; Zheng, J.; Wang, C.; Gu, M., Designing principle for Ni-rich cathode materials with high energy density for practical applications. *Nano Energy* **2018,** *49*, 434-452.
131. Wu, F.; Liu, N.; Chen, L.; Su, Y.; Tan, G.; Bao, L.; Zhang, Q.; Lu, Y.; Wang, J.; Chen, S.; Tan, J., Improving the reversibility of the H2-H3 phase transitions for layered Ni-rich oxide cathode towards retarded structural transition and enhanced cycle stability. *Nano Energy* **2019,** *59*, 50-57.
132. Li, W.; Reimers, J. N.; Dahn, J. R., In situ x-ray diffraction and electrochemical studies of $Li_{1-x}NiO_2$. *Solid State Ionics* **1993,** *67* (1), 123-130.
133. Yang, X. Q.; Sun, X.; McBreen, J., New findings on the phase transitions in $Li_{1-x}NiO_2$: in situ synchrotron X-ray diffraction studies. *Electrochem. Commun.* **1999,** *1* (6), 227-232.
134. Dixit, M.; Markovsky, B.; Schipper, F.; Aurbach, D.; Major, D. T., Origin of Structural Degradation During Cycling and Low Thermal Stability of Ni-Rich Layered Transition Metal-Based Electrode Materials. *J. Phys. Chem. C* **2017,** *121* (41), 22628-22636.
135. Langdon, J.; Manthiram, A., A perspective on single-crystal layered oxide cathodes for lithium-ion batteries. *Energy Storage Mater.* **2021,** *37*, 143-160.
136. Van der Ven, A.; Aydinol, M. K.; Ceder, G.; Kresse, G.; Hafner, J., First-principles investigation of phase stability in Li_xCoO_2. *Phys. Rev. B* **1998,** *58* (6), 2975-2987.
137. Dokko, K., In Situ Observation of $LiNiO_2$ Single-Particle Fracture during Li-Ion Extraction and Insertion. *Electrochem. Solid-State Lett.* **1999,** *3* (3), 125.

138. Kikkawa, J.; Terada, S.; Gunji, A.; Nagai, T.; Kurashima, K.; Kimoto, K., Chemical States of Overcharged $LiCoO_2$ Particle Surfaces and Interiors Observed Using Electron Energy-Loss Spectroscopy. *J. Phys. Chem. C* **2015,** *119* (28), 15823-15830.
139. Tang, X.; Jia, Q.; Yang, L.; Bai, M.; Wu, W.; Wang, Z.; Gong, M.; Sa, S.; Tao, S.; Sun, M.; Ma, Y., Towards the high-energy-density battery with broader temperature adaptability: Self-discharge mitigation of quaternary nickel-rich cathode. *Energy Storage Mater.* **2020,** *33*, 239-249.
140. Chen, Z.; Lu, Z.; Dahn, J., Staging Phase Transitions in Li_xCoO_2. *J. Electrochem. Soc.* **2002,** *149*, A1604.
141. Xia, H.; Lu, L.; Meng, Y. S.; Ceder, G., Phase Transitions and High-Voltage Electrochemical Behavior of $LiCoO_2$ Thin Films Grown by Pulsed Laser Deposition. *J. Electrochem. Soc.* **2007,** *154* (4), A337.
142. Akhilash, M.; Salini, P. S.; John, B.; Mercy, T. D., A journey through layered cathode materials for lithium ion cells – From lithium cobalt oxide to lithium-rich transition metal oxides. *J. Alloys Compd.* **2021,** *869*, 159239.
143. Chebiam, R. V.; Kannan, A. M.; Prado, F.; Manthiram, A., Comparison of the chemical stability of the high energy density cathodes of lithium-ion batteries. *Electrochem. Commun.* **2001,** *3* (11), 624-627.
144. Choi, J.; Manthiram, A., Role of Chemical and Structural Stabilities on the Electrochemical Properties of Layered $LiNi_{1/3}Mn_{1/3}Co_{1/3}O_2$ Cathodes. *J. Electrochem. Soc.* **2005,** *152* (9), A1714.
145. Yano, A.; Taguchi, N.; Kanzaki, H.; Shikano, M.; Sakaebe, H., Capability and Reversibility of $LiCoO_2$ during Charge/Discharge with O3/H1−3 Layered Structure Change. *J. Electrochem. Soc.* **2021,** *168* (5), 050517.
146. Gabrisch, H.; Yazami, R.; Fultz, B., Hexagonal to Cubic Spinel Transformation in Lithiated Cobalt Oxide. *J. Electrochem. Soc.* **2004,** *151* (6), A891.
147. Jung, S.-K.; Gwon, H.; Hong, J.; Park, K.-Y.; Seo, D.-H.; Kim, H.; Hyun, J.; Yang, W.; Kang, K., Understanding the Degradation Mechanisms of $LiNi_{0.5}Co_{0.2}Mn_{0.3}O_2$ Cathode Material in Lithium Ion Batteries. *Adv. Energy Mater.* **2014,** *4* (1), 1300787.
148. Wang, L.; Chen, B.; Ma, J.; Cui, G.; Chen, L., Reviving lithium cobalt oxide-based lithium secondary batteries-toward a higher energy density. *Chem. Soc. Rev.* **2018,** *47* (17), 6505-6602.
149. Nam, K.-W.; Bak, S.-M.; Hu, E.; Yu, X.; Zhou, Y.; Wang, X.; Wu, L.; Zhu, Y.; Chung, K.-Y.; Yang, X.-Q., Combining In Situ Synchrotron X-Ray Diffraction and Absorption Techniques with Transmission Electron Microscopy to Study the Origin of Thermal Instability in Overcharged Cathode Materials for Lithium-Ion Batteries. *Adv. Funct. Mater.* **2013,** *23* (8), 1047-1063.
150. Wang, H.; Jang, Y. I.; Huang, B.; Sadoway, D. R.; Chiang, Y. M., TEM Study of Electrochemical Cycling-Induced Damage and Disorder in $LiCoO_2$ Cathodes for Rechargeable Lithium Batteries. *J. Electrochem. Soc.* **1999,** *146* (2), 473-480.
151. Lin, F.; Markus, I. M.; Nordlund, D.; Weng, T.-C.; Asta, M. D.; Xin, H. L.; Doeff, M. M., Surface reconstruction and chemical evolution of stoichiometric layered cathode materials for lithium-ion batteries. *Nat. Commun.* **2014,** *5* (1).
152. Xiong, X.; Wang, Z.; Yue, P.; Guo, H.; Wu, F.; Wang, J.; Li, X., Washing effects on electrochemical performance and storage characteristics of $LiNi_{0.8}Co_{0.1}Mn_{0.1}O_2$ as cathode material for lithium-ion batteries. *J. Power Sources* **2013,** *222*, 318-325.
153. Yabuuchi, N.; Kim, Y.-T.; Li, H. H.; Shao-Horn, Y., Thermal Instability of Cycled $LixNi_{0.5}Mn_{0.5}O_2$ Electrodes: An in Situ Synchrotron X-ray Powder Diffraction Study. *Chem. Mater.* **2008,** *20* (15), 4936-4951.
154. Reed, J.; Ceder, G., Role of Electronic Structure in the Susceptibility of Metastable

Transition-Metal Oxide Structures to Transformation. *Chem. Rev.* **2004,** *104* (10), 4513-4534.
155. Sharifi-Asl, S.; Lu, J.; Amine, K.; Shahbazian-Yassar, R., Oxygen Release Degradation in Li-Ion Battery Cathode Materials: Mechanisms and Mitigating Approaches. *Adv. Energy Mater.* **2019,** *9* (22), 1900551.
156. Wang, C.; Han, L.; Zhang, R.; Cheng, H.; Mu, L.; Kisslinger, K.; Zou, P.; Ren, Y.; Cao, P.; Lin, F.; Xin, H. L., Resolving atomic-scale phase transformation and oxygen loss mechanism in ultrahigh-nickel layered cathodes for cobalt-free lithium-ion batteries. *Matter* **2021,** *4* (6), 2013-2026.
157. Wang, L.; Maxisch, T.; Ceder, G., A First-Principles Approach to Studying the Thermal Stability of Oxide Cathode Materials. *Chem. Mater.* **2007,** *19* (3), 543-552.
158. Yang, T.; Lu, Y.; Li, L.; Ge, D.; Yang, H.; Leng, W.; Zhou, H.; Han, X.; Schmidt, N.; Ellis, M.; Li, Z., An Effective Relithiation Process for Recycling Lithium-Ion Battery Cathode Materials. *Adv. Sustain. Syst.* **2020,** *4* (1), 1900088.
159. Park, K.; Yu, J.; Coyle, J.; Dai, Q.; Frisco, S.; Zhou, M.; Burrell, A., Direct Cathode Recycling of End-Of-Life Li-Ion Batteries Enabled by Redox Mediation. *ACS Sustain. Chem. Eng.* **2021,** *9* (24), 8214-8221.
160. Ma, T.; Guo, Z.; Shen, Z.; Wu, Q.; Li, Y.; Yang, G., Molten salt-assisted regeneration and characterization of submicron-sized $LiNi_{0.5}Co_{0.2}Mn_{0.3}O_2$ crystals from spent lithium ion batteries. *J. Alloys Compd.* **2020,** *848*, 156591.
161. Wang, T.; Luo, H.; Bai, Y.; Li, J.; Belharouak, I.; Dai, S., Direct Recycling of Spent NCM Cathodes through Ionothermal Lithiation. *Adv. Energy Mater.* **2020,** *10* (30), 2001204.
162. Li, X.; Dogan, F.; Lu, Y.; Antunes, C.; Shi, Y.; Burrell, A.; Ban, C., Fast Determination of Lithium Content in Spent Cathodes for Direct Battery Recycling. *Adv. Sustain. Syst.* **2020,** *4* (8), 2000073.
163. Chen, S.; He, T.; Lu, Y.; Su, Y.; Tian, J.; Li, N.; Chen, G.; Bao, L.; Wu, F., Renovation of $LiCoO_2$ with outstanding cycling stability by thermal treatment with Li_2CO_3 from spent Li-ion batteries. *J. Energy Storage* **2016,** *8*, 262-273.
164. Fan, M.; Chang, X.; Guo, Y.-J.; Chen, W.-P.; Yin, Y.-X.; Yang, X.; Meng, Q.; Wan, L.-J.; Guo, Y.-G., Increased residual lithium compounds guided design for green recycling of spent lithium-ion cathodes. *Energy Environ. Sci.* **2021,** *14* (3), 1461-1468.
165. Shi, Y.; Chen, G.; Liu, F.; Yue, X.; Chen, Z., Resolving the Compositional and Structural Defects of Degraded $LiNi_xCo_yMn_zO_2$ Particles to Directly Regenerate High-Performance Lithium-Ion Battery Cathodes. *ACS Energy Lett.* **2018,** *3* (7), 1683-1692.
166. Garcia, B.; Farcy, J.; Pereira-Ramos, J. P.; Perichon, J.; Baffier, N., Low-temperature cobalt oxide as rechargeable cathodic material for lithium batteries. *J. Power Sources* **1995,** *54* (2), 373-377.
167. Gummow, R. J.; Liles, D. C.; Thackeray, M. M., Spinel versus layered structures for lithium cobalt oxide synthesised at 400°C. *Mater. Res. Bull.* **1993,** *28* (3), 235-246.
168. Garcia, B.; Barboux, P.; Ribot, F.; Kahn-Harari, A.; Mazerolles, L.; Baffier, N., The structure of low temperature crystallized $LiCoO_2$. *Solid State Ionics* **1995,** *80* (1), 111-118.
169. Xu, P.; Dai, Q.; Gao, H.; Liu, H.; Zhang, M.; Li, M.; Chen, Y.; An, K.; Meng, Y. S.; Liu, P.; Li, Y.; Spangenberger, J. S.; Gaines, L.; Lu, J.; Chen, Z., Efficient Direct Recycling of Lithium-Ion Battery Cathodes by Targeted Healing. *Joule* **2020,** *4* (12), 2609-2626.
170. Xu, P.; Yang, Z.; Yu, X.; Holoubek, J.; Gao, H.; Li, M.; Cai, G.; Bloom, I.; Liu, H.; Chen, Y.; An, K.; Pupek, K. Z.; Liu, P.; Chen, Z., Design and Optimization of the Direct Recycling of Spent Li-Ion Battery Cathode Materials. *ACS Sustain. Chem. Eng.* **2021,** *9* (12), 4543-4553.

171. Park, K.-Y.; Park, I.; Kim, H.; Lim, H.-d.; Hong, J.; Kim, J.; Kang, K., Anti-Site Reordering in $LiFePO_4$: Defect Annihilation on Charge Carrier Injection. *Chem. Mater.* **2014,** *26* (18), 5345-5351.
172. Cho, J.; Kim, T.-J.; Kim, Y. J.; Park, B., High-Performance ZrO_2-Coated $LiNiO_2$ Cathode Material. *Electrochem. Solid-State Lett.* **2001,** *4* (10), A159.
173. Han, B.; Key, B.; Lapidus, S. H.; Garcia, J. C.; Iddir, H.; Vaughey, J. T.; Dogan, F., From Coating to Dopant: How the Transition Metal Composition Affects Alumina Coatings on Ni-Rich Cathodes. *ACS Appl. Mater. Interfaces* **2017,** *9* (47), 41291-41302.
174. Li, Q.; Zhuang, W.; Li, Z.; Wu, S.; Li, N.; Gao, M.; Li, W.; Wang, J.; Lu, S., Realizing Superior Cycle Stability of a Ni-Rich Layered $LiNi_{0.83}Co_{0.12}Mn_{0.05}O_2$ Cathode with a B_2O_3 Surface Modification. *ChemElectroChem* **2020,** *7* (4), 998-1006.
175. Hwang, B. J.; Wu, Y. W.; Venkateswarlu, M.; Cheng, M. Y.; Santhanam, R., Influence of synthesis conditions on electrochemical properties of high-voltage $Li_{1.02}Ni_{0.5}Mn_{1.5}O_4$ spinel cathode material. *J. Power Sources* **2009,** *193* (2), 828-833.
176. Zhu, Z.; Yu, D.; Shi, Z.; Gao, R.; Xiao, X.; Waluyo, I.; Ge, M.; Dong, Y.; Xue, W.; Xu, G.; Lee, W.-K.; Hunt, A.; Li, J., Gradient-morph $LiCoO_2$ single crystals with stabilized energy density above 3400 W h L^{-1}. *Energy Environ. Sci.* **2020,** *13* (6), 1865-1878.
177. Meng, X.; Cao, H.; Hao, J.; Ning, P.; Xu, G.; Sun, Z., Sustainable Preparation of $LiNi_{1/3}Co_{1/3}Mn_{1/3}O_2$–$V_2O_5$ Cathode Materials by Recycling Waste Materials of Spent Lithium-Ion Battery and Vanadium-Bearing Slag. *ACS Sustain. Chem. Eng.* **2018,** *6* (5), 5797-5805.
178. Zhang, Y.; Hao, T.; Huang, X.; Duan, J.; Meng, Q.; Wang, D.; Lin, Y.; Xu, M.; Dong, P., Synthesis of high performance nano-over-lithiated oxide coated $LiNi_{0.6}Co_{0.2}Mn_{0.2}O_2$ from spent lithium ion batteries. *Mater. Res. Express* **2019,** *6* (8), 085521.
179. Wu, N.; Wu, H.; Kim, J.-K.; Liu, X.; Zhang, Y., Restoration of Degraded Nickel-Rich Cathode Materials for Long-Life Lithium-Ion Batteries. *ChemElectroChem* **2018,** *5* (1), 78-83.
180. Chen, T.; Wang, F.; Li, X.; Yan, X.; Wang, H.; Deng, B.; Xie, Z.; Qu, M., Dual functional $MgHPO_4$ surface modifier used to repair deteriorated Ni-Rich $LiNi_{0.8}Co_{0.15}Al_{0.05}O_2$ cathode material. *Applied Surface Science* **2019,** *465*, 863-870.
181. Fan, X.; Tan, C.; Li, Y.; Chen, Z.; Li, Y.; Huang, Y.; Pan, Q.; Zheng, F.; Wang, H.; Li, Q., A green, efficient, closed-loop direct regeneration technology for reconstructing of the $LiNi_{0.5}Co_{0.2}Mn_{0.3}O_2$ cathode material from spent lithium-ion batteries. *J. Hazard. Mater.* **2021,** *410*, 124610.
182. Xu, B.; Dong, P.; Duan, J.; Wang, D.; Huang, X.; Zhang, Y., Regenerating the used $LiFePO_4$ to high performance cathode via mechanochemical activation assisted V^{5+} doping. *Ceram. Int.* **2019,** *45* (9), 11792-11801.
183. Wu, J.; Lin, J.; Fan, E.; Chen, R.; Wu, F.; Li, L., Sustainable Regeneration of High-Performance $Li_{1-x}Na_xCoO_2$ from Cathode Materials in Spent Lithium-Ion Batteries. *ACS Appl. Energy Mater.* **2021,** *4* (3), 2607-2615.
184. Parikh, V. P.; Ahmadi, A.; Parekh, M. H.; Sadeghi, F.; Pol, V. G., Upcycling of Spent Lithium Cobalt Oxide Cathodes from Discarded Lithium-Ion Batteries as Solid Lubricant Additive. *Environ. Sci. Technol.* **2019,** *53* (7), 3757-3763.
185. Zhang, Y.; Wang, Y.; Zhang, H.; Li, Y.; Zhang, Z.; Zhang, W., Recycling spent lithium-ion battery as adsorbents to remove aqueous heavy metals: Adsorption kinetics, isotherms, and regeneration assessment. *Resour. Conserv. Recycl.* **2020,** *156*, 104688.
186. Lv, H.; Huang, H.; Huang, C.; Gao, Q.; Yang, Z.; Zhang, W., Electric field driven de-lithiation: A strategy towards comprehensive and efficient recycling of electrode materials from

spent lithium ion batteries. *Appl. Catal. B* **2021,** *283*, 119634.
187. Yang, Y.; Yang, H.; Cao, H.; Wang, Z.; Liu, C.; Sun, Y.; Zhao, H.; Zhang, Y.; Sun, Z., Direct preparation of efficient catalyst for oxygen evolution reaction and high-purity Li_2CO_3 from spent $LiNi_{0.5}Mn_{0.3}Co_{0.2}O_2$ batteries. *J. Clean. Prod.* **2019,** *236*, 117576.
188. Guo, M.; Li, K.; Liu, L.; Zhang, H.; Guo, W.; Hu, X.; Meng, X.; Jia, J.; Sun, T., Manganese-based multi-oxide derived from spent ternary lithium-ions batteries as high-efficient catalyst for VOCs oxidation. *J. Hazard. Mater.* **2019,** *380*, 120905.
189. PRNewswire Global Lithium-Ion Battery Market (2021 to 2030) - Declining Prices of Lithium-Ion Batteries Presents Opportunities. https://www.prnewswire.com/news-releases/global-lithium-ion-battery-market-2021-to-2030---declining-prices-of-lithium-ion-batteries-presents-opportunities-301333864.html (accessed 31 October).
190. Chen, X.; Li, S.; Wang, Y.; Jiang, Y.; Tan, X.; Han, W.; Wang, S., Recycling of $LiFePO_4$ cathode materials from spent lithium-ion batteries through ultrasound-assisted Fenton reaction and lithium compensation. *Waste Manag.* **2021,** *136*, 67-75.
191. Zhang, X.; Jiang, W. J.; Mauger, A.; Qilu; Gendron, F.; Julien, C. M., Minimization of the cation mixing in $Li_{1+x}(NMC)_{1-x}O_2$ as cathode material. *J. Power Sources* **2010,** *195* (5), 1292-1301.
192. Zhang, J.-N.; Li, Q.; Wang, Y.; Zheng, J.; Yu, X.; Li, H., Dynamic evolution of cathode electrolyte interphase (CEI) on high voltage $LiCoO_2$ cathode and its interaction with Li anode. *Energy Storage Mater.* **2018,** *14*, 1-7.